Surface Wave Effects on Oceanic Fronts, Filaments, and Turbulence

Baylor Fox-Kemper (Brown Geo.)

with Jim McWilliams (UCLA), Qing Li (Brown Geo), Nobu Suzuki (Brown Geo), and Sean Haney (CU-ATOC),

Expanding on past work with:

Peter Hamlington (CU-Boulder), Luke Van Roekel (Northland College), Adrean Webb (TUMST), Keith Julien (CU-APPM), Greg Chini (UNH), Peter Sullivan (NCAR), Mark Hemer (CSIRO)

Kavli Institute for Theoretical Physics

Sponsors: NSF 1258907, 1245944, 0934737, NASA NNX09AF38G

Surface Wave Effects on Oceanic Fronts, Filaments, and Turbulence

Baylor Fox-Kemper (Brown Geo.)

with Jim McWilliams (UCLA), Qing Li (Brown Geo), Nobu Suzuki (Brown Geo), and Sean Haney (CU-ATOC),

Expanding on past work with:

Peter Hamlington (CU-Boulder), Luke Van Roekel (Northland College), Adrean Webb (TUMST), Keith Julien (CU-APPM), Greg Chini (UNH), Peter Sullivan (NCAR), Mark Hemer (CSIRO)

Kavli Institute for Theoretical Physics

Sponsors: NSF 1258907, 1245944, 0934737, NASA NNX09AF38G

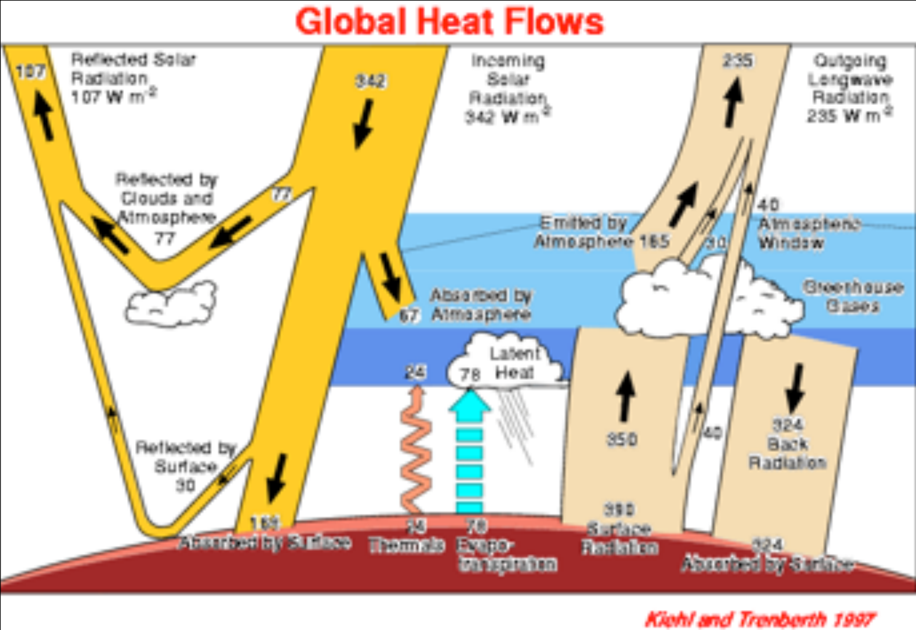

The Earth's Climate System is forced by the Sun on a global scale (24,000km)

Next-gen. ocean climate models simulate globe to 10km: Mesoscale Ocean Large Eddy Simulations (MOLES)

Turbulence cascades to scales about 10 billion times smaller O(1mm)

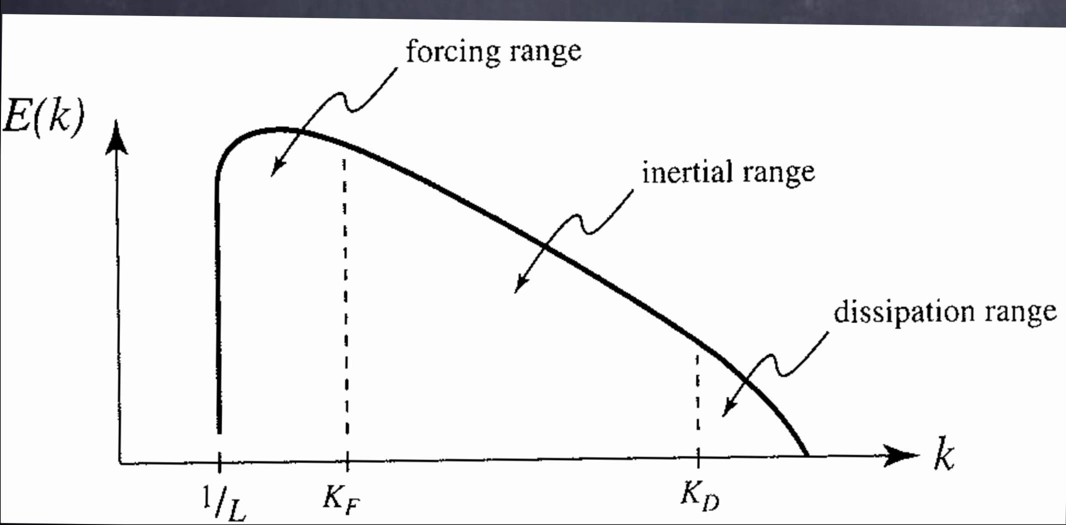

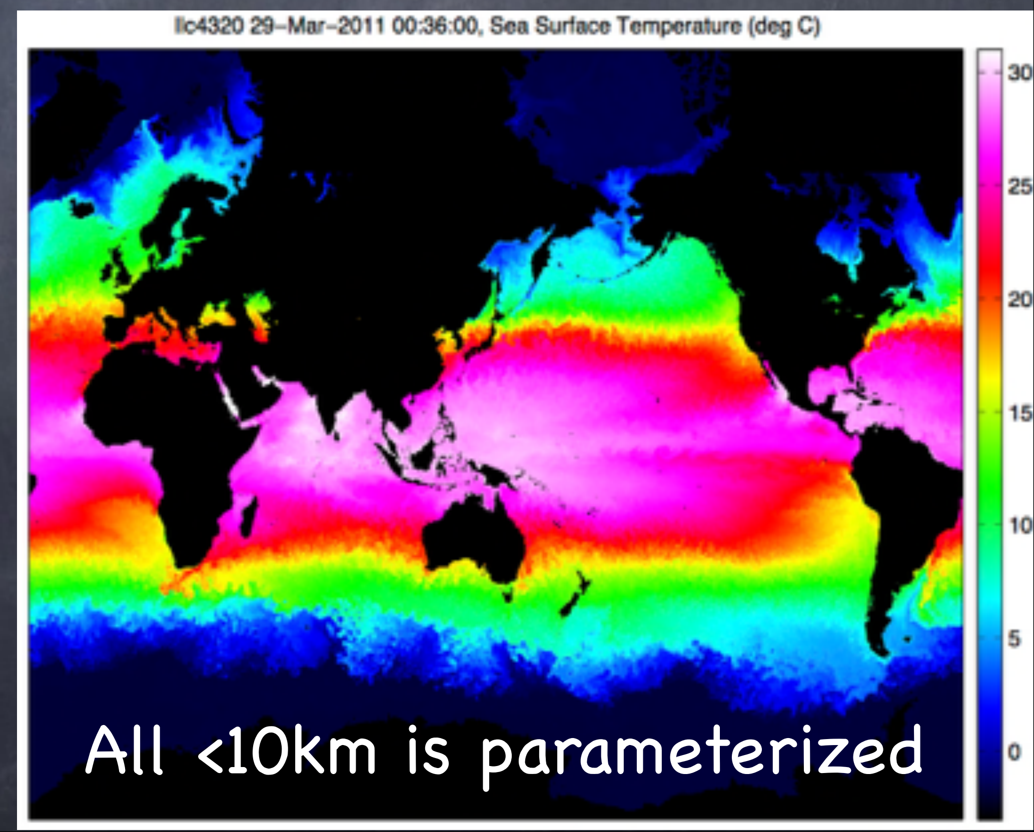

Air-Sea Flux Errors vs. Data

Heat capacity & mode of transport is different in A vs. O

>90% of GW is oceanic, 10m O=whole A

S. C. Bates, B. Fox-Kemper, S. R. Jayne, W. G. Large, S. Stevenson, and S. G. Yeager. Mean biases, variability, and trends in air-sea fluxes and SST in the CCSM4.Journal of Climate, 25(22):7781-7801, 2012.

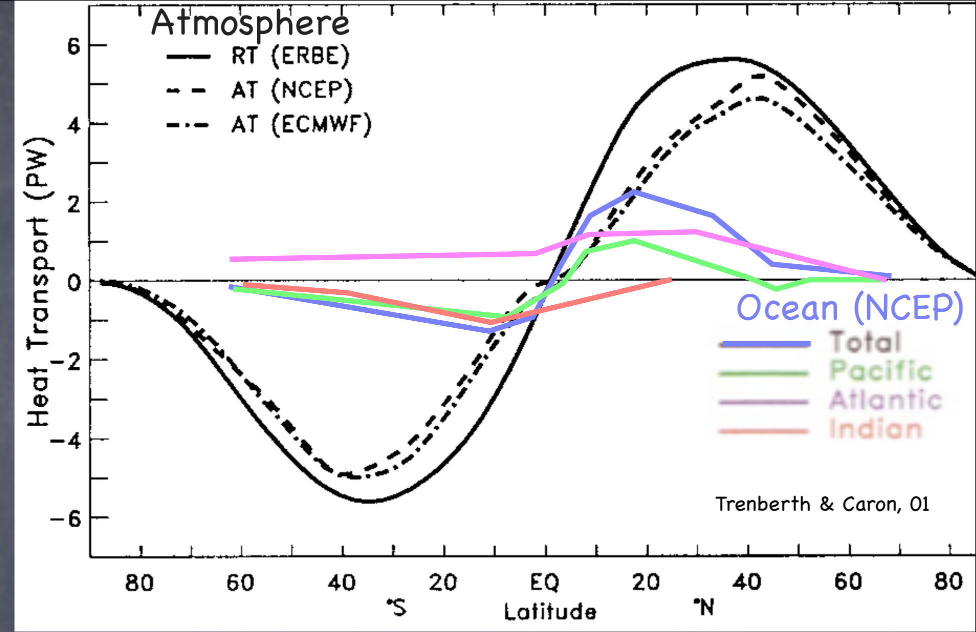

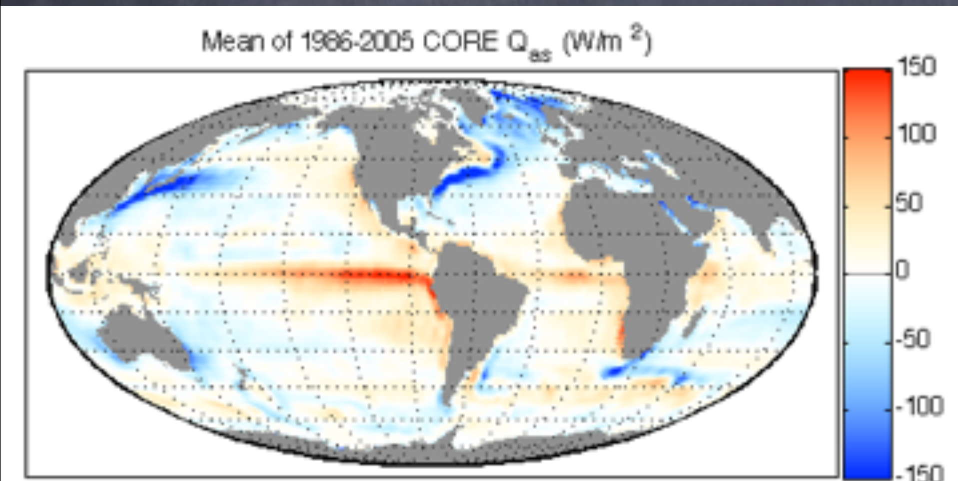

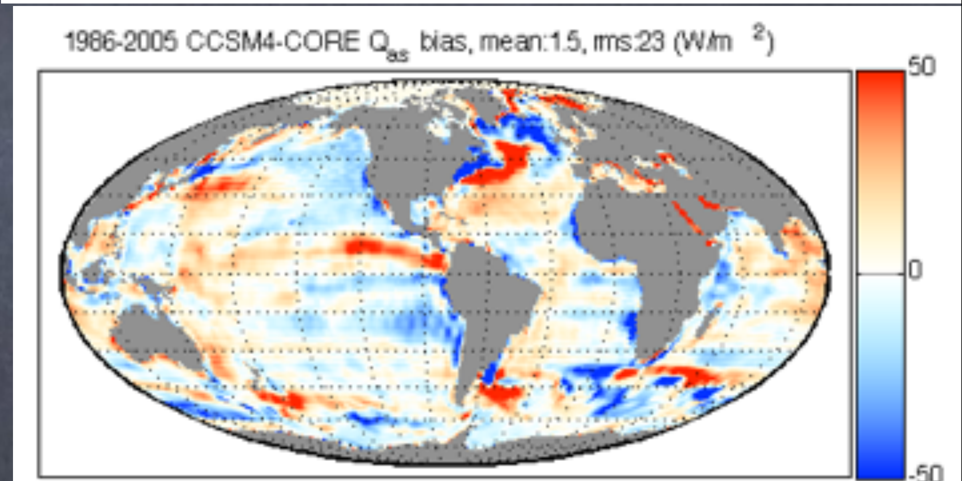

Mean

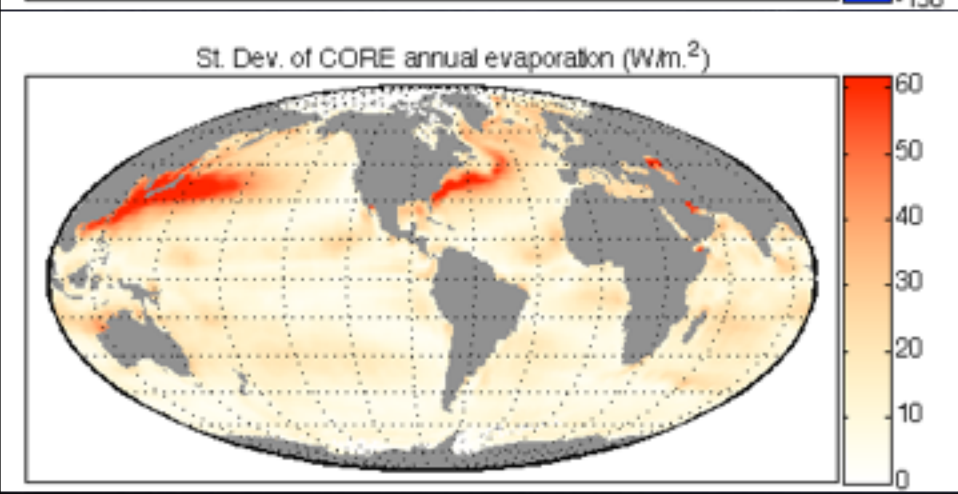

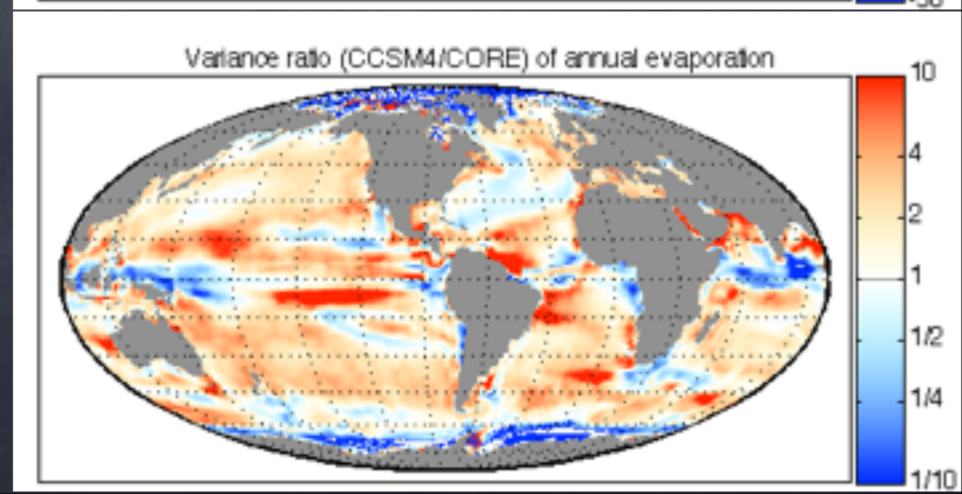

Annual 9-15mo

With nearly incompressible (small density variations) approximation & approximated rotating Earth:

A set of 5 vars

Summary of Boussinesq Equations

$$\frac{D?}{Dt} \equiv \frac{\partial ?}{\partial t} + \mathbf{v} \cdot \nabla ?$$

The simple Boussinesq equations are, for an inviscid fluid:

momentum equations:
$$\frac{\mathrm{D}\boldsymbol{v}}{\mathrm{D}t} + \boldsymbol{f} \times \boldsymbol{v} = -\nabla \phi + b\mathbf{k}, \quad \text{(B.1)}$$

mass conservation:
$$\nabla \cdot \boldsymbol{v} = 0, \quad \text{(B.2)}$$

buoyancy equation:
$$\frac{\mathrm{D}b}{\mathrm{D}t} = \dot{b}. \quad \text{(B.3)}$$

Vallis, 06

If you want, it's easy to distinguish buoyancy into contributions from Temperature and from Salinity

Don't blame me that they are inviscid—they are the vallis equations…

Geostrophy, Hydrostasy, & Thermal Wind

Traditional Oceanography & Resolved Flow in IPCC models inhabits a special distinguished limit:

Inviscid (Re>>1), rapidly rotating (Ro<<1), and thin* (L>>H)

Full Momentum

$$\frac{D\mathbf{v}}{Dt} + \mathbf{f} \times \mathbf{v} = -\nabla \phi + b\mathbf{k} + \nu \nabla^2 \mathbf{v}$$

$$Re = \frac{UL}{\nu} \qquad Ro = \frac{U}{fL} \qquad Ri = \frac{\frac{\partial b}{\partial z}}{\left(\frac{\partial U}{\partial z}\right)^2} \qquad \alpha = H/L$$

*closely related to strong statification & ocean dimensions

Geostrophy, Hydrostasy, & Thermal Wind

Traditional Oceanography & Resolved Flow in IPCC models
inhabits a special distinguished limit:
Inviscid (Re>>1), rapidly rotating (Ro<<1), and thin* (L>>H)

(Horizontal) Geostrophic Balance

$$\frac{D\mathbf{v}}{Dt} + \mathbf{f} \times \mathbf{v} = -\nabla\phi + b\mathbf{k} + \nu\nabla^2\mathbf{v}$$

$$Re = \frac{UL}{\nu} \qquad Ro = \frac{U}{fL} \qquad Ri = \frac{\frac{\partial b}{\partial z}}{\left(\frac{\partial U}{\partial z}\right)^2} \qquad \alpha = H/L$$

*closely related to strong statification & ocean dimensions

Geostrophy, Hydrostasy, & Thermal Wind

Traditional Oceanography & Resolved Flow in IPCC models inhabits a special distinguished limit:
Inviscid (Re>>1), rapidly rotating (Ro<<1), and thin* (L>>H)

(Vertical) Hydrostatic Balance

$$\frac{D\mathbf{v}}{Dt} + \mathbf{f} \times \mathbf{v} = -\nabla\phi + b\mathbf{k} + \nu\nabla^2\mathbf{v}$$

$$Re = \frac{UL}{\nu} \qquad Ro = \frac{U}{fL} \qquad Ri = \frac{\frac{\partial b}{\partial z}}{\left(\frac{\partial U}{\partial z}\right)^2} \qquad \alpha = H/L$$

*closely related to strong statification & ocean dimensions

Geostrophy, Hydrostasy, & Thermal Wind

Traditional Oceanography & Resolved Flow in IPCC models inhabits a special distinguished limit:

Inviscid (Re>>1), rapidly rotating (Ro<<1), and thin* (L>>H)

(Combined) Thermal Wind Balance

$$\mathbf{f} \times \frac{\partial \mathbf{v}}{\partial z} = -\nabla b$$

Taken together with the forcing (air-sea) of buoyancy and the advection of buoyancy by this flow--you have the tools to study large-scale ocean physics!

Dimensionless Boussinesq

Spanning Mesoscale to Stratified Turbulence

McWilliams (85)

$$Ro\left[v_{i,t}+v_jv_{i,j}\right]+\frac{M_{Ro}}{Ri}wv_{i,z}+\boxed{\epsilon_{izj}v_j=-M_{Ro}\pi_{,i}}+\frac{Ro}{Re}v_{i,jj}$$

$$\frac{\alpha^2}{Ri}\left[w_{,t}+v_jw_{,j}+\frac{M_{Ro}}{RoRi}ww_{,z}\right]=\boxed{-\pi_{,z}+b}+\frac{\alpha^2}{ReRi}w_{,jj}$$

$$b_t+v_jb_{,j}+\frac{M_{Ro}}{RoRi}wb_z+w=0$$

$$v_{j,j}+\frac{M_{Ro}}{RoRi}w_z=0$$

Plus boundary conditions

$$Re=\frac{UL}{\nu}\qquad Ro=\frac{U}{fL}\qquad Ri=\frac{N^2}{(U_{,z})^2}\qquad \alpha=H/L$$

$$M_{Ro}\equiv\max(1,Ro)\quad v=\text{horiz. vel.}\ \ w=\text{vert. vel.}$$

Let’s see some examples of
Bousinesq, Hydrostatic Models
at work in the
mesoscale (10-100km) &
submesoscale (100m-10km)

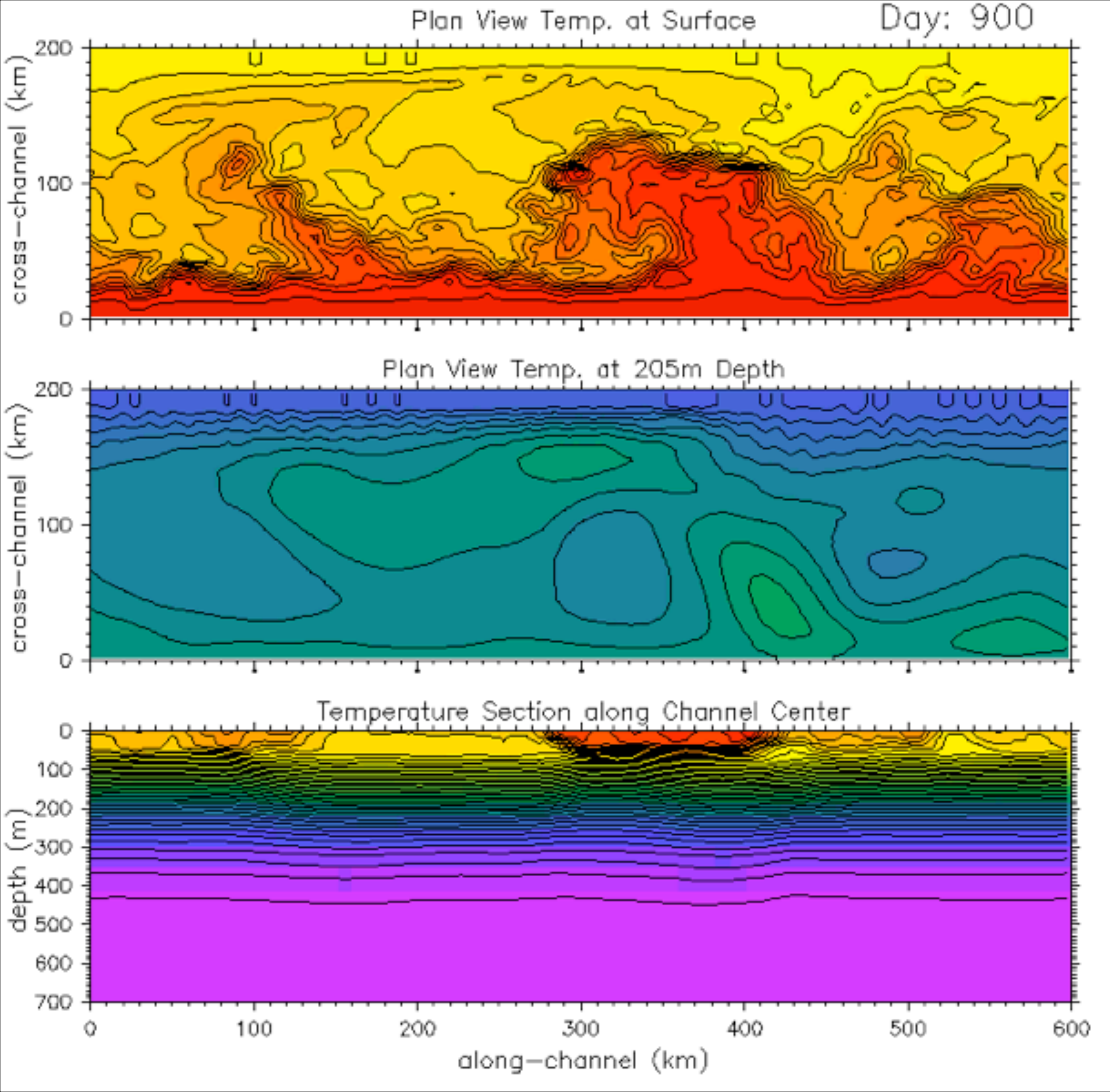

Big, Deep (mesoscale) w/ Little, Shallow (submeso)

Note mixed layer heat capacity!

B. Fox-Kemper, R. Ferrari, and R. W. Hallberg. Parameterization of mixed layer eddies. Part I: Theory and diagnosis. Journal of Physical Oceanography, 38(6):1145-1165, 2008.

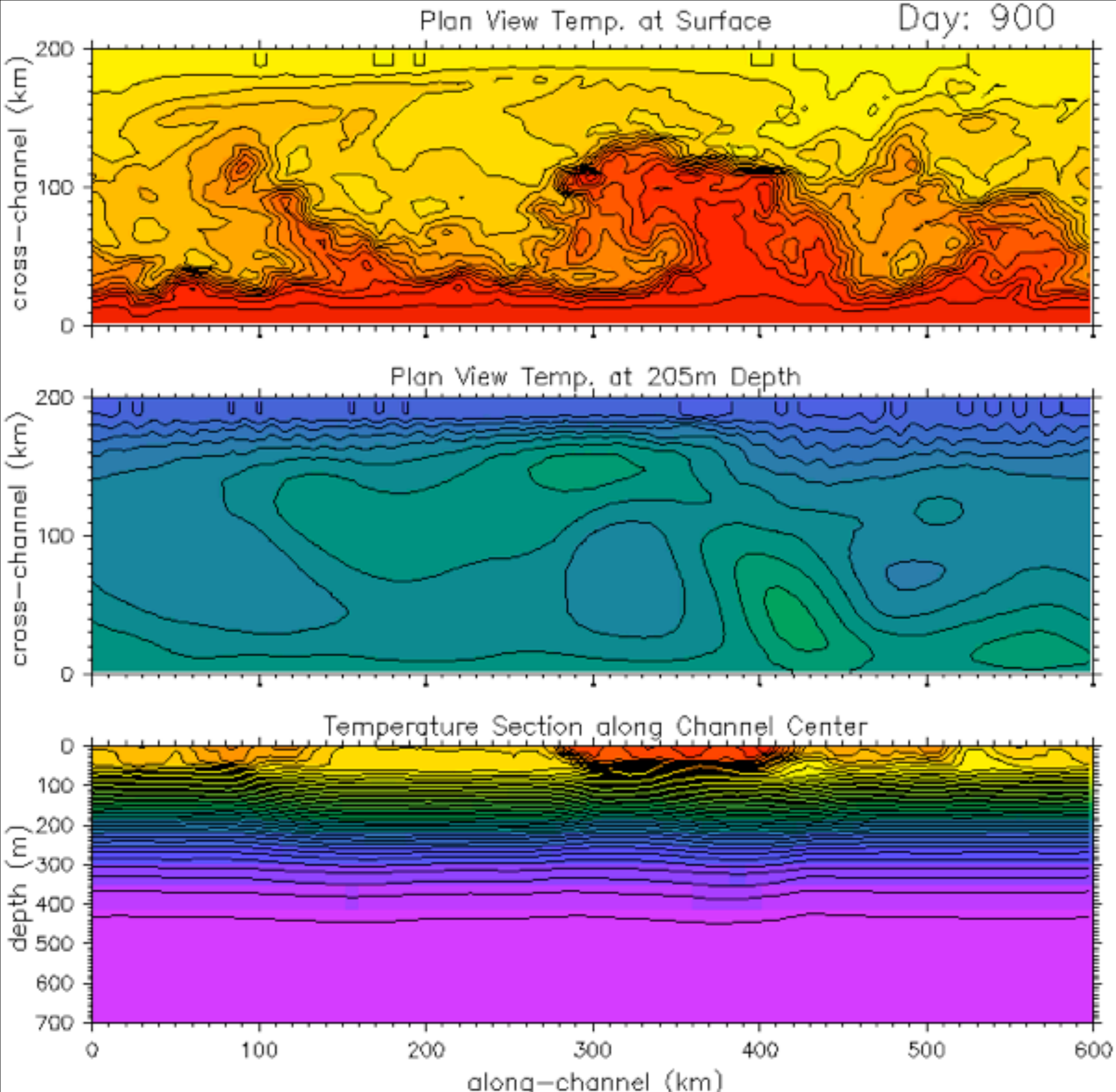

Big, Deep (mesoscale) w/ Little, Shallow (submeso)

Note mixed layer heat capacity!

B. Fox-Kemper, R. Ferrari, and R. W. Hallberg. Parameterization of mixed layer eddies. Part I: Theory and diagnosis. Journal of Physical Oceanography, 38(6):1145-1165, 2008.

The Character of the Mesoscale

100 km

(Capet et al., 2008)

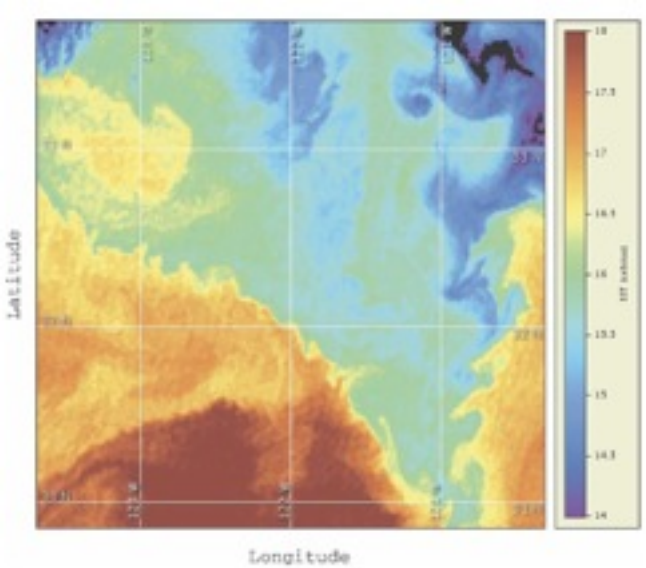

FIG. 16. Sea surface temperature measured at 1832 UTC 3 Jun 2006 off Point Conception in the California Current from CoastWatch (http://coastwatch.pfeg.noaa.gov). The fronts between recently upwelled water (i.e., 15°–16°C) and offshore water (≥17°C) show submesoscale instabilities with wavelengths around 30 km (right front) or 15 km (left front). Images for 1 day earlier and 4 days later show persistence of the instability events.

- Boundary Currents
- Eddies
- Ro=O(0.1)
- Ri=O(1000)
- Full Depth (4km)
- Eddies strain to produce Fronts
- 100km, months

(NASA GSFC Gallery)

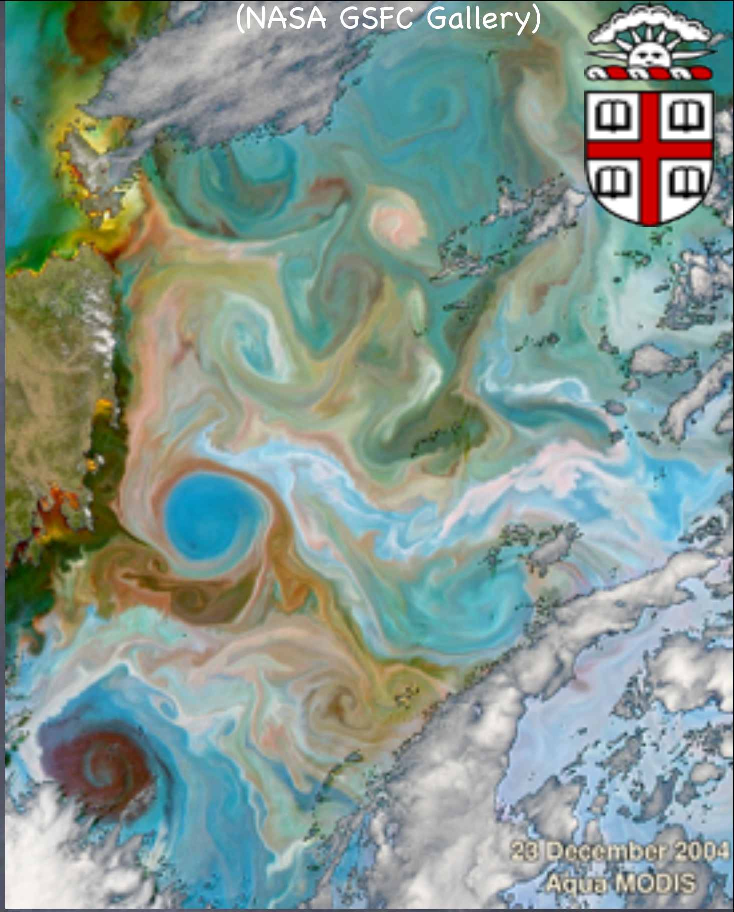

Eddy processes mainly baroclinic & barotropic instability. Parameterizations of baroclinic instability (GM, Visbeck...), will be routinely resolved in climate models in 2040

The Character of the Submesoscale

← 10 km

(NASA GSFC Gallery)

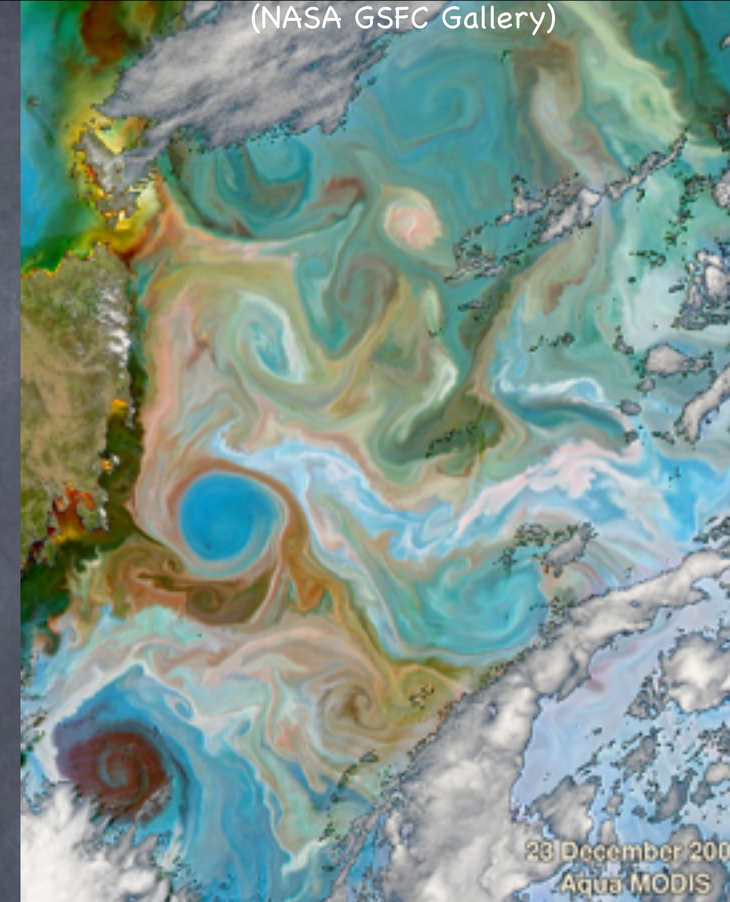

(Capet et al., 2008)

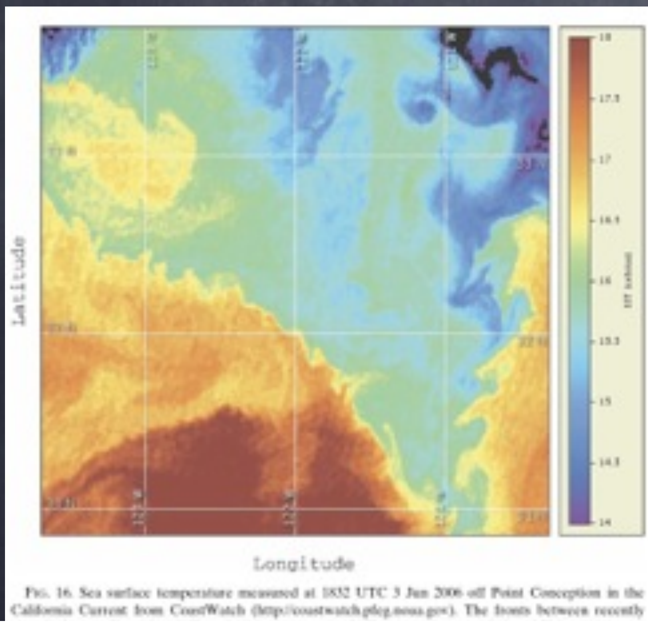

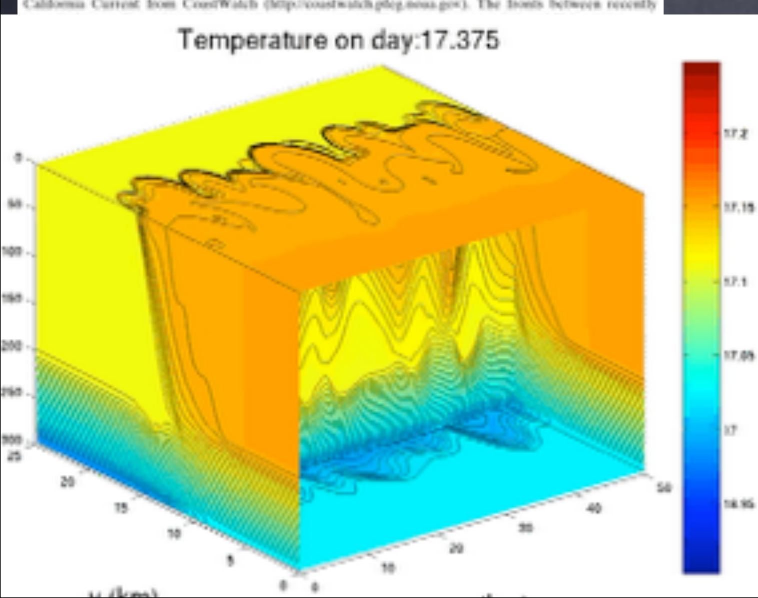

- Fronts
- Eddies
- Ro=O(1)
- Ri=O(1)
- near-surface (H=100m)
- 1-10km, days

Eddy processes often baroclinic instability

Parameterizations = F-K et al (08-11).

Routinely resolved in 2100

B. Fox-Kemper, R. Ferrari, and R. W. Hallberg. Parameterization of mixed layer eddies. Part I: Theory and diagnosis. Journal of Physical Oceanography, 38(6):1145-1165, 2008

S. Bachman and B. Fox-Kemper. Eddy parameterization challenge suite. I: Eady spindown. Ocean Modelling, 64:12-28, 2013

The Character of the Submesoscale

← 10 km

(Capet et al., 2008)

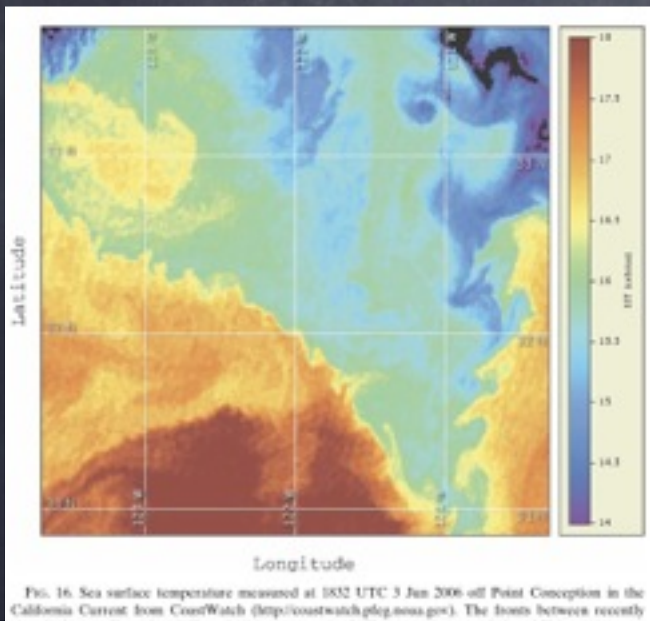

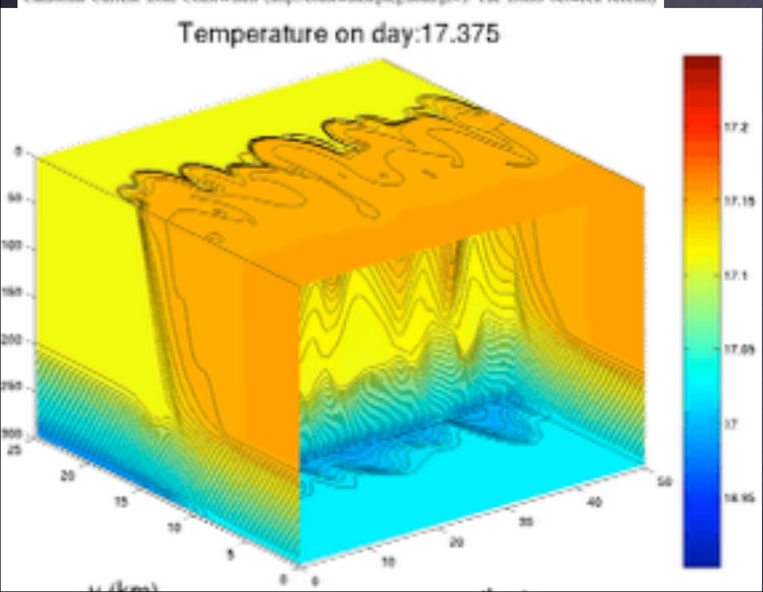

- Fronts
- Eddies
- Ro=O(1)
- Ri=O(1)
- near-surface (H=100m)
- 1-10km, days

Eddy processes often baroclinic instability

Parameterizations = F-K et al (08-11).

Routinely resolved in 2100

(NASA GSFC Gallery)

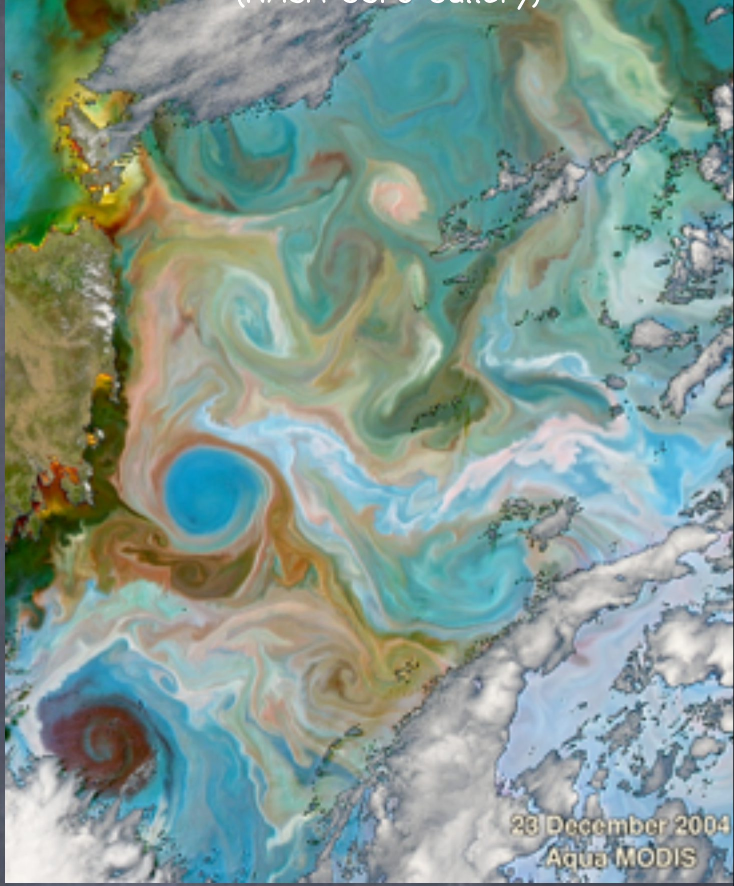

B. Fox-Kemper, R. Ferrari, and R. W. Hallberg. Parameterization of mixed layer eddies. Part I: Theory and diagnosis. Journal of Physical Oceanography, 38(6):1145-1165, 2008

S. Bachman and B. Fox-Kemper. Eddy parameterization challenge suite. I: Eady spindown. Ocean Modelling, 64:12-28, 2013

- We can study a small-scale system, derive parameterizations, and then use them to improve climate models & assess impact globally
  - This process often relies heavily on thermal wind scaling relationships
- But, what about the effects of things that aren't geostrophic & hydrostatic?
  - For example, waves and near-surface 3d turbulence

Surface Waves are...

fast, small, irrotational solutions of the Boussinesq Equations

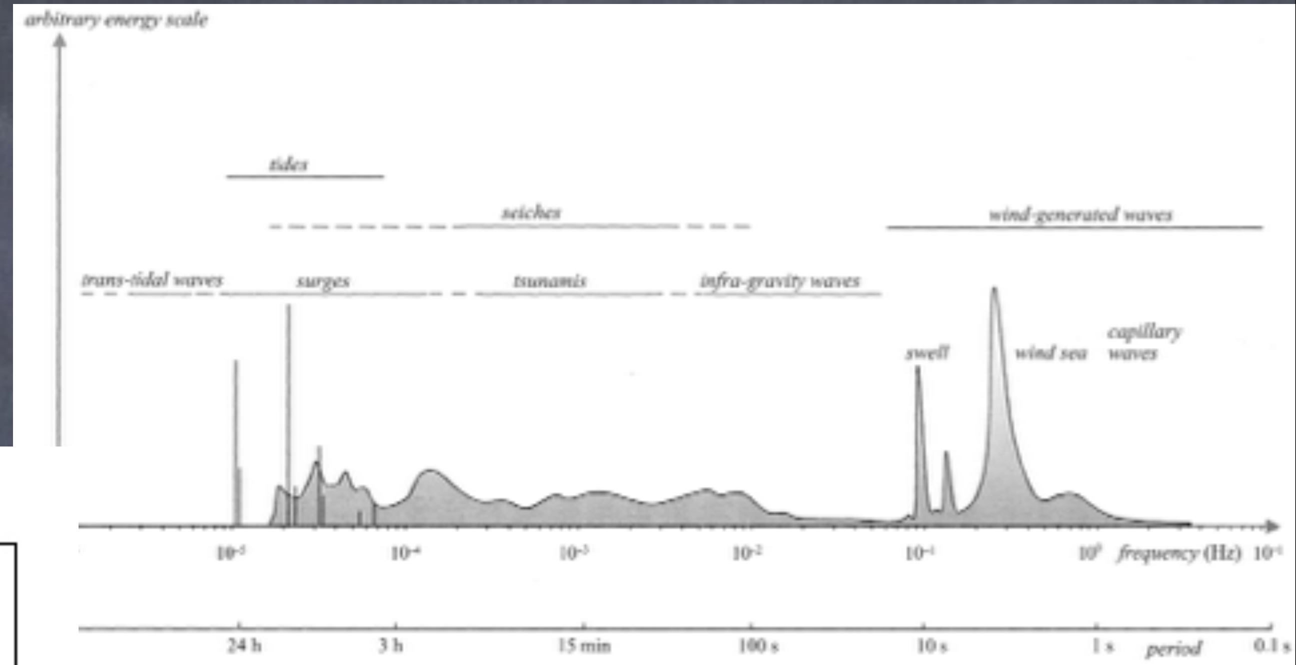

llustration of wave spectra from different types of ocean surface waves (Holthuijsen, 2007)

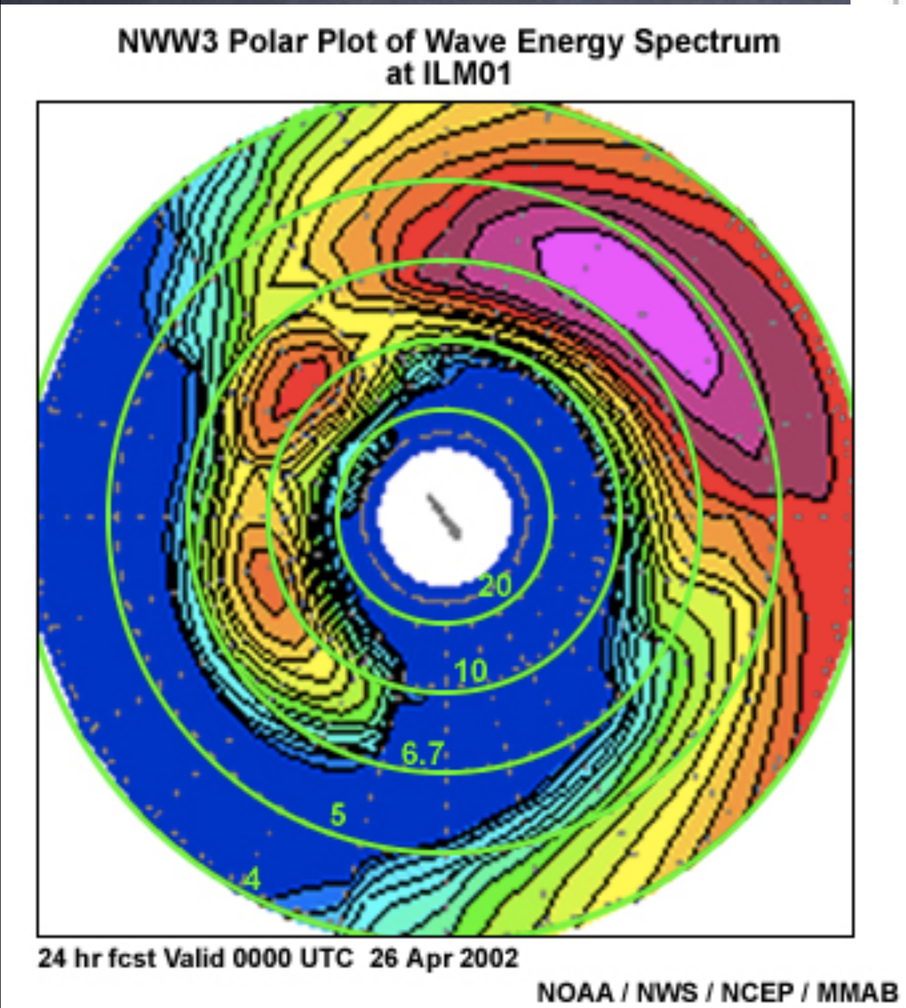

Surface Waves are...

fast, small, irrotational solutions of the Boussinesq Equations

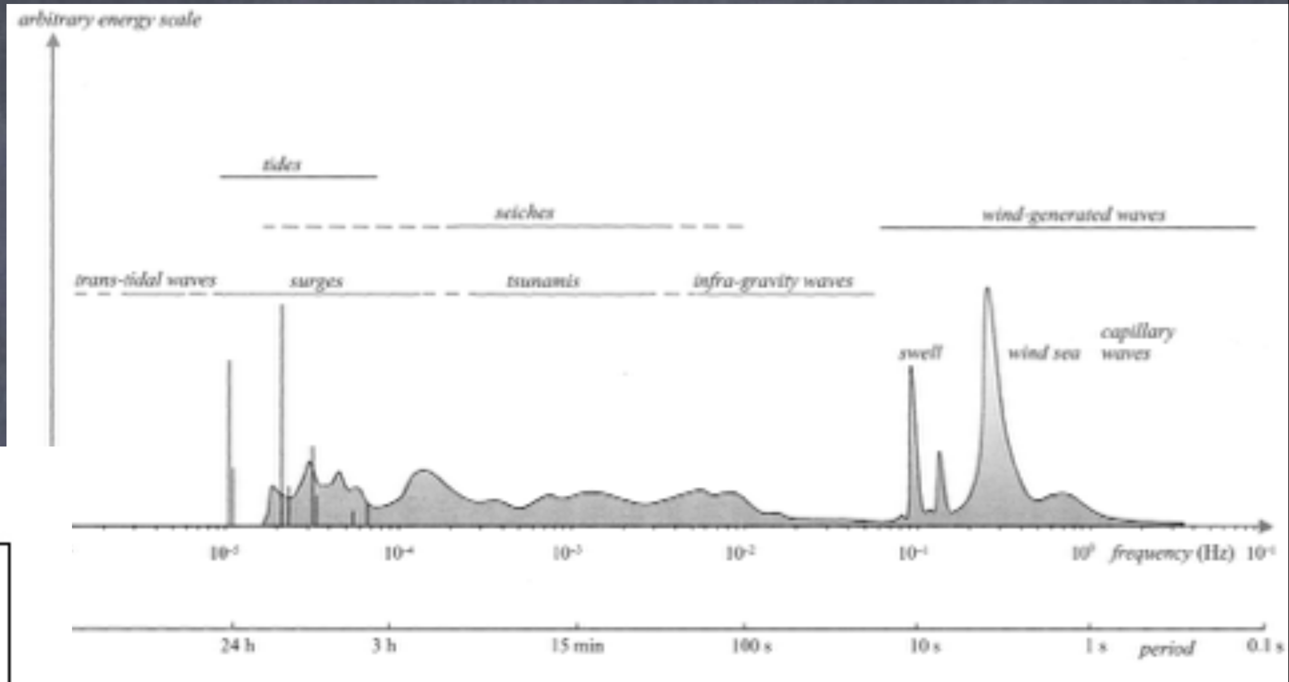

lustration of wave spectra from different types of ocean surface waves (Holthuijsen, 2007)

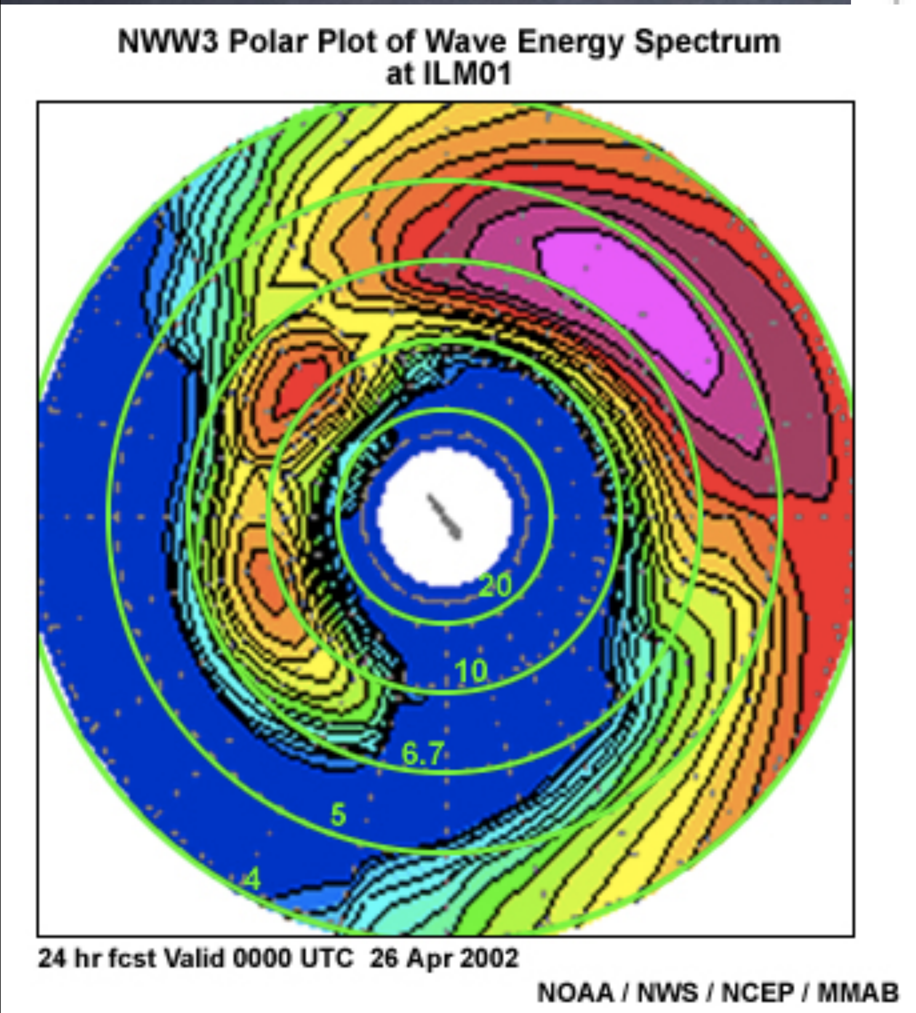

Craik-Leibovich Boussinesq Or Wave-Averaged Eqtns

- Formally a multiscale asymptotic equation set:
  - 3 classes: Small, Fast; Large, Fast; Large, Slow
  - Solve first 2 types of motion in the case of limited slope (ka), irrotational --> Deep Water Waves!
  - Average over deep water waves in space & time,
  - Arrive at Large, Slow equation set.

All Wave-Mean coupling terms involve the Stokes Drift

Craik & Leibovich 1976; Gjaja & Holm 1996; McWilliams *et al.* 2004

What is Stokes Drift?

Take wave solns, compare the velocity of trajectories vs. Eulerian velocity, Taylor Expand, calculate:

$$\boldsymbol{u}^L(\boldsymbol{x}_p(t_0),t) - \boldsymbol{u}^E(\boldsymbol{x}_p(t_0),t) \approx [\boldsymbol{x}_p(t) - \boldsymbol{x}_p(t_0)] \cdot \nabla \boldsymbol{u}^E(\boldsymbol{x}_p(t_0),t)$$
$$\approx \left[\int_{t_0}^{t} \boldsymbol{u}^E(\boldsymbol{x}_p(t_0),s')ds'\right] \cdot \nabla \boldsymbol{u}^E(\boldsymbol{x}_p(t_0),t)\,.$$

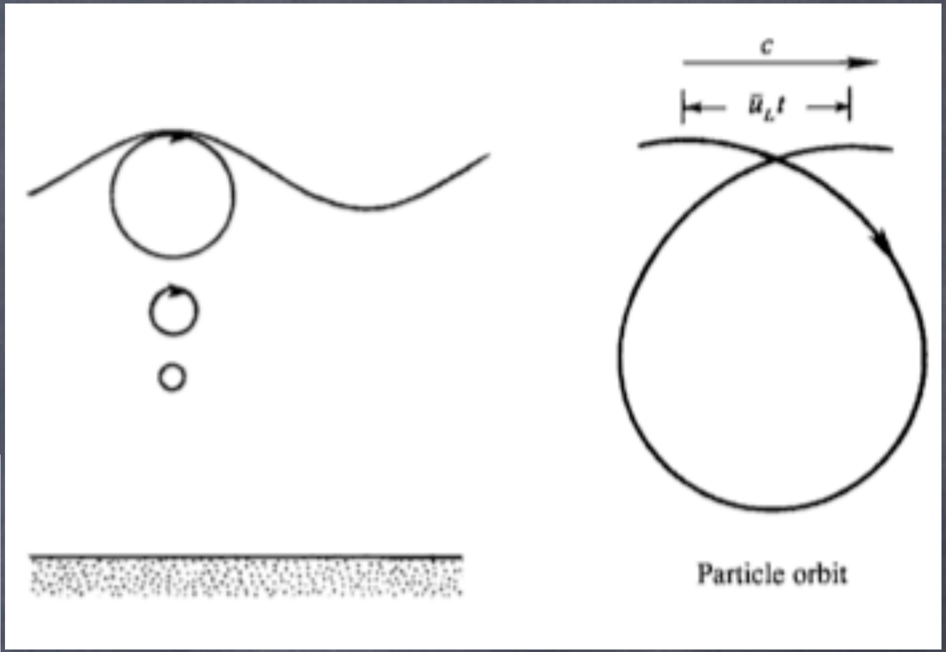

Examples:

Monochromatic: $$\boldsymbol{u}^S = \hat{\mathbf{e}}^{\mathrm{w}} \frac{8\pi^3 a^2 f_p^3}{g} e^{\frac{8\pi^2 f_p^2}{g} z} = \hat{\mathbf{e}}^{\mathrm{w}} a^2 \sqrt{g k^3} e^{2kz}.$$

Spectrum: $$\boldsymbol{u}^S = \frac{16\pi^3}{g} \int_0^\infty \int_{-\pi}^{\pi} (\cos\theta, \sin\theta, 0) f^3 S_{f\theta}(f,\theta) e^{\frac{8\pi^2 f^2}{g} z} d\theta df.$$

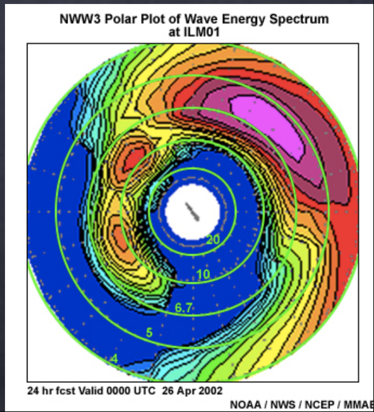

A. Webb and B. Fox-Kemper. Wave spectral moments and Stokes drift estimation. Ocean Modelling, 40(3-4):273-288, 2011.

Wave-Averaged Equations following McWilliams & F-K (13) and Suzuki & F-K (14)

$$\varepsilon = \frac{V^s H}{f L H_s}$$

(for horizontally uniform Stokes drift)

$$Ro\left[v_{i,t} + v_j^L v_{i,j}\right] + \frac{M_{Ro}}{Ri} w v_{i,z} + \epsilon_{izj} v_j^L = -M_{Ro}\pi_{,i} + \frac{Ro}{Re} v_{i,jj}$$

$$\frac{\alpha^2}{Ri}\left[w_{,y} + v_j^L w_{,j} + \frac{M_{Ro}}{RoRi}\right] = -\pi_{,z} + b + \boxed{\varepsilon v_j^L v_{j,z}^s} + \frac{\alpha^2}{ReRi} w_{,jj}$$

$$b_t + v_j^L b_{,j} + \frac{M_{Ro}}{RoRi} w b_z + w = 0$$

$$v_{j,j} + \frac{M_{Ro}}{RoRi} w_z = 0$$

Plus boundary conditions

LAGRANGIAN (Eulerian+Stokes) advection of Eulerian momentum

Coriolis Effect is on LAGRANGIAN velocity

Stokes Shear Force is NEW in vertical momentum equation.

The Character of the Langmuir Scale

- Near-surface
- Langmuir Cells & Langmuir Turb.
- Ro>>1
- Ri<1: Nonhydro
- 1-100m (H=L)
- 10s to 1hr
- w, u=O(10cm/s)
- Stokes drift
- Eqtns:Craik-Leibovich
- Params: McWilliams & Sullivan, 2000, Van Roekel et al. 2011
- Resolved routinely in 2170

image:
Thorpe, 04

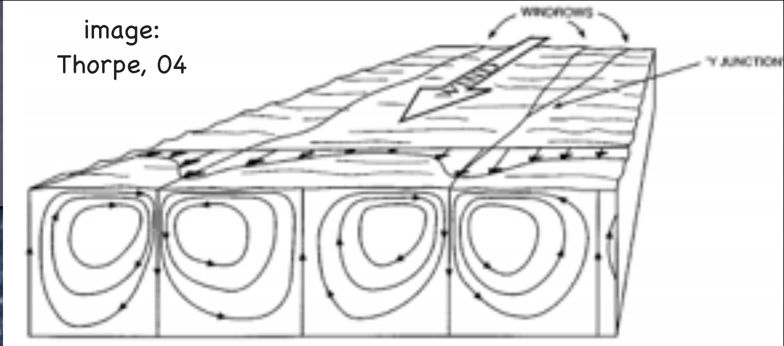

Figure 1 Sketch showing the pattern of mean flow in idealized Langmuir circulation. The windrows may be 2 m to 300 m apart, and the cell form is roughly square (as shown). In practice the flow is turbulent, especially near the water surface, and the windrows (Figure 2 amalgamate and meander in space and time. Bands of bubbles or buoyant algae may form within the downward-going (or downwelling) flow (see Figure 3).

Image: NPR.org, Deep Water Horizon Spill

Data + LES scaling, Southern Ocean mixing energy:

One way to estimate

So, waves can drive mixing via Stokes drift (combines with cooling & winds)

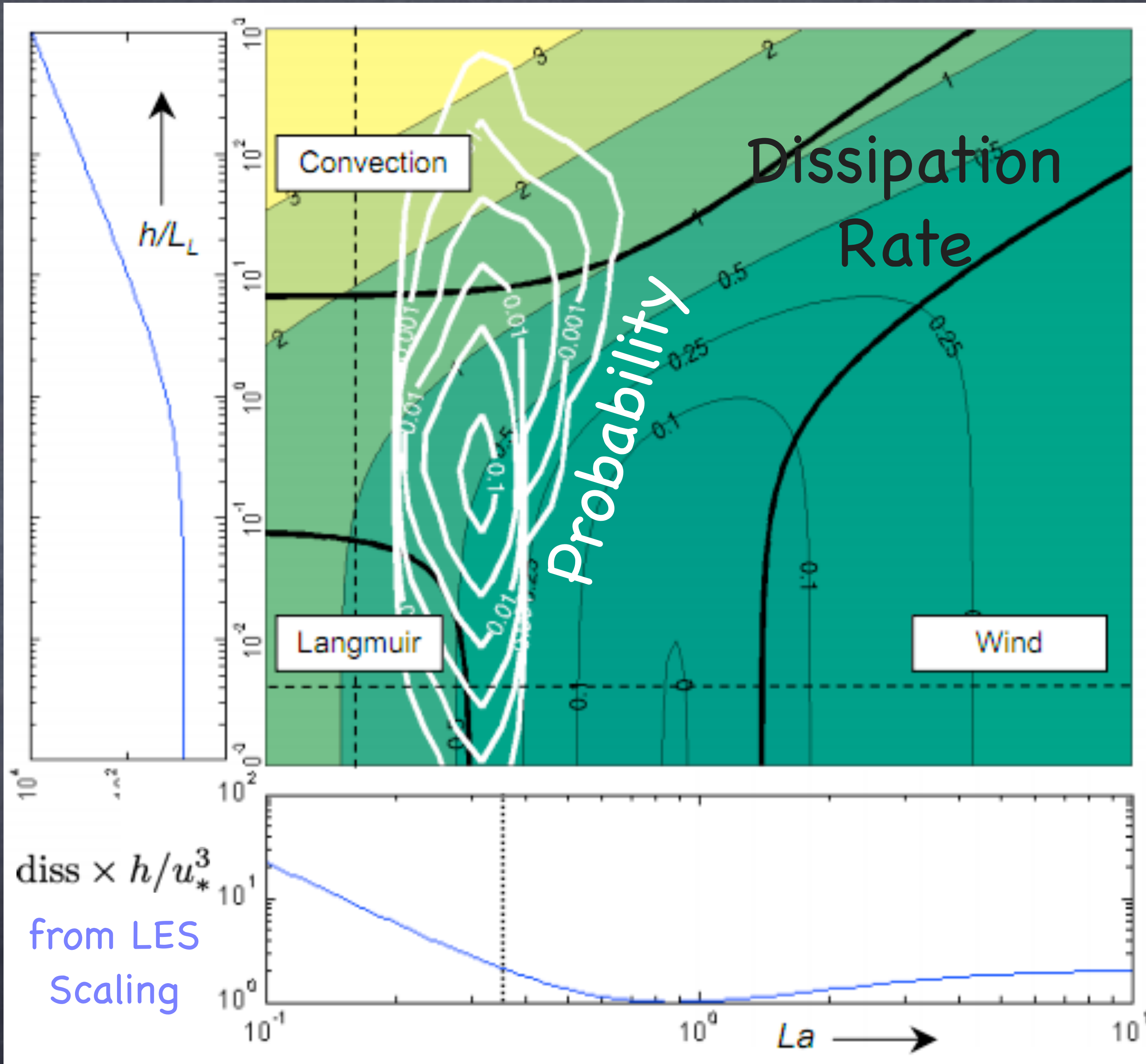

S. E. Belcher, A. A. L. M. Grant, K. E. Hanley, B. Fox-Kemper, L. Van Roekel, P. P. Sullivan, W. G. Large, A. Brown, A. Hines, D. Calvert, A. Rutgersson, H. Petterson, J. Bidlot, P. A. E. M. Janssen, and J. A. Polton. A global perspective on Langmuir turbulence in the ocean surface boundary layer. Geophysical Research Letters, 39(18):L18605, 9pp, 2012.

Data-driven offline parameterization:

Another way to estimate

Including Wave-driven Mixing (Harcourt 2013) Deepens the Mixed Layer!

E. A. D'Asaro, J. Thomson, A. Y. Shcherbina, R. R. Harcourt, M. F. Cronin, M. A. Hemer, and B. Fox-Kemper. Quantifying upper ocean turbulence driven by surface waves. Geophysical Research Letters, 41(1): 102-107, January 2014.

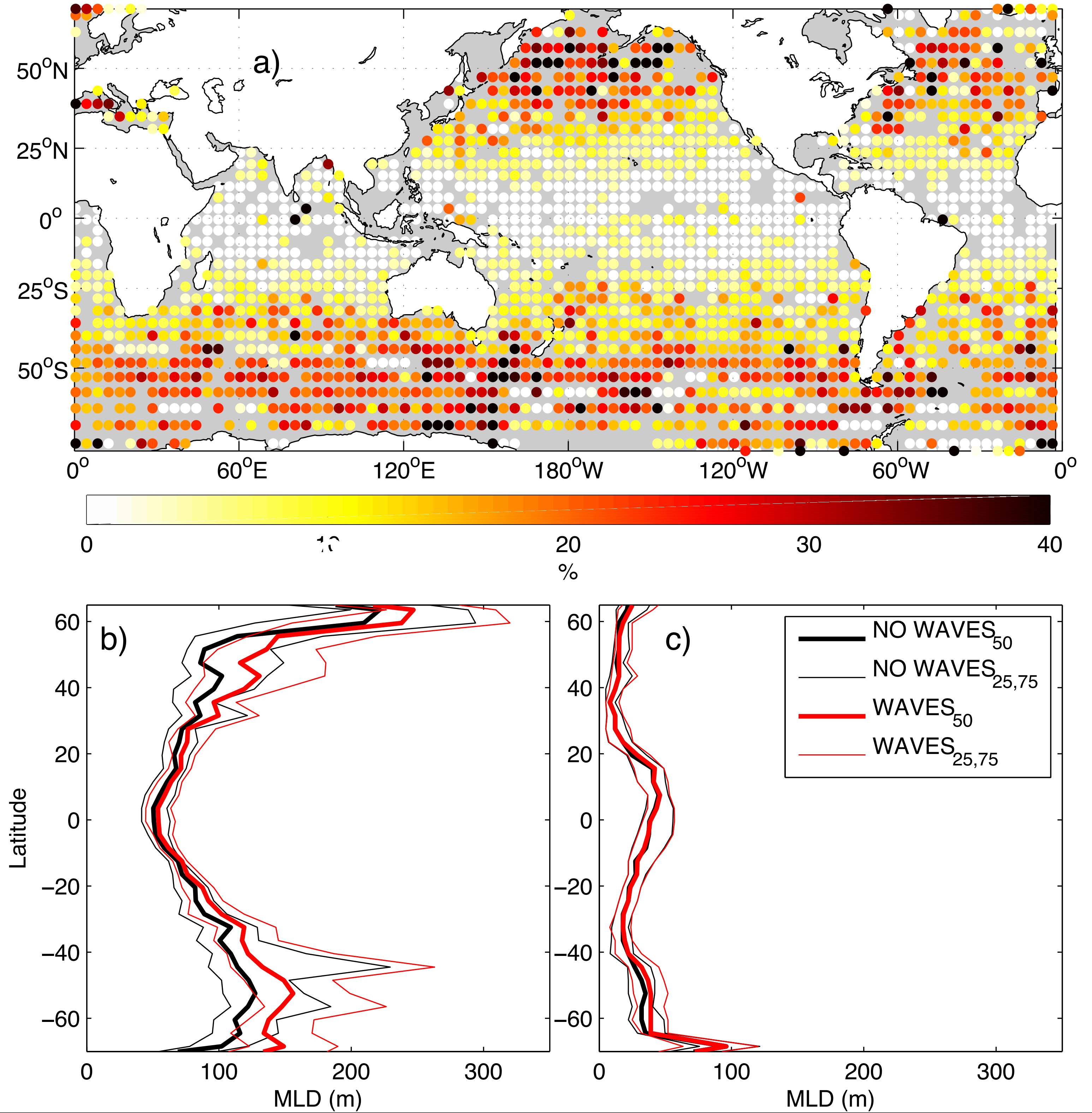

Parameterization in a climate model: Better estimate

Winter Waves in NCAR Community Earth System Model

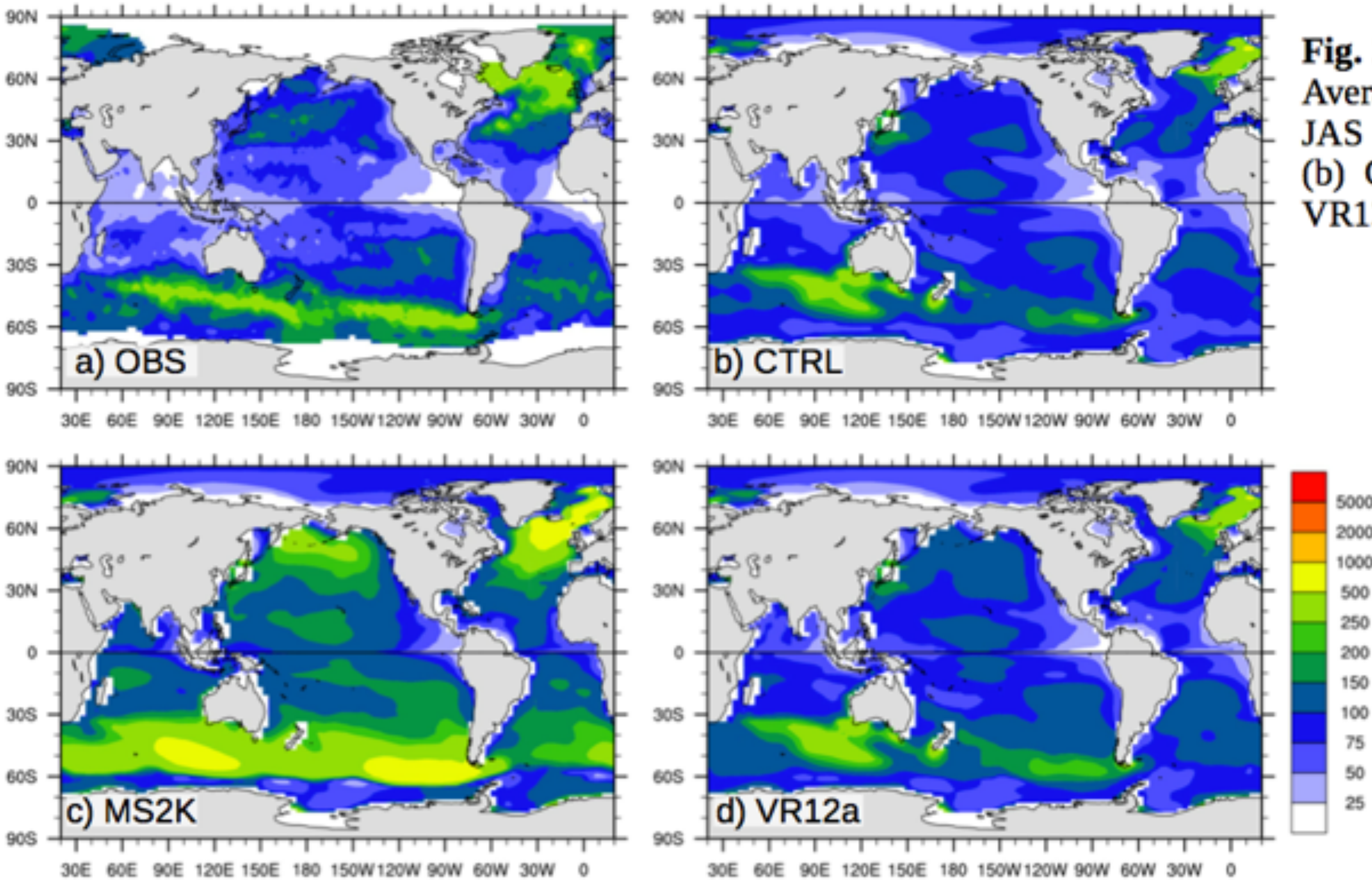

Fig. 2. Winter mean MLD (m; Averaged over JFM for NH and JAS for SH) for cases (a) OBS, (b) CTRL, (c) MS2K and (d) VR12a.

RMSE (m)

	Global	90°S-30°S
CTRL	59.57	63.46
MS2K	135.55	184.87
VR12a	54.86	53.93

Li et al., in prep.

L. P. Van Roekel, B. Fox-Kemper, P. P. Sullivan, P. E. Hamlington, and S. R. Haney. The form and orientation of Langmuir cells for misaligned winds and waves. Journal of Geophysical Research-Oceans, 117:C05001, 22pp, 2012.

Summer Waves in NCAR Community Earth System Model

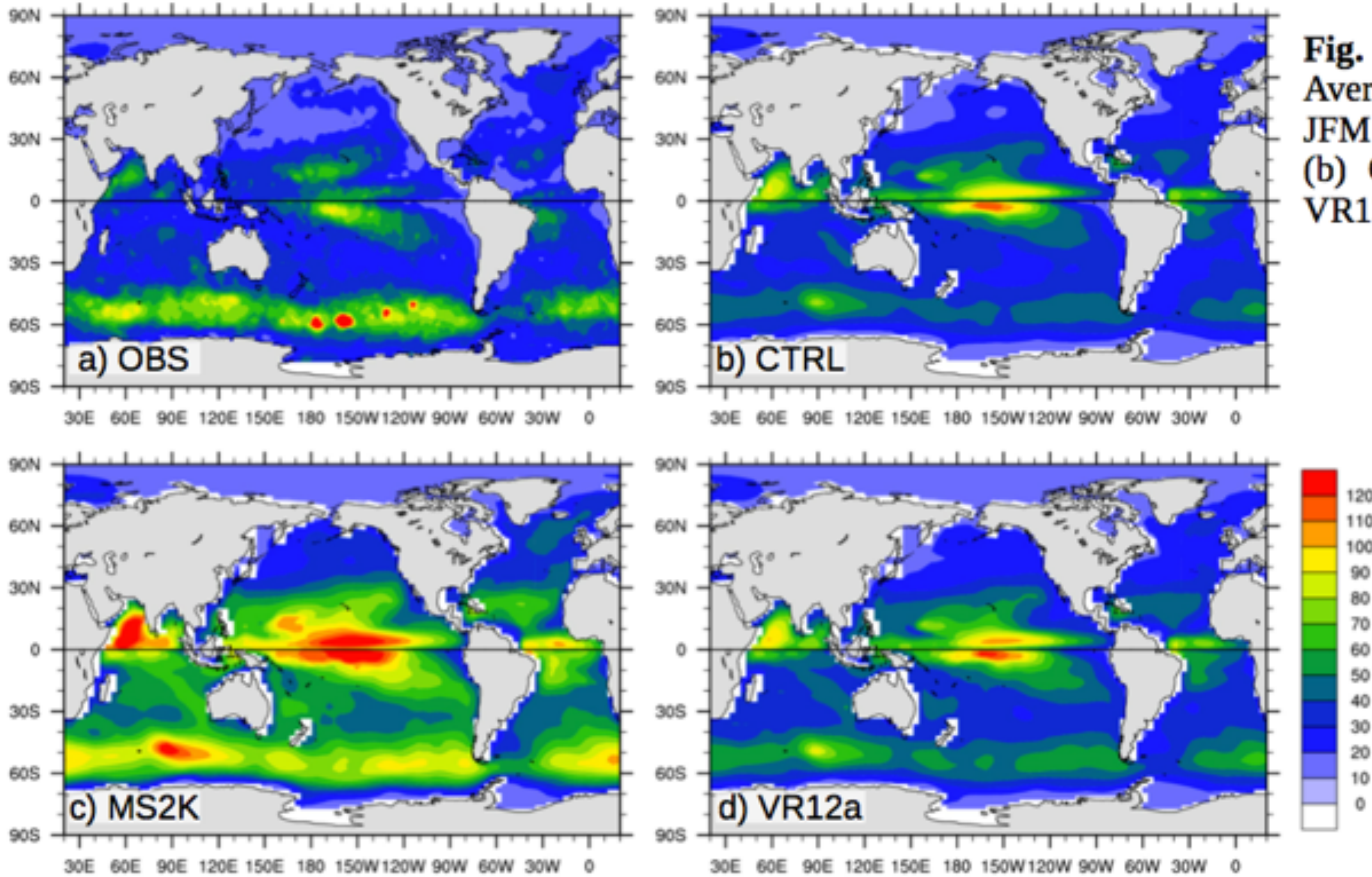

Fig. 1. Summer mean MLD (m; Averaged over JAS for NH and JFM for SH) for cases (a) OBS, (b) CTRL, (c) MS2K and (d) VR12a.

RMSE (m)

	Global	90°S-30°S
CTRL	14.94	20.53
MS2K	25.95	20.56
VR12a	14.92	16.67

Li et al., in prep.

L. P. Van Roekel, B. Fox-Kemper, P. P. Sullivan, P. E. Hamlington, and S. R. Haney. The form and orientation of Langmuir cells for misaligned winds and waves. Journal of Geophysical Research-Oceans, 117:C05001, 22pp, 2012.

Multi-Model Ensemble: Best Estimate

- Results similar in pattern and magnitude to ours (in NCAR CESM) were found by Fan & Griffies (2014) using the NOAA Geophysical Fluid Dynamics Laboratory CM2M model.

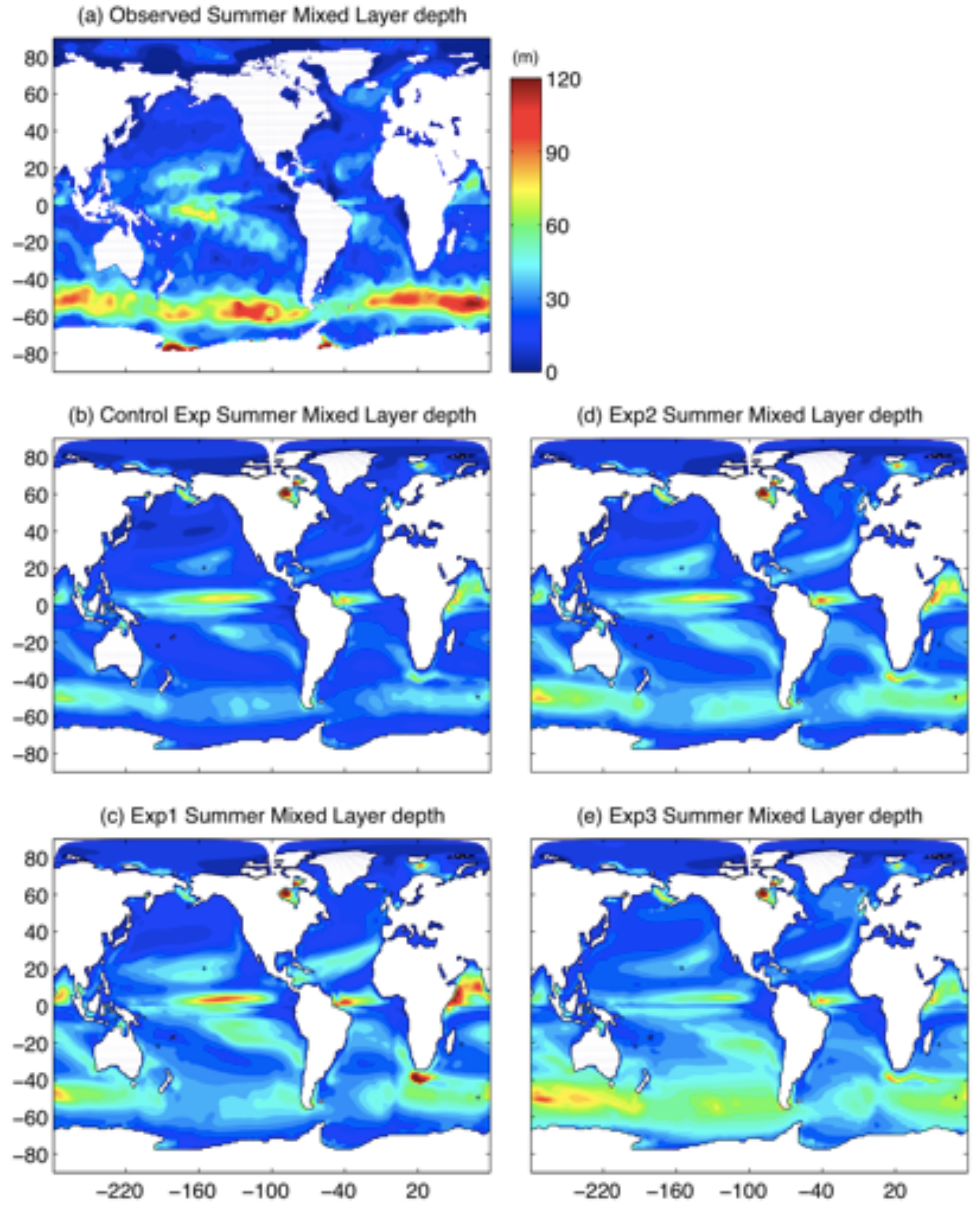

Figure 3. Summer mean (July – September and January – March averages in the Northern and Southern Hemispheres, respectively) mixed layer depth from (a) observational estimate based on world ocean atlas data obtained from the national oceanographic data center (http://data.nodc.noaa.gov/woa/WOA09/), and the (b) Control, (c) Exp1, (d) Exp2, and (e) Exp3 experiments.

Wave-Averaged Equations following McWilliams & F-K (13) and Suzuki & F-K (14)

$$\varepsilon = \frac{V^s H}{f L H_s}$$

(for horizontally uniform Stokes drift)

$$Ro\left[v_{i,t} + v_j^L v_{i,j}\right] + \frac{M_{Ro}}{Ri} w v_{i,z} + \epsilon_{izj} v_j^L = -M_{Ro}\pi_{,i} + \frac{Ro}{Re} v_{i,jj}$$

$$\frac{\alpha^2}{Ri}\left[w_{,y} + v_j^L w_{,j} + \frac{M_{Ro}}{RoRi}\right] = -\pi_{,z} + b + \boxed{\varepsilon v_j^L v_{j,z}^s} + \frac{\alpha^2}{ReRi} w_{,jj}$$

$$b_t + v_j^L b_{,j} + \frac{M_{Ro}}{RoRi} w b_z + w = 0$$

$$v_{j,j} + \frac{M_{Ro}}{RoRi} w_z = 0$$

Plus boundary conditions

LAGRANGIAN advection of Eulerian momentum

Coriolis Effect is on LAGRANGIAN velocity

Stokes Shear force is NEW in vertical momentum equation.

J. C. McWilliams and B. F-K. Oceanic wave-balanced surface fronts and filaments. Journal of Fluid Mechanics, 730:464-490, 2013.

So, Waves can Drive turbulence that affect larger scales indirectly:

What about direct effects of waves on larger scales?

(Combined) Lagrangian Thermal Wind Balance

$$\mathbf{f} \times \frac{\partial}{\partial z}(\mathbf{v} + \mathbf{v}_s) = \mathbf{f} \times \frac{\partial \mathbf{v}_L}{\partial z} = -\nabla b$$

Now the temperature gradients govern the Lagrangian flow, not the not the Eulerian!

J. C. McWilliams and B. F-K. Oceanic wave-balanced surface fronts and filaments. Journal of Fluid Mechanics, 730:464-490, 2013.

Estimated importance of Stokes vortex on (sub)mesoscale: McWilliams & F-K (13)

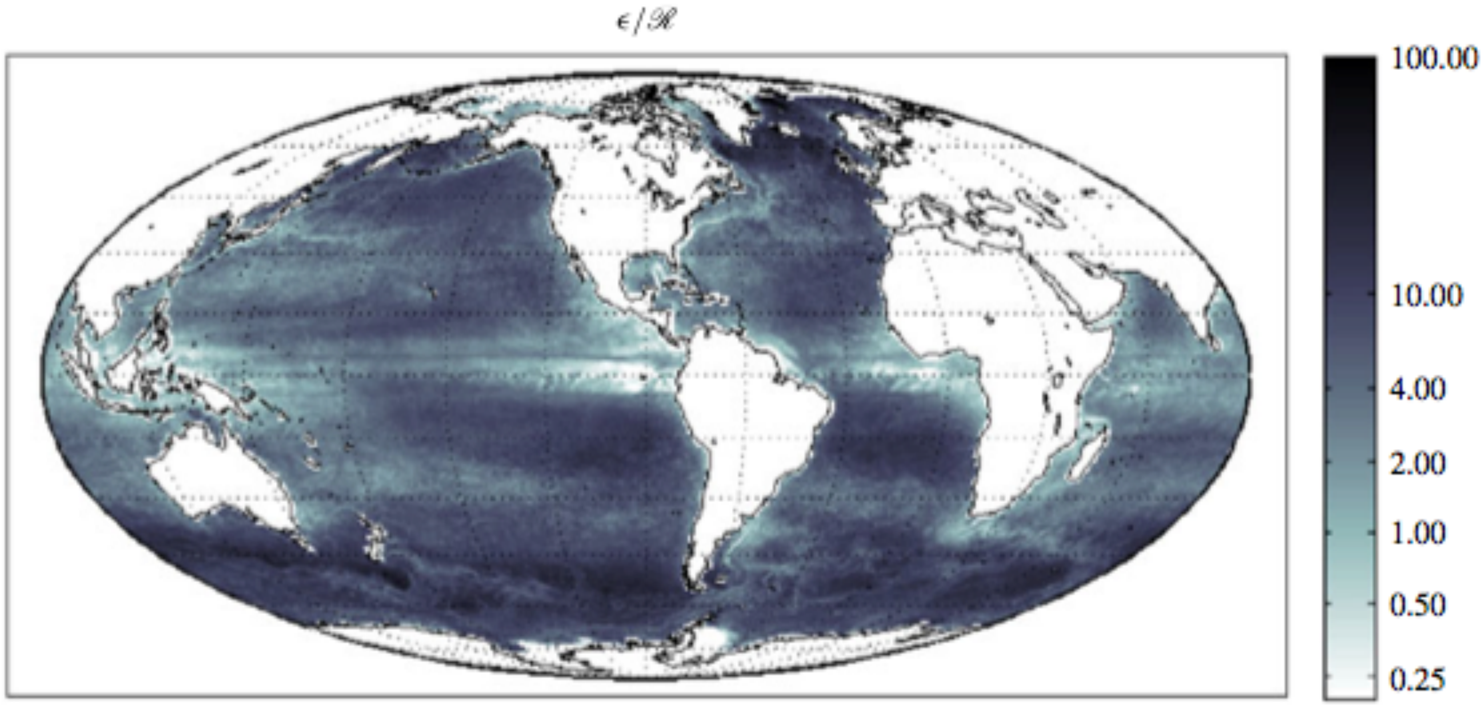

FIGURE 1. (Colour online) Estimated ratio $\epsilon/\mathscr{R} \approx (|\boldsymbol{u}_s \cdot \boldsymbol{u}|h)/(|\boldsymbol{u}|^2 h_s)$ governing the relative importance of Stokes effects versus nonlinearity. Eulerian velocity ($\boldsymbol{u}$) is taken as the AVISO weekly satellite geostrophic velocity or $-\boldsymbol{u}_s$ (for anti-Stokes flow) if $|\boldsymbol{u}_s| > |\boldsymbol{u}|$. The front/filament depth (h) is estimated as the mixed layer depth from the de Boyer Montégut *et al.* (2004) climatology. An exponential fit to the Stokes drift of the upper 9 m projected onto the AVISO geostrophic velocity provides $\boldsymbol{u}_s \cdot \boldsymbol{u}$ and h_s. Stokes drift is taken from the Wave Watch 3 simulation described in Webb & Fox-Kemper (2011). $\boldsymbol{u}$, $\boldsymbol{u}_s$, and h_s are all for the year 2000, while h is from a climatology of observations over 1961–2008. The year 2000 average of $\epsilon/\mathscr{R}$ is shown.

$$\varepsilon = \frac{V^s H}{f L H_s}$$

$$Ro = \frac{U}{f L}$$

J. C. McWilliams and B. F-K. Oceanic wave-balanced surface fronts and filaments. Journal of Fluid Mechanics, 730:464-490, 2013.

Wave-Averaged Equations following McWilliams & F-K (13) and Suzuki & F-K (14)

$$\varepsilon = \frac{V^s H}{f L H_s}$$

(for horizontally uniform Stokes drift)

$$Ro\left[v_{i,t} + v_j^L v_{i,j}\right] + \frac{M_{Ro}}{Ri} w v_{i,z} + \epsilon_{izj} v_j^L = -M_{Ro}\pi_{,i} + \frac{Ro}{Re} v_{i,jj}$$

$$\frac{\alpha^2}{Ri}\left[w_{,y} + v_j^L w_{,j} + \frac{M_{Ro}}{RoRi}\right] = -\pi_{,z} + b + \boxed{\varepsilon v_j^L v_{j,z}^s} + \frac{\alpha^2}{ReRi} w_{,jj}$$

$$b_t + v_j^L b_{,j} + \frac{M_{Ro}}{RoRi} w b_z + w = 0$$

$$v_{j,j} + \frac{M_{Ro}}{RoRi} w_z = 0$$

Plus boundary conditions

LAGRANGIAN advection of Eulerian momentum

Coriolis Effect is on LAGRANGIAN velocity

Stokes Shear force is NEW in vertical momentum equation.

J. C. McWilliams and B. F-K. Oceanic wave-balanced surface fronts and filaments. Journal of Fluid Mechanics, 730:464-490, 2013.

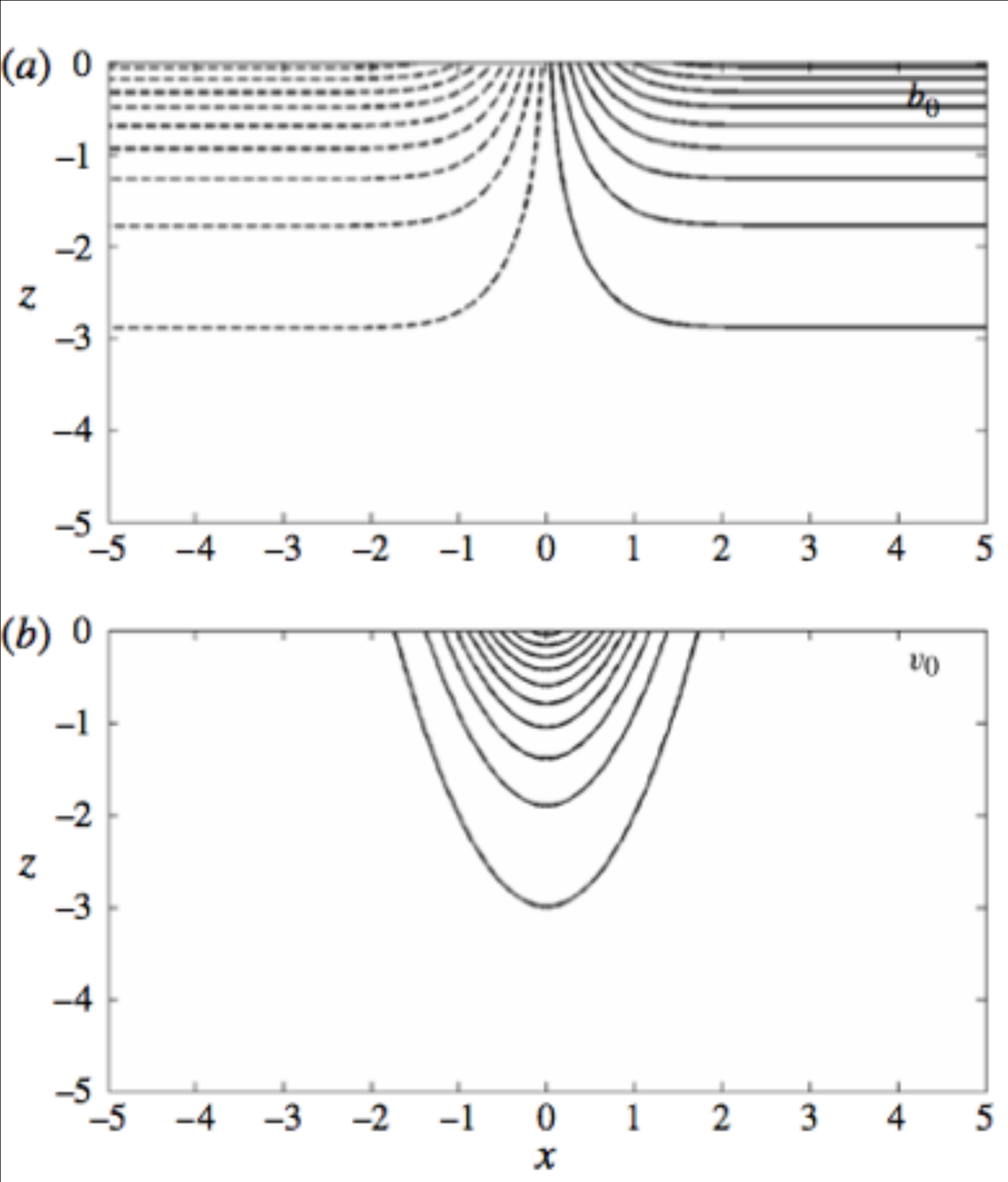

1) Consider a plane parallel balanced flow with b(y,z), q(y,z)
2) Perturb this flow by introducing Stokes forces (turn on waves)
3) Adiabatically rearrange the b(y,z) and q(y,z) until new forces are balanced
4) This solution amounts to solving for b′ and v′ in:

$$\partial_x^2 b' + \partial_z^2 \left(\frac{b'}{N^2}\right) = \mathscr{F}' + \partial_z \left(\frac{\epsilon \mathscr{Q}'}{N^2}\right) - \partial_x \epsilon \mathscr{P}'$$

$$v' = -\int_{-\infty}^{x} \left[\partial_z \left(\frac{b'}{N^2}\right) + \frac{S_s}{N^2} \partial_z v_0 + \epsilon S_s \frac{\partial_x b'}{N^2}\right] \mathrm{d}x'.$$

Waves (Stokes Drift Vortex Force) -> Submeso, Meso, an example for $\varepsilon \ll 1$ near the "sweet spot"

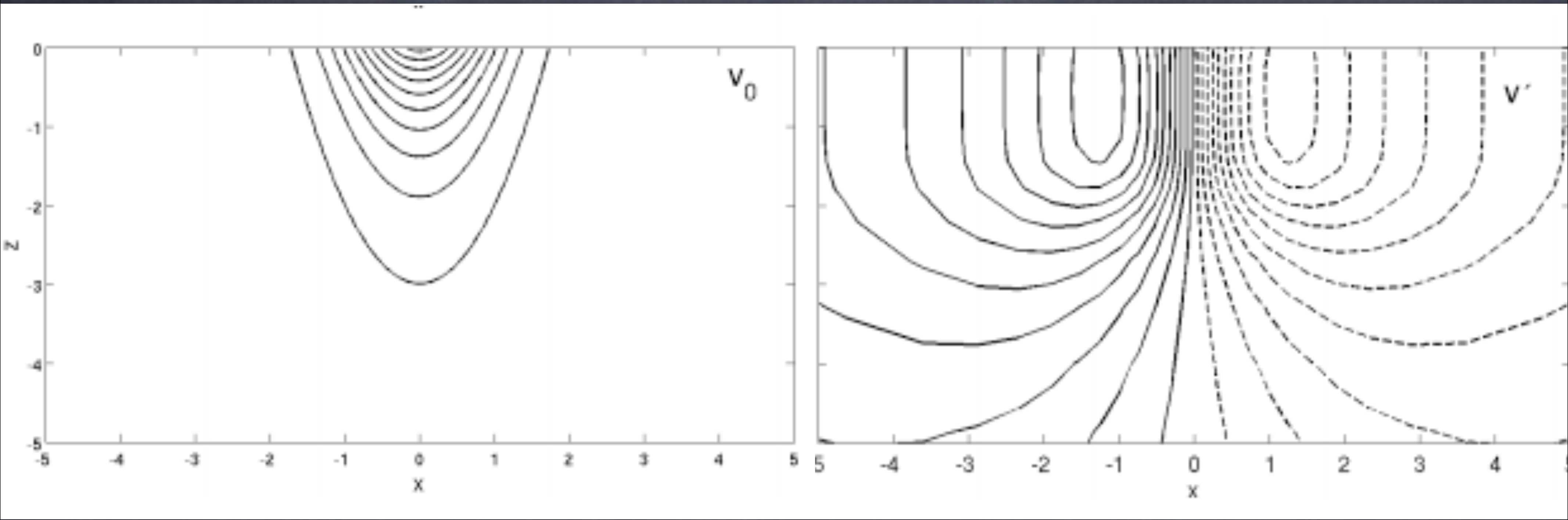

Initial Submeso Front

Max: 1

Perturbation on that scale due to waves

Max: 7.1ε

J. C. McWilliams and B. F-K. Oceanic wave-balanced surface fronts and filaments. Journal of Fluid Mechanics, 730:464-490, 2013.

Waves (Stokes Drift Vortex Force) -> Submeso, Meso, an example for finite waves

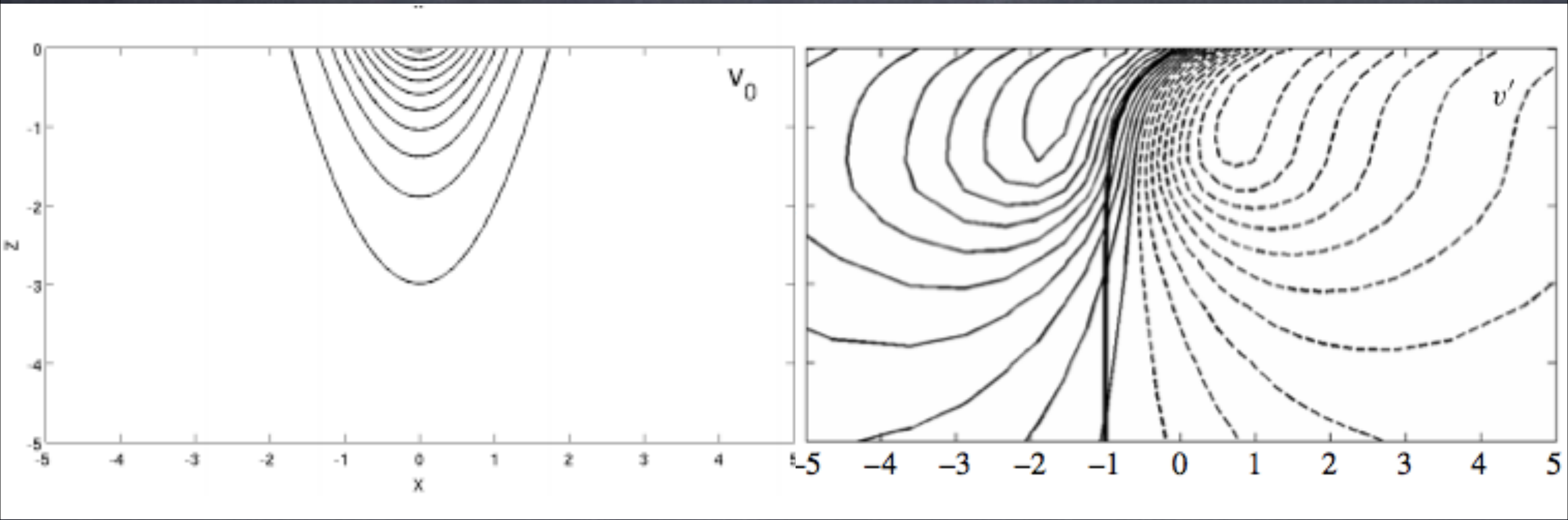

Initial Submeso Front

Max: 1

Perturbation on that scale due to waves

Max: $6.8\varepsilon = 13.6$

J. C. McWilliams and B. F-K. Oceanic wave-balanced surface fronts and filaments. Journal of Fluid Mechanics, 730:464-490, 2013.

LES of Langmuir-Submeso Interactions?

Perform large eddy simulations (LES) of Langmuir turbulence with a submesoscale temperature front

Use NCAR LES model to solve Craik-Leibovich equations (Moeng, 1984, McWilliams et al, 1997)

$$\frac{\partial \rho}{\partial t} + \mathbf{u}_L \cdot \nabla \rho = \mathrm{SGS} \qquad \nabla \cdot \mathbf{u} = 0$$

$$\frac{\partial \mathbf{u}}{\partial t} + (\boldsymbol{\omega} + f\hat{\mathbf{z}}) \times \mathbf{u}_L = -\nabla \pi - \frac{g\rho\hat{\mathbf{z}}}{\rho_0} + \mathrm{SGS}$$

Computational parameters:

Domain size: 20km x 20km x -160m

Grid points: 4096 x 4096 x 128

Resolution: 5m x 5m x -1.25m

1000x more gridpoints than CESM

Movie: P. Hamlington

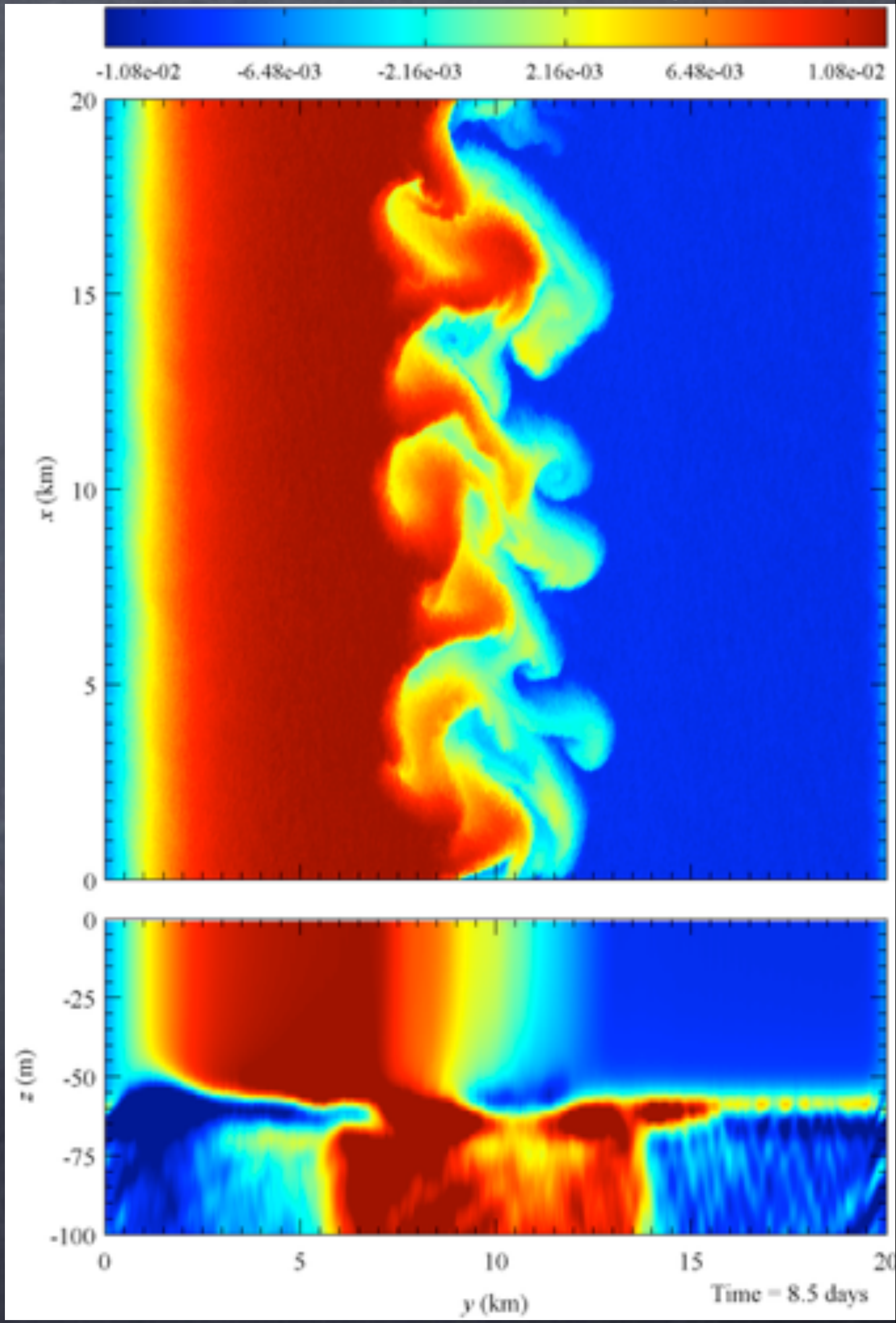

P. E. Hamlington, L. P. Van Roekel, B. Fox-Kemper, K. Julien, and G. P. Chini. Langmuir-submesoscale interactions: Descriptive analysis multiscale frontal spin-down simulations. Journal of Physical Oceanography, 2013. Submitted.

LES of Langmuir-Submeso Interactions?

Perform large eddy simulations (LES) of Langmuir turbulence with a submesoscale temperature front

Use NCAR LES model to solve Craik-Leibovich equations (Moeng, 1984, McWilliams et al, 1997)

$$\frac{\partial \rho}{\partial t} + \mathbf{u}_L \cdot \nabla \rho = \mathrm{SGS} \qquad \nabla \cdot \mathbf{u} = 0$$

$$\frac{\partial \mathbf{u}}{\partial t} + (\boldsymbol{\omega} + f\hat{\mathbf{z}}) \times \mathbf{u}_L = -\nabla \pi - \frac{g\rho\hat{\mathbf{z}}}{\rho_0} + \mathrm{SGS}$$

Computational parameters:

Domain size: 20km x 20km x -160m

Grid points: 4096 x 4096 x 128

Resolution: 5m x 5m x -1.25m

1000x more gridpoints than CESM

Movie: P. Hamlington

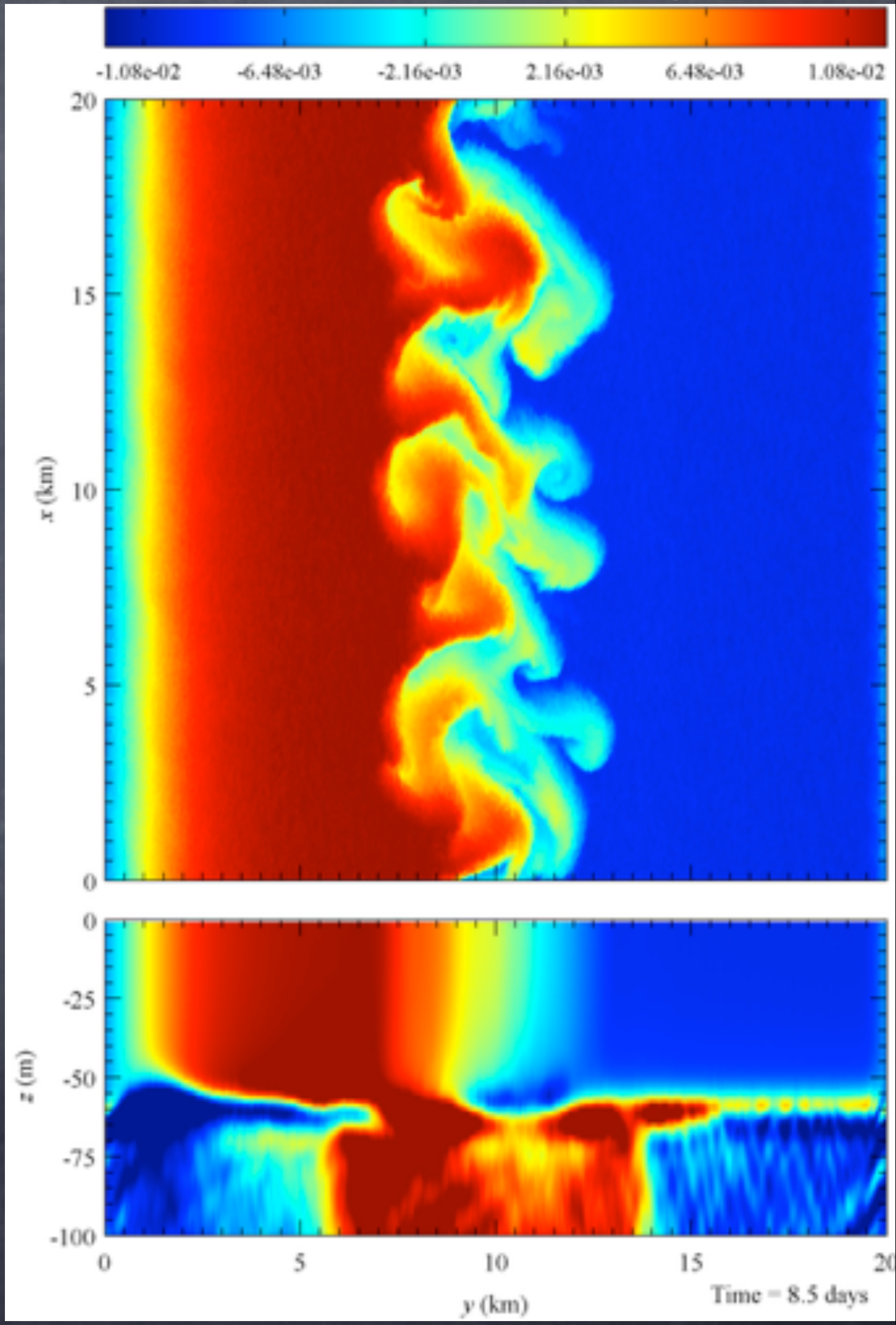

P. E. Hamlington, L. P. Van Roekel, B. Fox-Kemper, K. Julien, and G. P. Chini. Langmuir-submesoscale interactions: Descriptive analysis multiscale frontal spin-down simulations. Journal of Physical Oceanography, 2013. Submitted.

Zoom: Submeso-Langmuir Interaction!

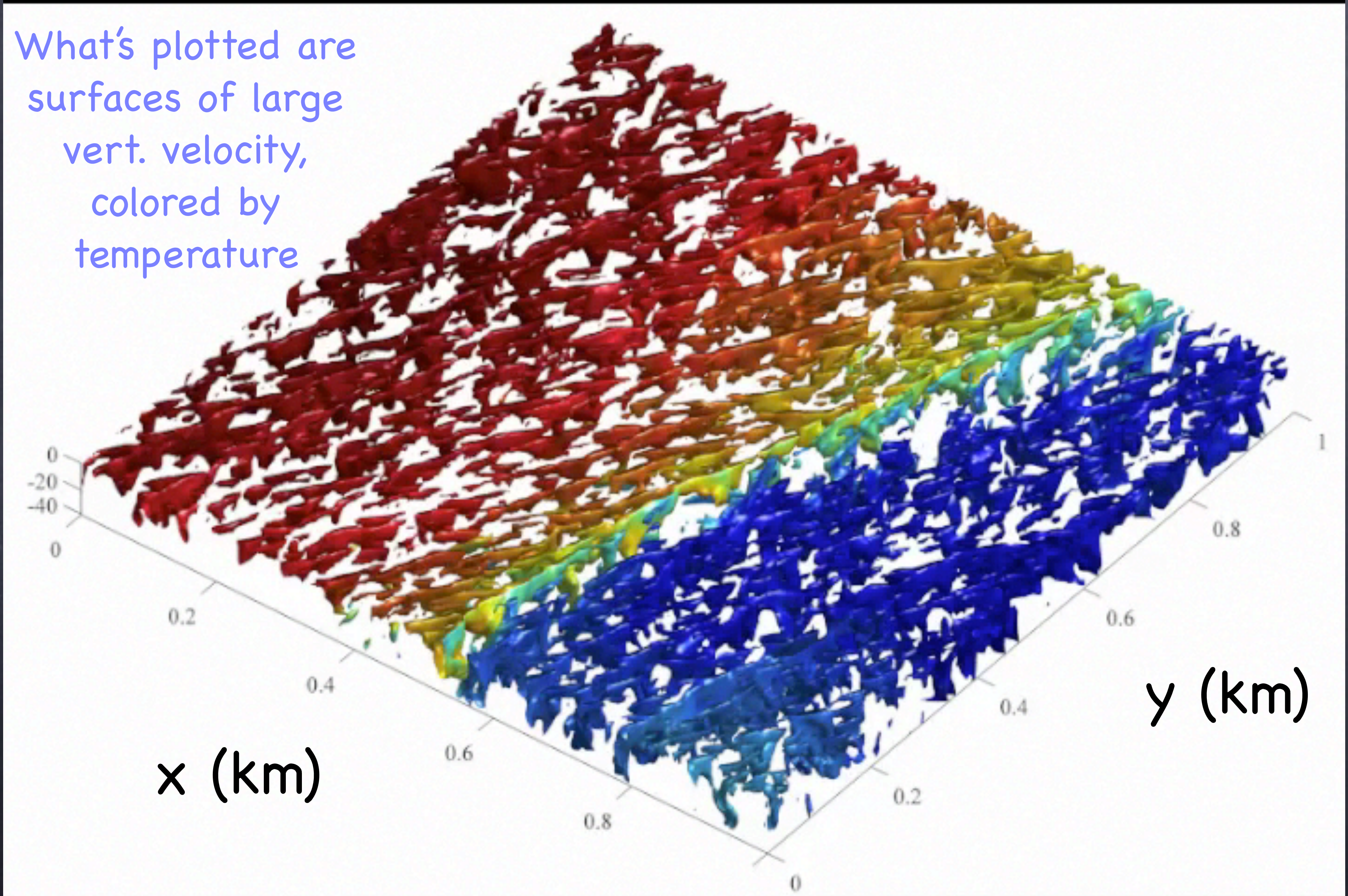

P. E. Hamlington, L. P. Van Roekel, B. Fox-Kemper, K. Julien, and G. P. Chini. Langmuir-submesoscale interactions: Descriptive analysis multiscale frontal spin-down simulations. Journal of Physical Oceanography, 2013. Submitted.

Zoom: Submeso-Langmuir Interaction!

What's plotted are surfaces of large vert. velocity, colored by temperature

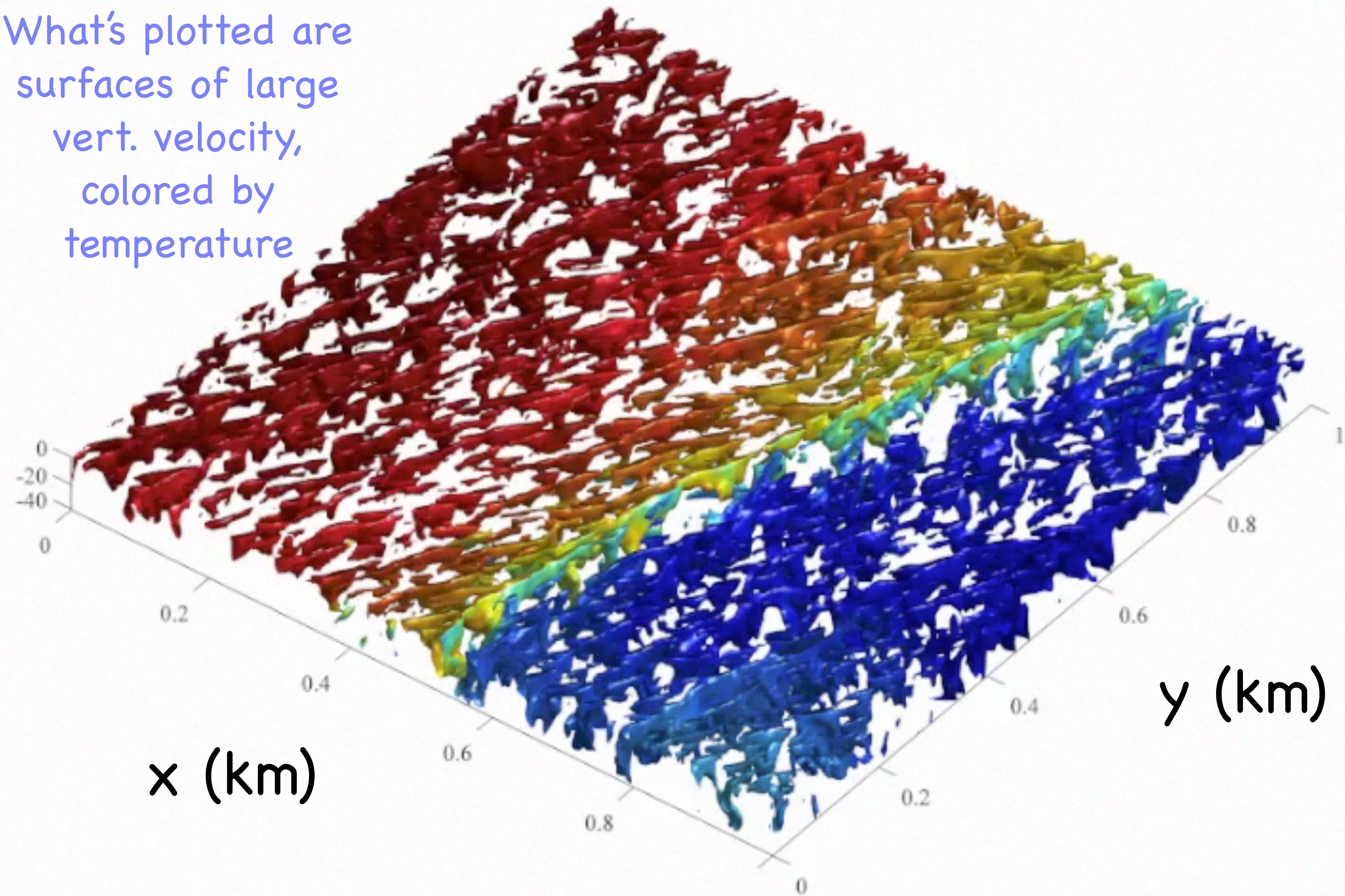

P. E. Hamlington, L. P. Van Roekel, B. Fox-Kemper, K. Julien, and G. P. Chini. Langmuir-submesoscale interactions: Descriptive analysis multiscale frontal spin-down simulations. Journal of Physical Oceanography, 2013. Submitted.

Diverse types of interaction

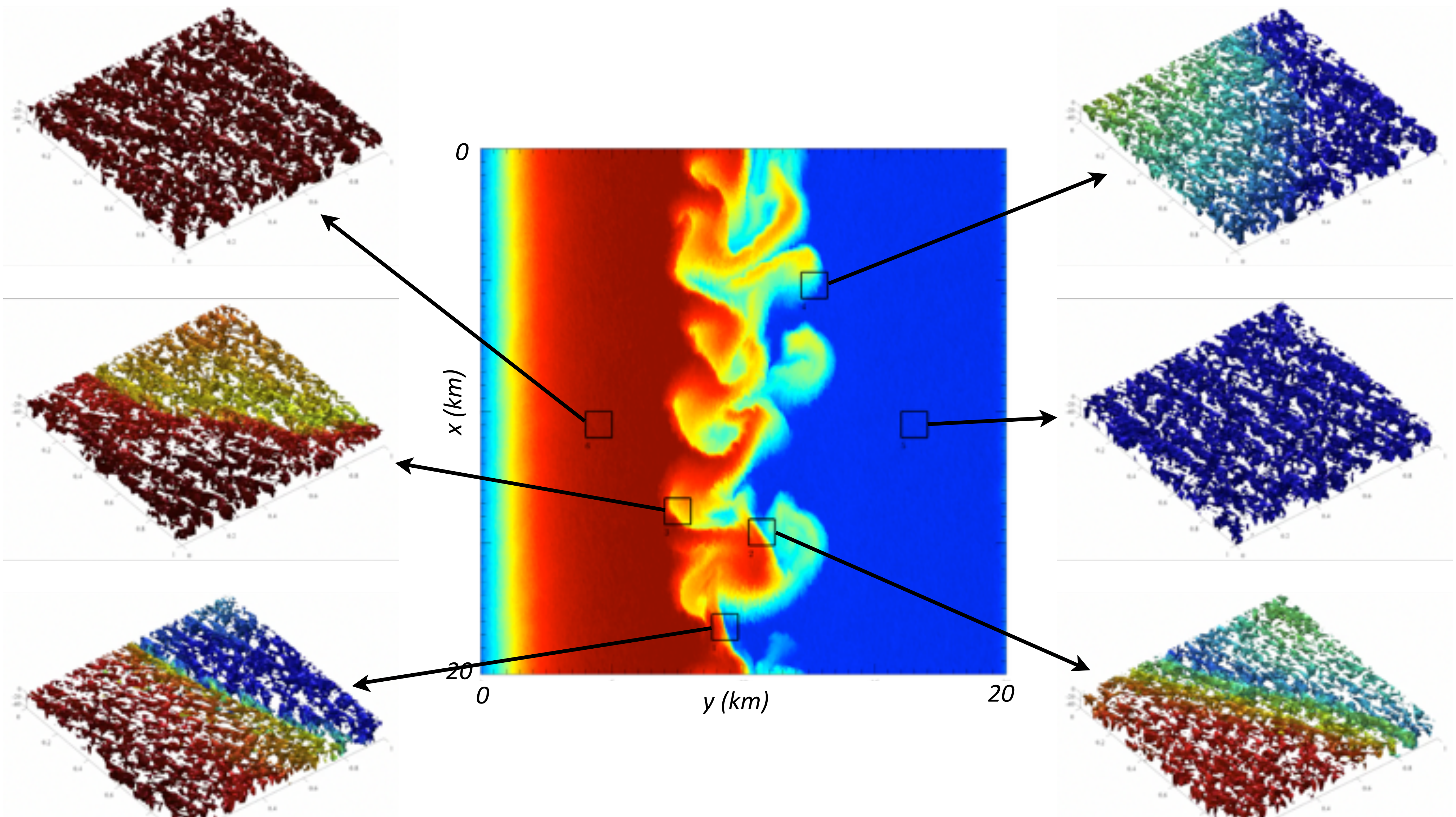

Slide & Movies by Peter Hamlington

P. E. Hamlington, L. P. Van Roekel, B. Fox-Kemper, K. Julien, and G. P. Chini. Langmuir-submesoscale interactions: Descriptive analysis of multiscale frontal spin-down simulations. Journal of Physical Oceanography, 2013. Submitted.

Diverse types of interaction

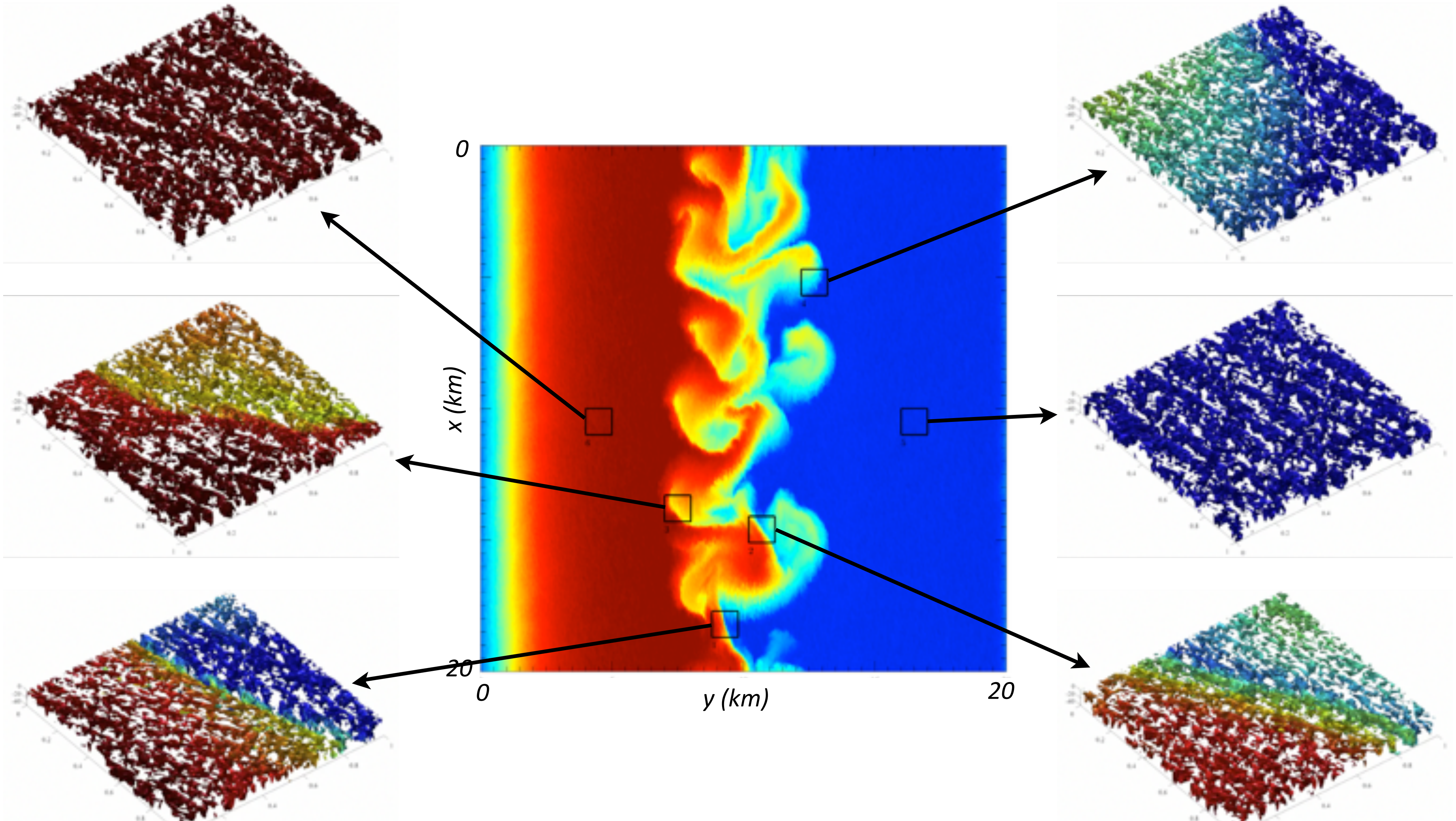

Slide & Movies by Peter Hamlington

P. E. Hamlington, L. P. Van Roekel, B. Fox-Kemper, K. Julien, and G. P. Chini. Langmuir-submesoscale interactions: Descriptive analysis of multiscale frontal spin-down simulations. Journal of Physical Oceanography, 2013. Submitted.

Wave-influenced Sawyer-Eliassen eq.

Suzuki & F-K in prep

$$N_*^2 \frac{\partial^2 \psi}{\partial y^2} + F_*^2 \frac{\partial^2 \psi}{\partial z^2} + 2M_*^2 \frac{\partial^2 \psi}{\partial y \partial z} = 2Q_2 + S_{turb} + S_{SSF}$$

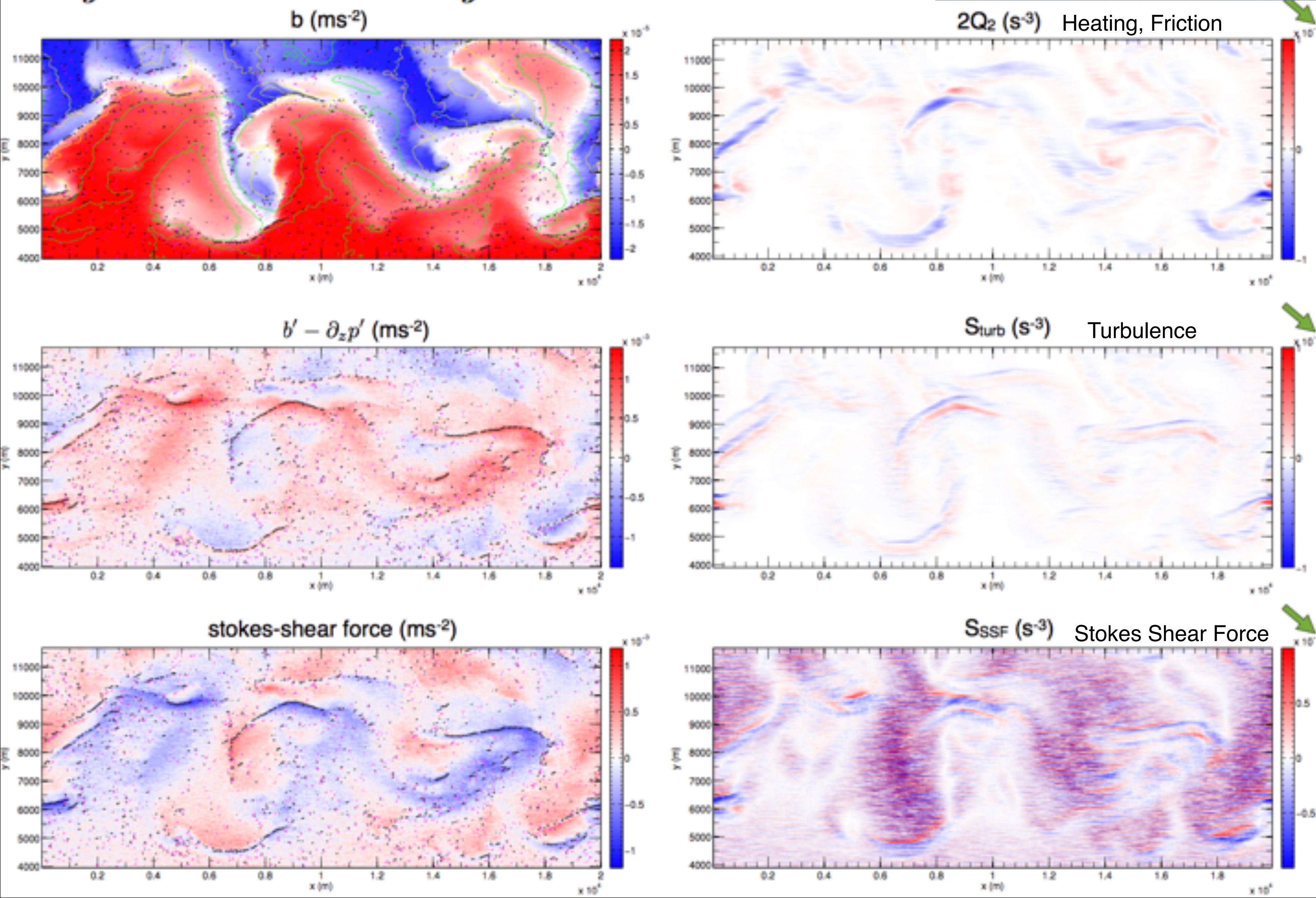

10^{-11}

10^{-11}

10^{-10}

Conclusions

- Climate modeling is challenging partly due to the vast and diverse scales of fluid motions
- In the upper ocean, horizontal scales as big as basins, and as small as meters contribute non-negligibly to the air-sea exchange and climate
- Interesting transition occurs on the Submeso to Langmuir scale boundary, as nonhydro. & ageostrophic effects begin to dominate
- The effects of the Stokes forces on mesoscale and submesoscale dynamics are under-appreciated.
- All papers at: fox-kemper.com/pubs

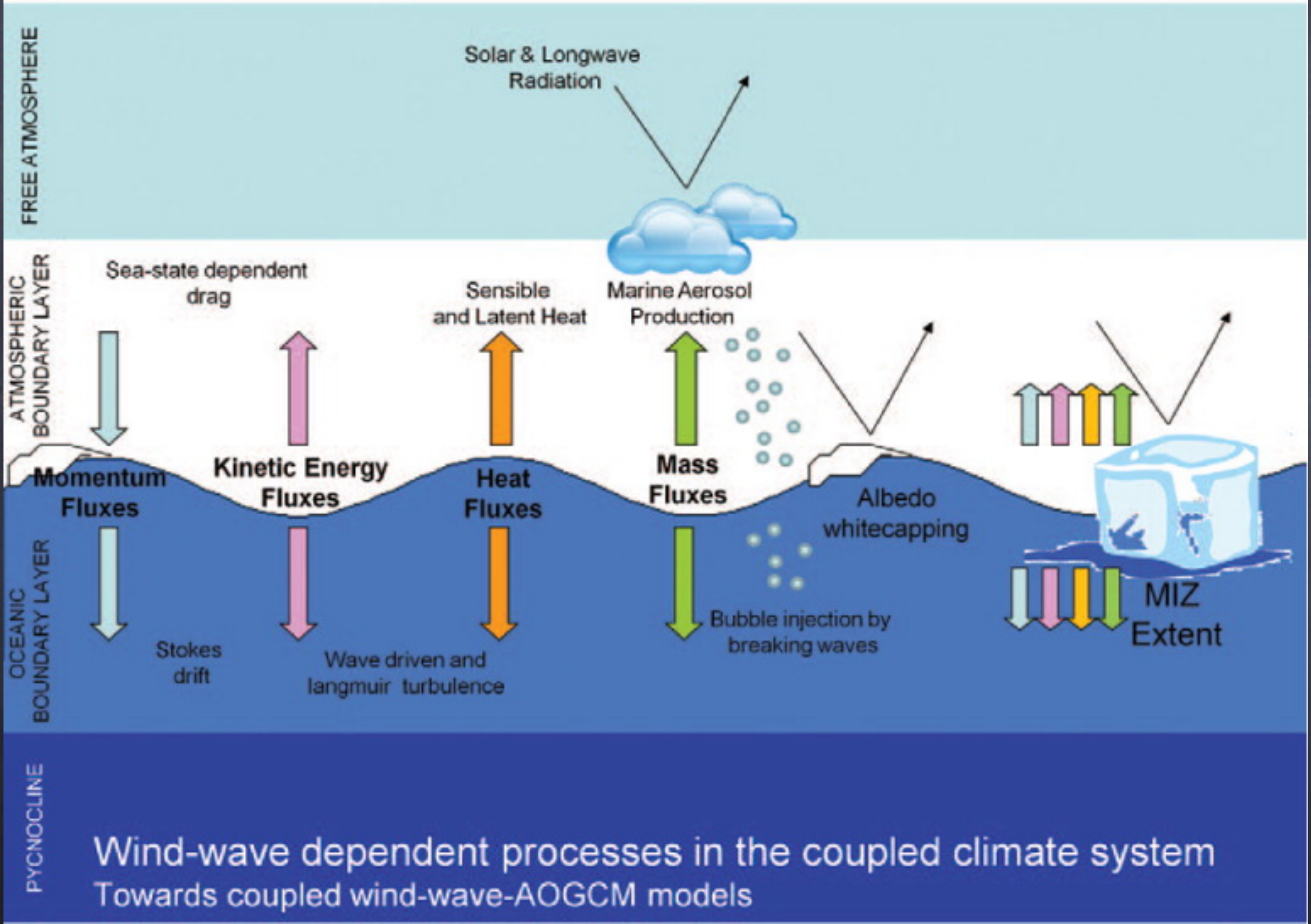

L. Cavaleri, B. Fox-Kemper, and M. Hemer. Wind waves in the coupled climate system. Bulletin of the American Meteorological Society, 93(11):1651-1661, 2012.

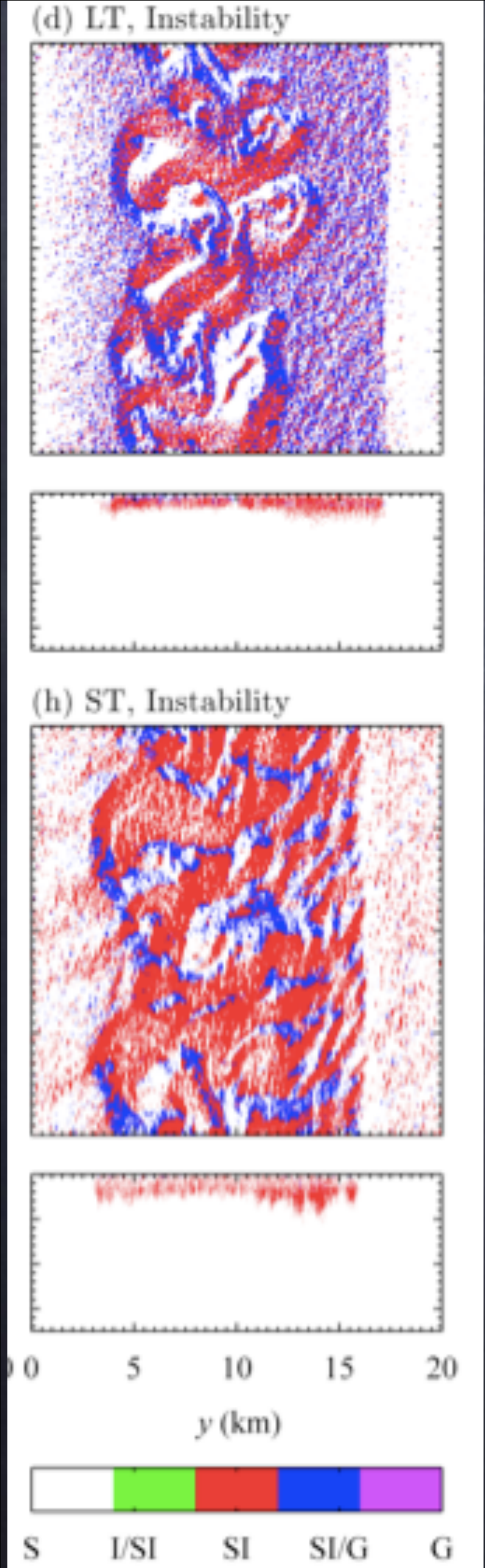

P. E. Hamlington, L. P. Van Roekel, B. Fox-Kemper, K. Julien, and G. P. Chini. Langmuir-submesoscale interactions: Descriptive analysis of multiscale frontal spin-down simulations. Journal of Physical Oceanography, 2013. Submitted.

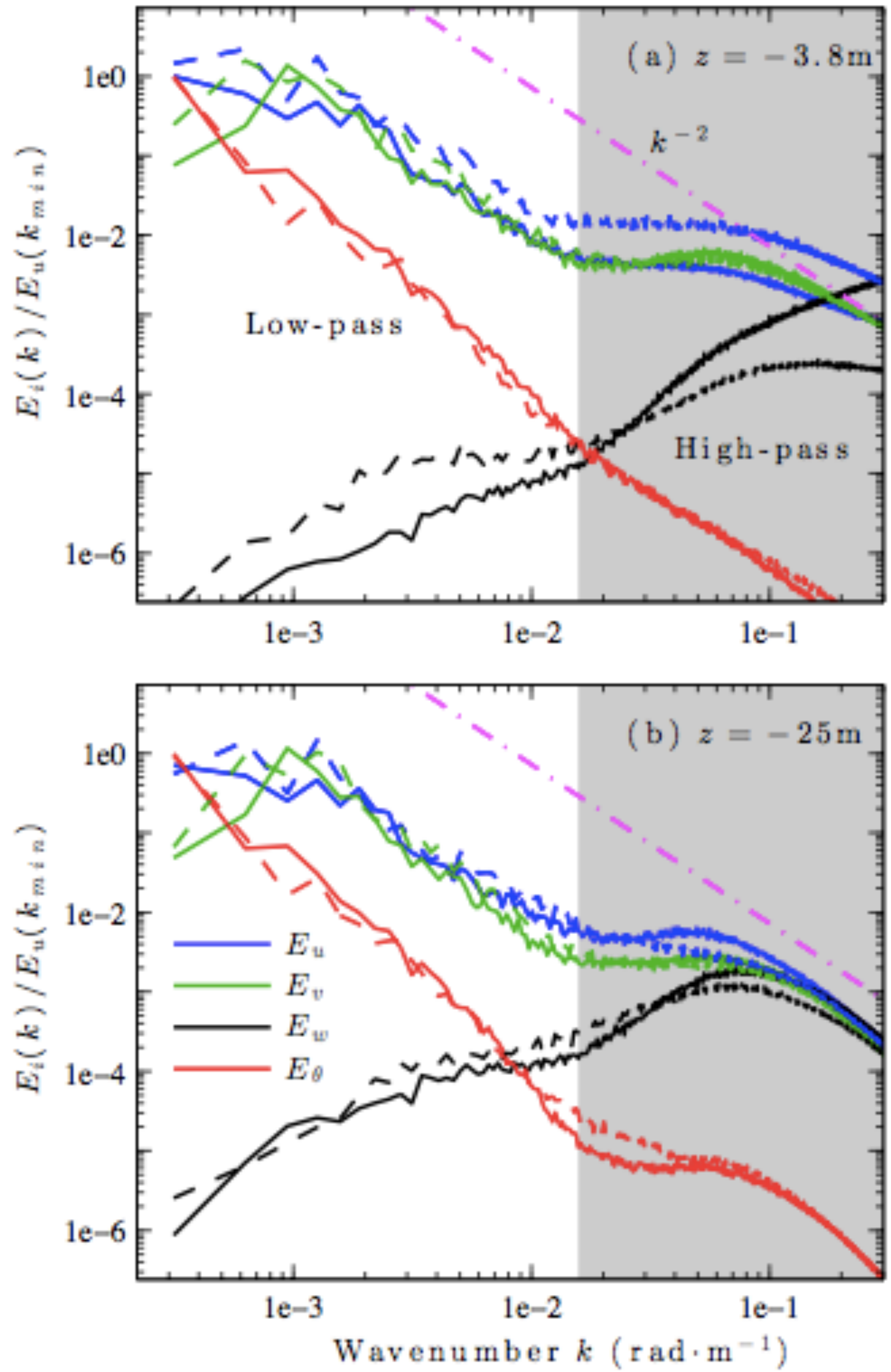

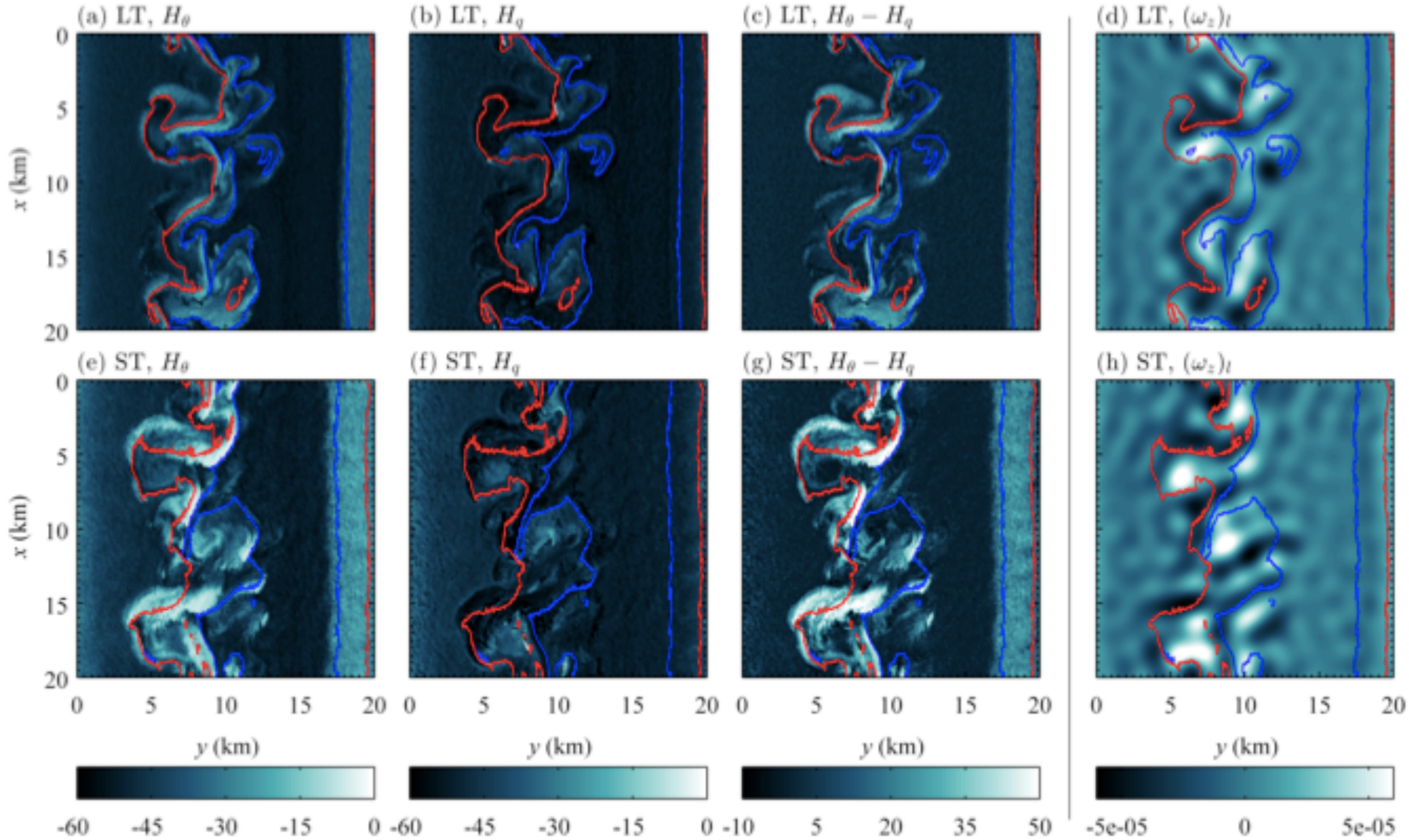

FIG. 13. Fields of the mixed layer depth (in m) based on temperature, denoted H_θ, (a,e) and on potential vorticity, denoted H_q, (b,f) for the LT (a,b) and ST (e,f) cases. The difference $H_\theta - H_q$ is shown in (c,g) and low-pass (submesoscale) vertical vorticity fields are shown in (d,h), where the filter cutoff for the vorticity fields is at 2km. Contour lines correspond to temperature contours taken from Figure 2.

P. E. Hamlington, L. P. Van Roekel, B. Fox-Kemper, K. Julien, and G. P. Chini. Langmuir-submesoscale interactions: Descriptive analysis of multiscale frontal spin-down simulations. Journal of Physical Oceanography, 2013. Submitted.

So, no problems? Just crunch away with CLB?

- Let's revisit our assumptions for scale separation:
  - CLB wave equations require limited *wave steepness* and irrotational flow
  - Real wind-waves are not monochromatic, but incorporate a spectrum of waves, and...

Power Spectrum of wave height

$$\langle \eta^2 \rangle = \int_0^\infty E(k)dk = C_0 + \int_{k_h}^\infty C_1 k^{-2} dk$$

Power Spectrum of wave steepness: INFINITE!

$$\langle k^2 \eta^2 \rangle = \int_0^\infty k^2 E(k)dk = D_0 + \int_{k_h}^\infty D_1 dk$$

Steep waves break->vortex motion & small scale turbulence!

So, no problems? Just crunch away with CLB?

- Let's revisit our assumptions for scale separation:
  - CLB wave equations require limited *wave steepness* and irrotational flow
  - Real wind-waves are not monochromatic, but incorporate a spectrum of waves, and...

Power Spectrum of wave height

$$\langle \eta^2 \rangle = \int_0^\infty E(k)dk = C_0 + \int_{k_h}^\infty C_1 k^{-2} dk$$

Power Spectrum of wave steepness: INFINITE!

$$\langle k^2 \eta^2 \rangle = \int_0^\infty k^2 E(k)dk = D_0 + \int_{k_h}^\infty D_1 dk$$

Steep waves break->vortex motion & small scale turbulence!

Physical Sensitivity of Ocean Climate to MLE: (submeso) Mixed Layer Eddy Restratification

Improves CFCs (water masses)

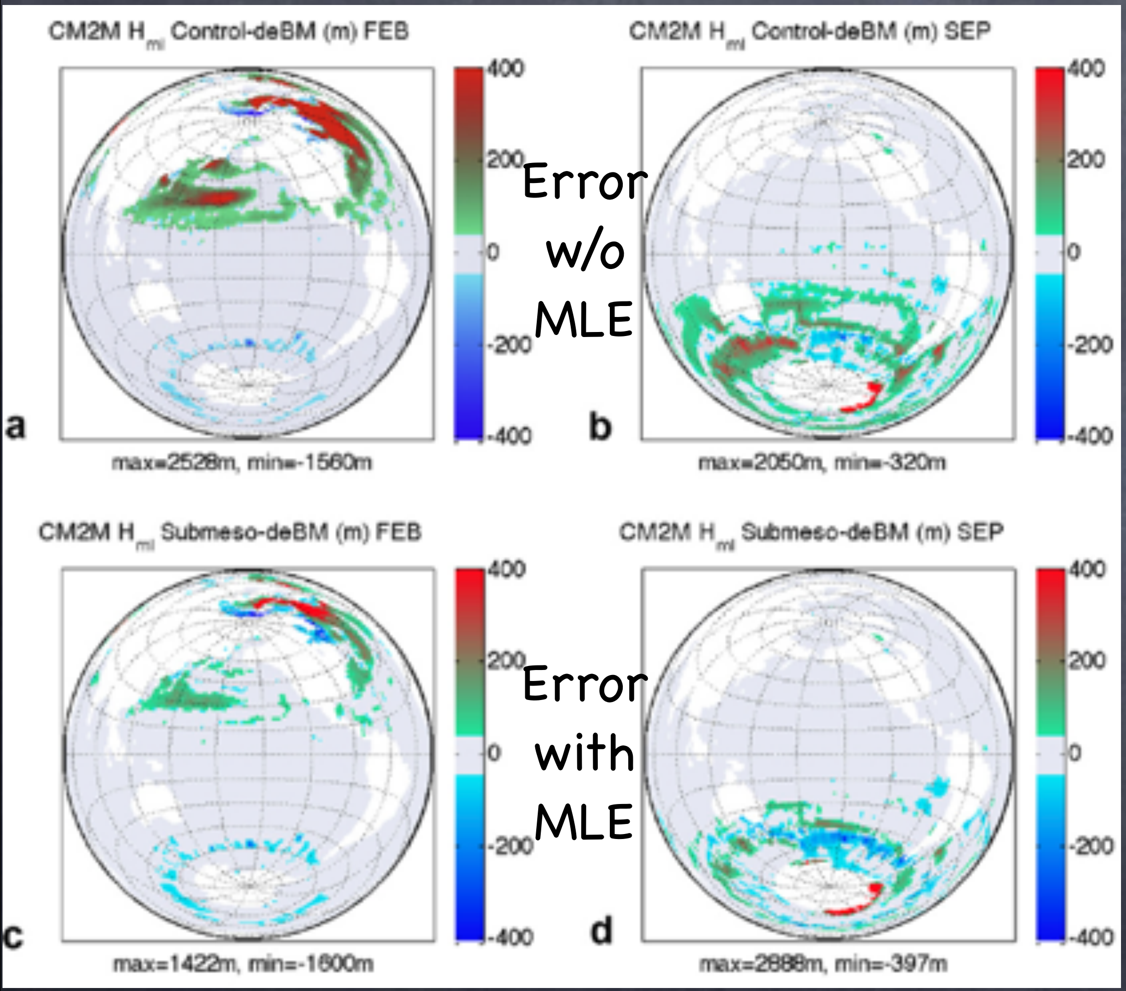

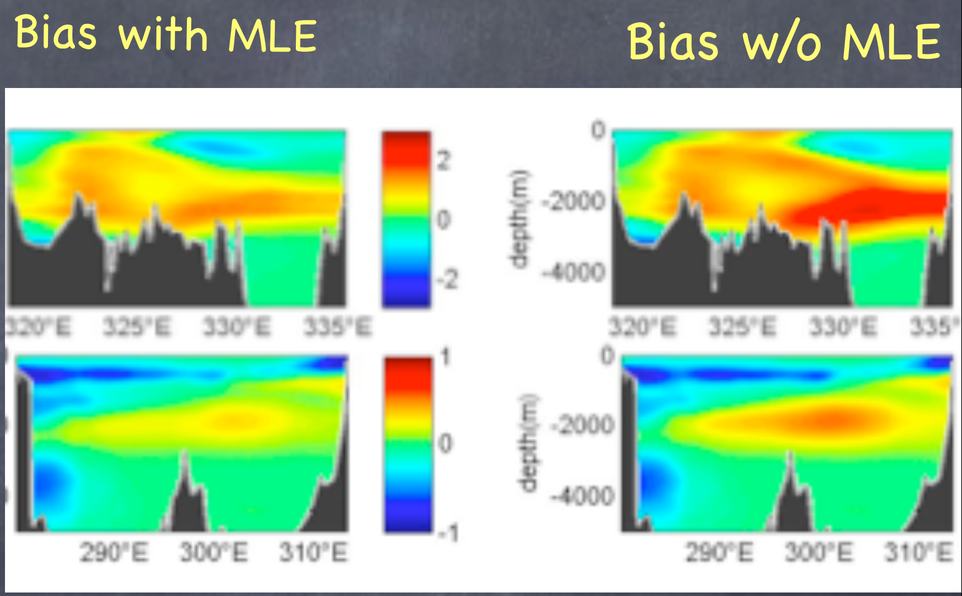

B. Fox-Kemper, G. Danabasoglu, R. Ferrari, S. M. Griffies, R. W. Hallberg, M. M. Holland, M. E. Maltrud, S. Peacock, and B. L. Samuels. Parameterization of mixed layer eddies. III: Implementation and impact in global ocean climate simulations. *Ocean Modelling*, 39:61-78, 2011.

Physical Sensitivity of Ocean Climate to MLE:
(submeso) Mixed Layer Eddy Restratification

Improves CFCs (water masses)

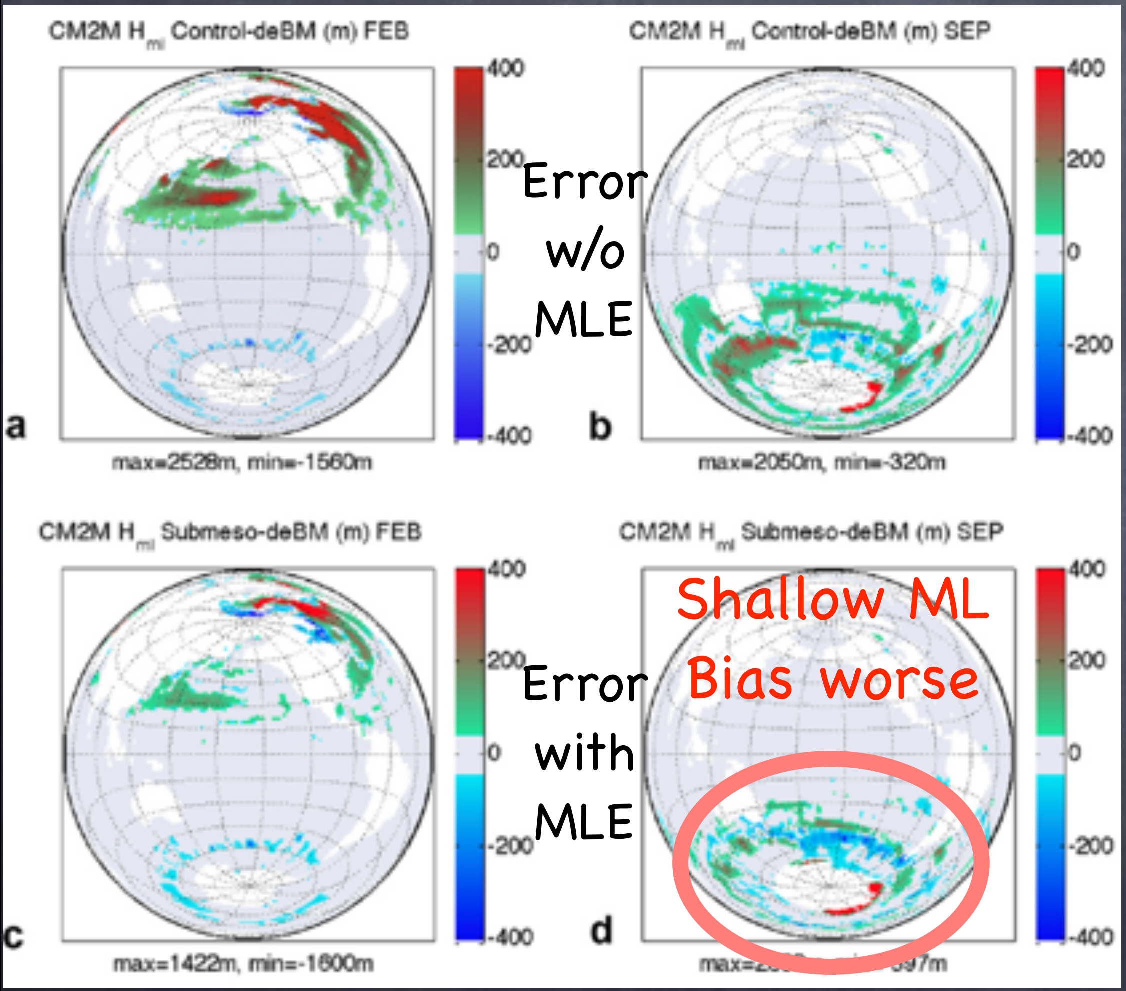

Bias with MLE

Bias w/o MLE

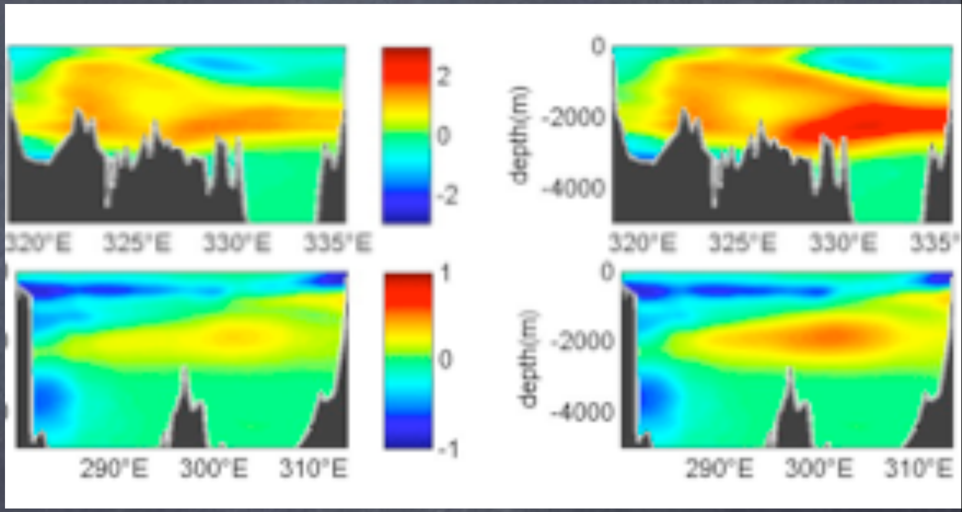

B. Fox-Kemper, G. Danabasoglu, R. Ferrari, S. M. Griffies, R. W. Hallberg, M. M. Holland, M. E. Maltrud, S. Peacock, and B. L. Samuels. Parameterization of mixed layer eddies. III: Implementation and impact in global ocean climate simulations. *Ocean Modelling*, 39:61-78, 2011.

Physical Sensitivity of Ocean Climate to MLE: (submeso) Mixed Layer Eddy Restratification

Improves CFCs (water masses)

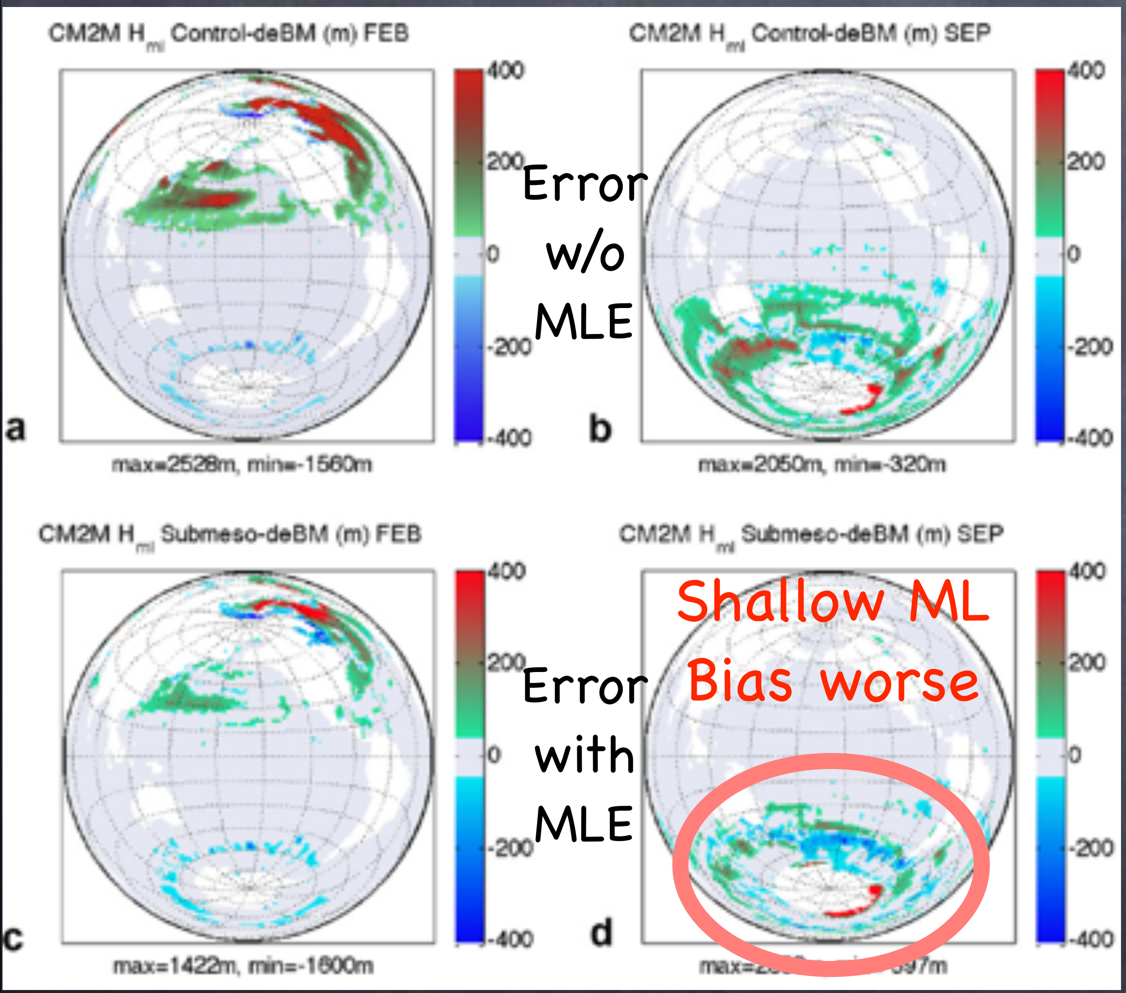

Bias with MLE

Bias w/o MLE

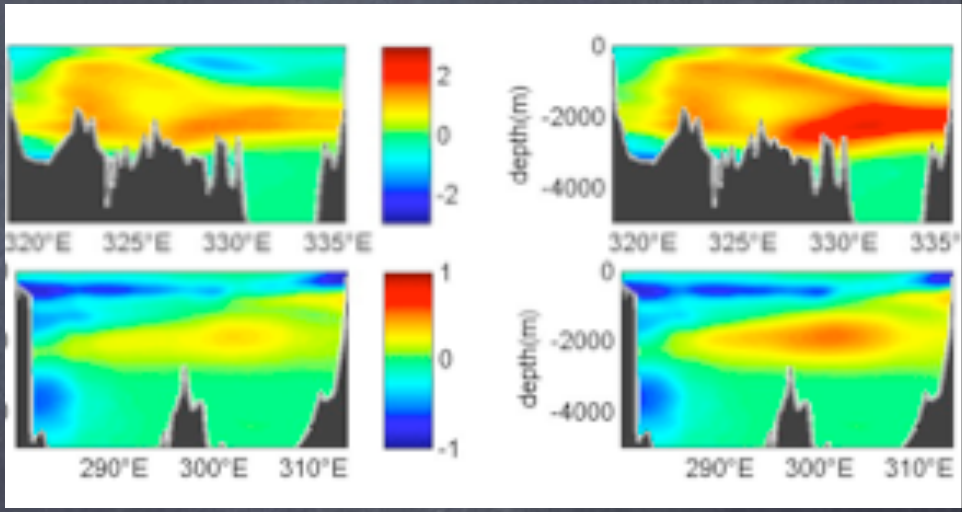

A consistently restratifying,

$$\overline{w'b'} \propto \frac{H^2}{|f|}\left|\nabla_H \bar{b}\right|^2$$

B. Fox-Kemper, G. Danabasoglu, R. Ferrari, S. M. Griffies, R. W. Hallberg, M. M. Holland, M. E. Maltrud, S. Peacock, and B. L. Samuels. Parameterization of mixed layer eddies. III: Implementation and impact in global ocean climate simulations. *Ocean Modelling*, 39:61-78, 2011.

Physical Sensitivity of Ocean Climate to MLE:
(submeso) Mixed Layer Eddy Restratification

Improves CFCs (water masses)

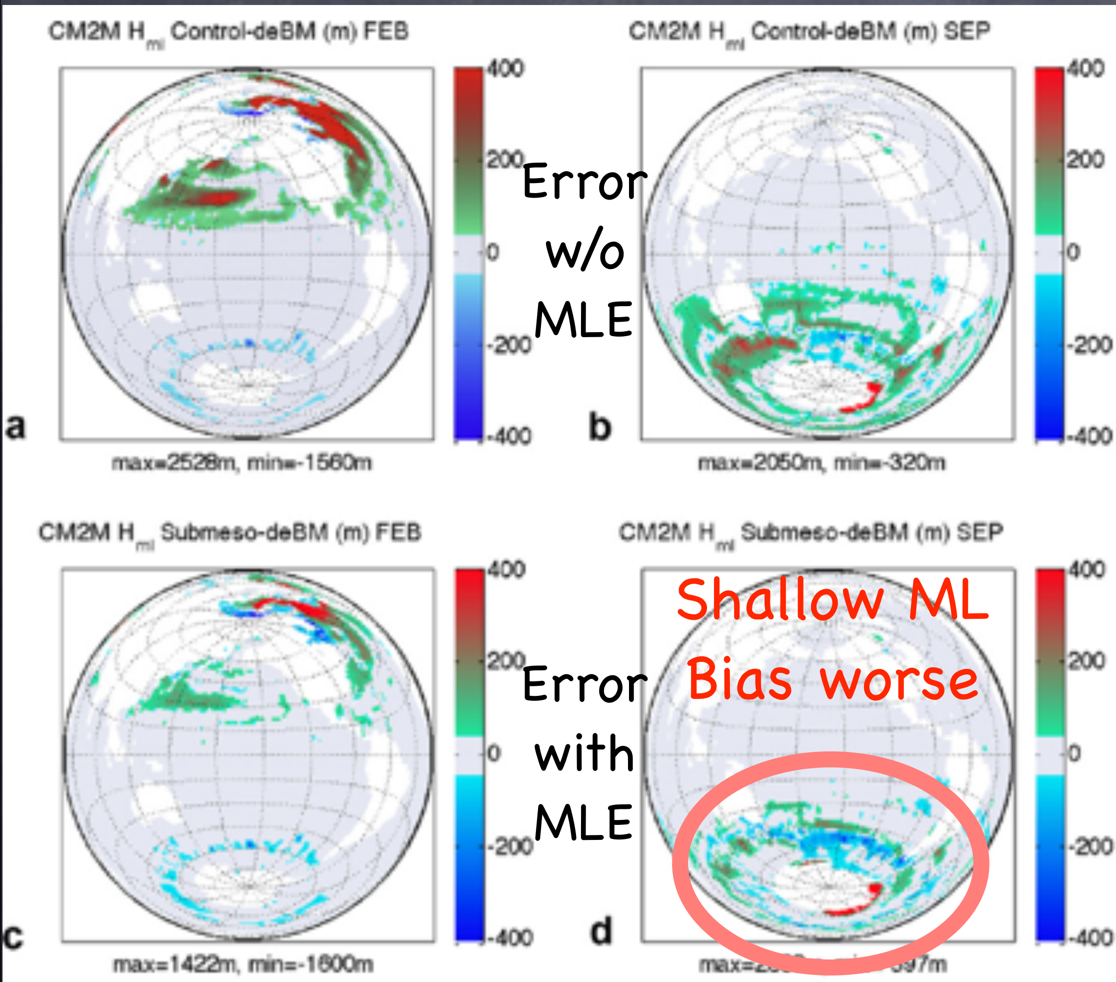

Bias with MLE

Bias w/o MLE

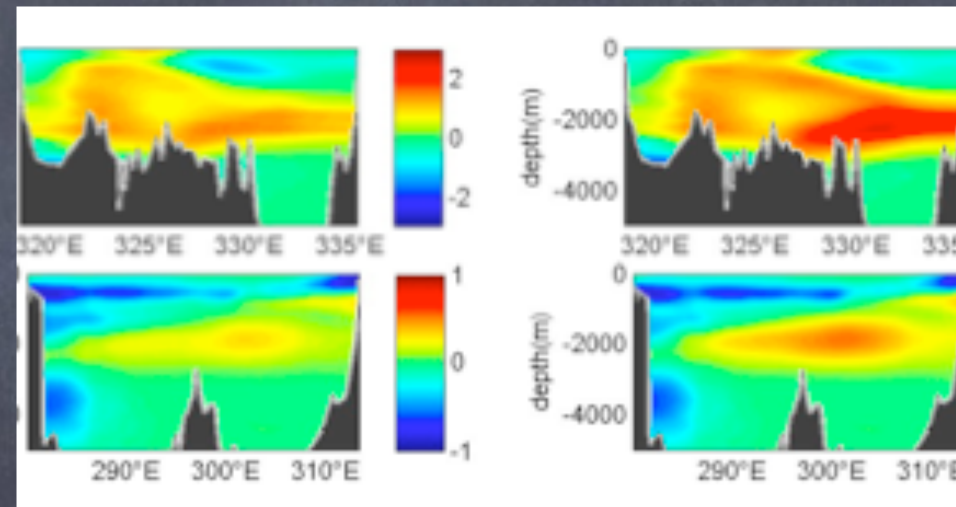

A consistently restratifying,

$$\overline{w'b'} \propto \frac{H^2}{|f|}\left|\nabla_H \bar{b}\right|^2$$

and horizontally downgradient flux.

$$\overline{\mathbf{u}'_H b'} \propto \frac{-H^2 \frac{\partial \bar{b}}{\partial z}}{|f|}\nabla_H \bar{b}$$

B. Fox-Kemper, G. Danabasoglu, R. Ferrari, S. M. Griffies, R. W. Hallberg, M. M. Holland, M. E. Maltrud, S. Peacock, and B. L. Samuels. Parameterization of mixed layer eddies. III: Implementation and impact in global ocean climate simulations. *Ocean Modelling*, 39:61-78, 2011.

Mixed Layer Eddy Restratification

Estimating eddy buoyancy/density fluxes:

$$\overline{\mathbf{u}'b'} \equiv \mathbf{\Psi} \times \nabla \bar{b}$$

A submeso eddy-induced overturning:

$$\mathbf{\Psi} = \frac{C_e H^2 \mu(z)}{|f|} \nabla \bar{b} \times \hat{\mathbf{z}}$$

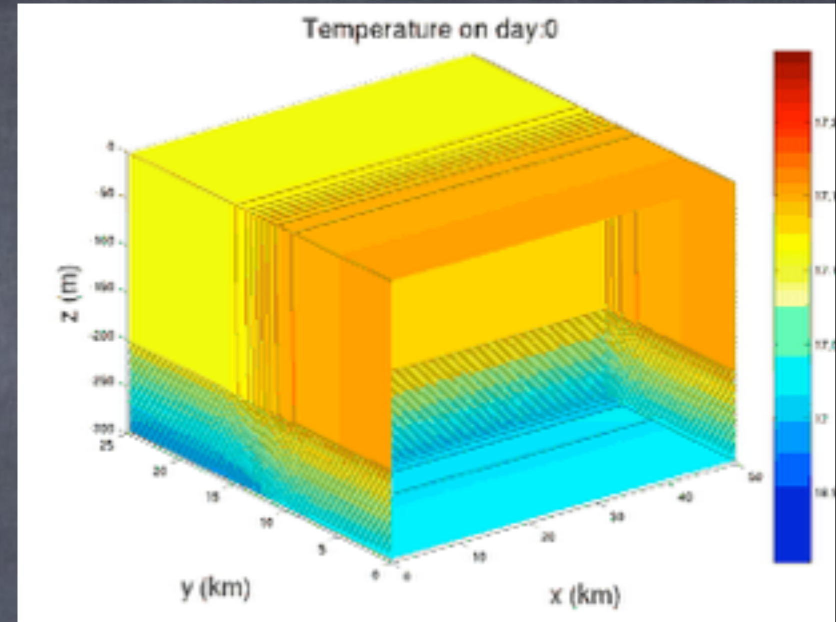

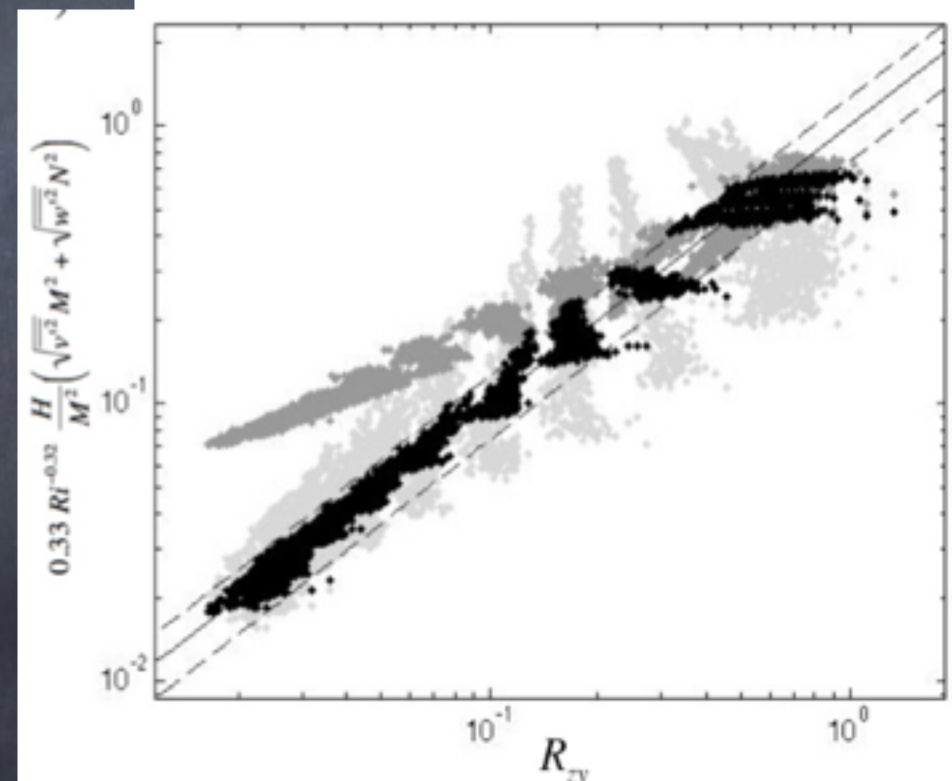

S. Bachman and B. Fox-Kemper. Eddy parameterization challenge suite. I: Eady spindown. Ocean Modelling, 64:12-28, 2013

Mixed Layer Eddy Restratification

Estimating eddy buoyancy/density fluxes:

$$\overline{\mathbf{u}'b'} \equiv \mathbf{\Psi} \times \nabla \bar{b}$$

A submeso eddy-induced overturning:

$$\mathbf{\Psi} = \frac{C_e H^2 \mu(z)}{|f|} \nabla \bar{b} \times \hat{\mathbf{z}}$$

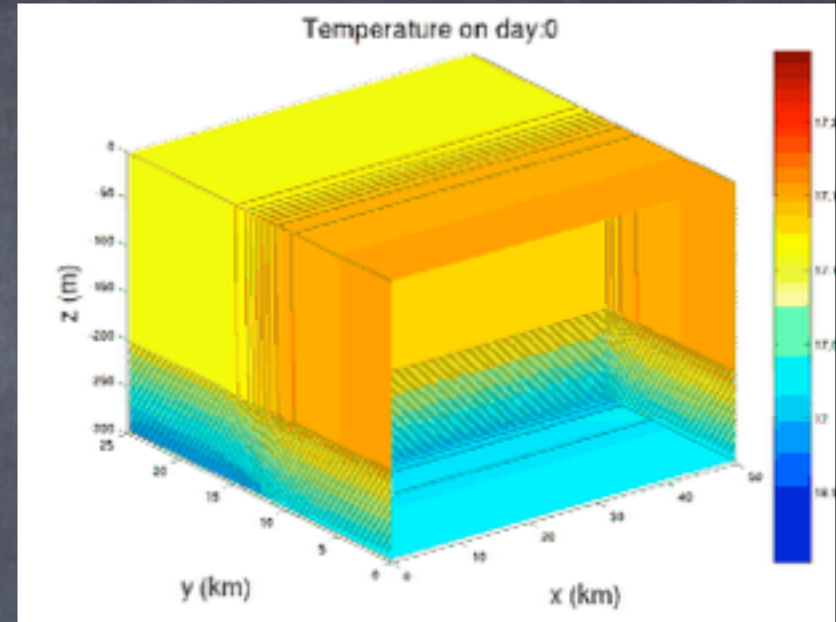

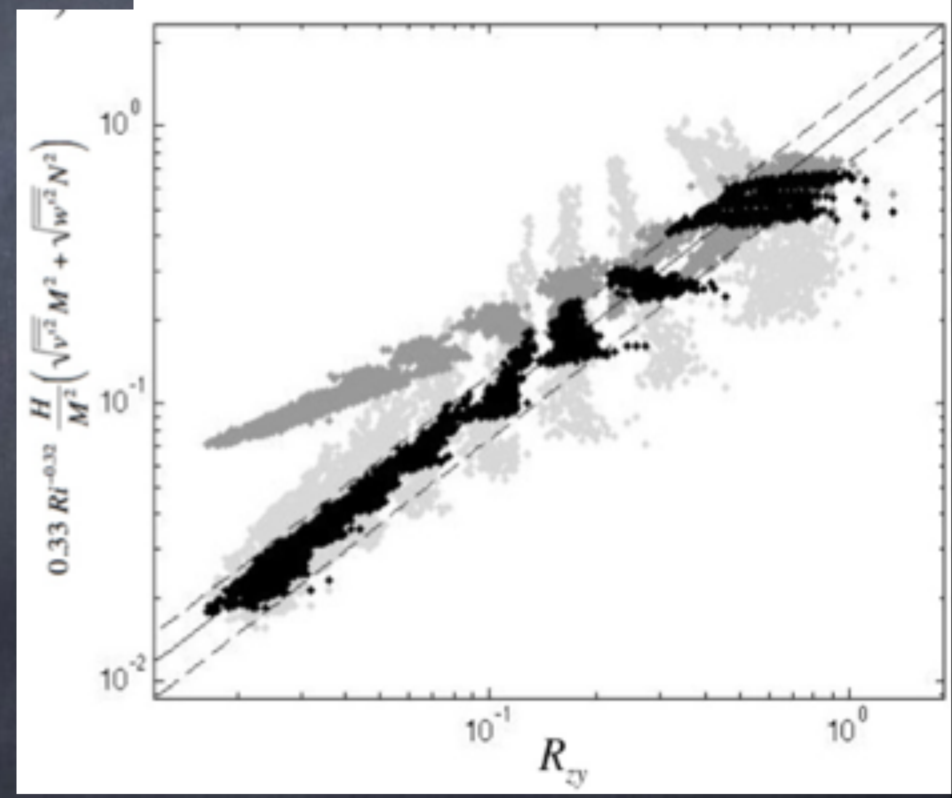

S. Bachman and B. Fox-Kemper. Eddy parameterization challenge suite. I: Eady spindown. Ocean Modelling, 64:12-28, 2013

Mixed Layer Eddy Restratification

Estimating eddy buoyancy/density fluxes:

$$\overline{\mathbf{u}'b'} \equiv \mathbf{\Psi} \times \nabla \bar{b}$$

A submeso eddy-induced overturning:

$$\mathbf{\Psi} = \frac{C_e H^2 \mu(z)}{|f|} \nabla \bar{b} \times \hat{\mathbf{z}}$$

in ML only:

$$\mu(z) = 0 \text{ if } z < -H$$

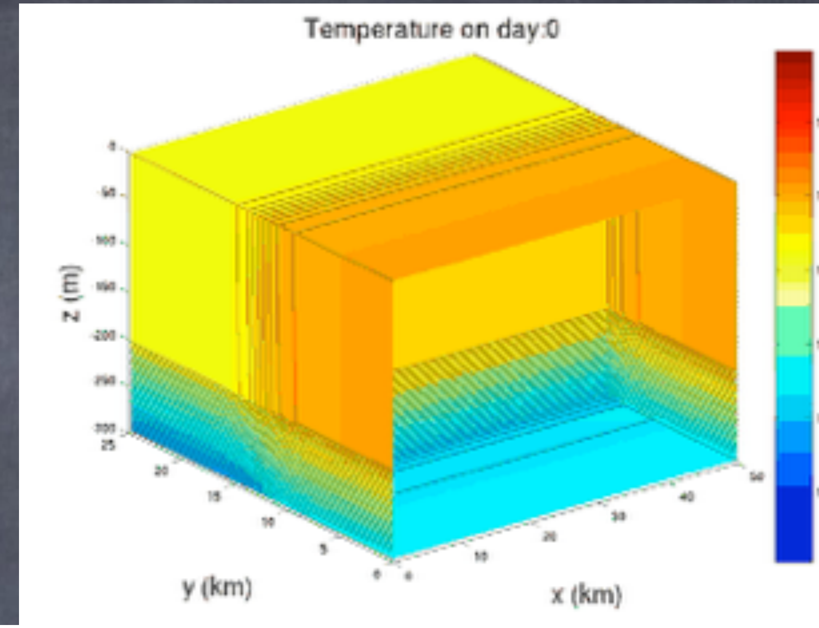

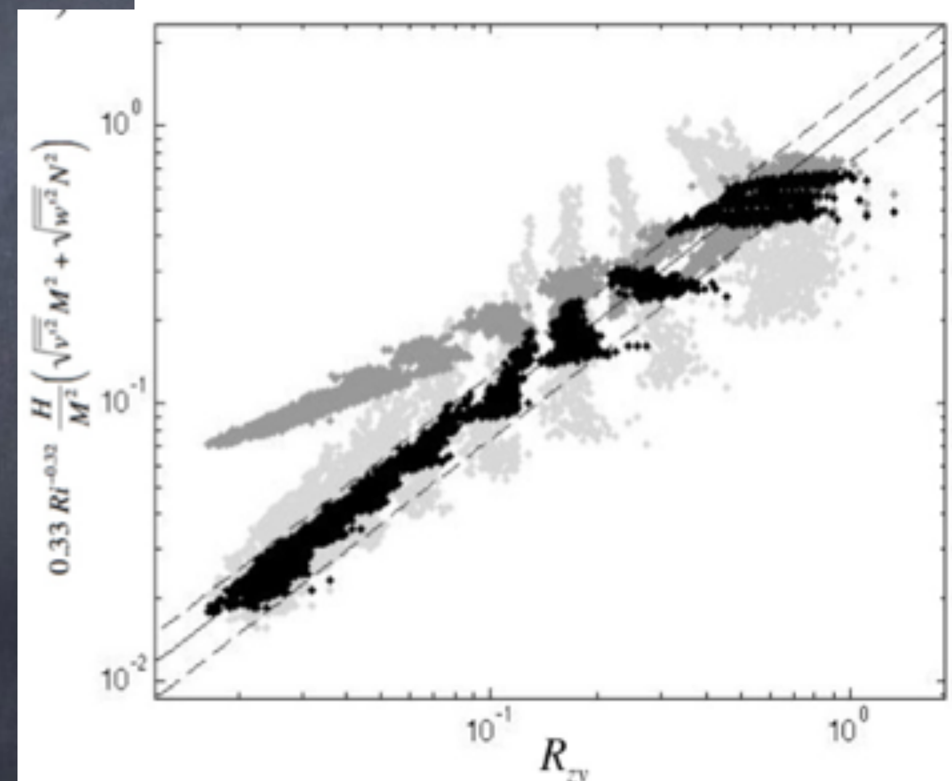

S. Bachman and B. Fox-Kemper. Eddy parameterization challenge suite. I: Eady spindown. Ocean Modelling, 64:12-28, 2013

Mixed Layer Eddy Restratification

Estimating eddy buoyancy/density fluxes:

$$\overline{\mathbf{u}'b'} \equiv \mathbf{\Psi} \times \nabla \bar{b}$$

A submeso eddy-induced overturning:

$$\mathbf{\Psi} = \frac{C_e H^2 \mu(z)}{|f|} \nabla \bar{b} \times \hat{\mathbf{z}}$$

in ML only:

$$\mu(z) = 0 \text{ if } z < -H$$

For a consistently restratifying,

$$\overline{w'b'} \propto \frac{H^2}{|f|} \left|\nabla_H \bar{b}\right|^2$$

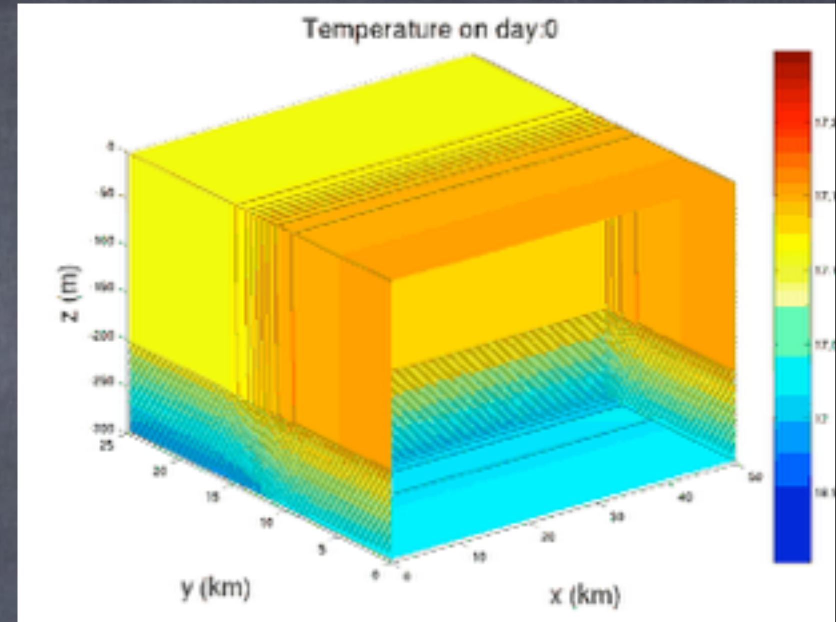

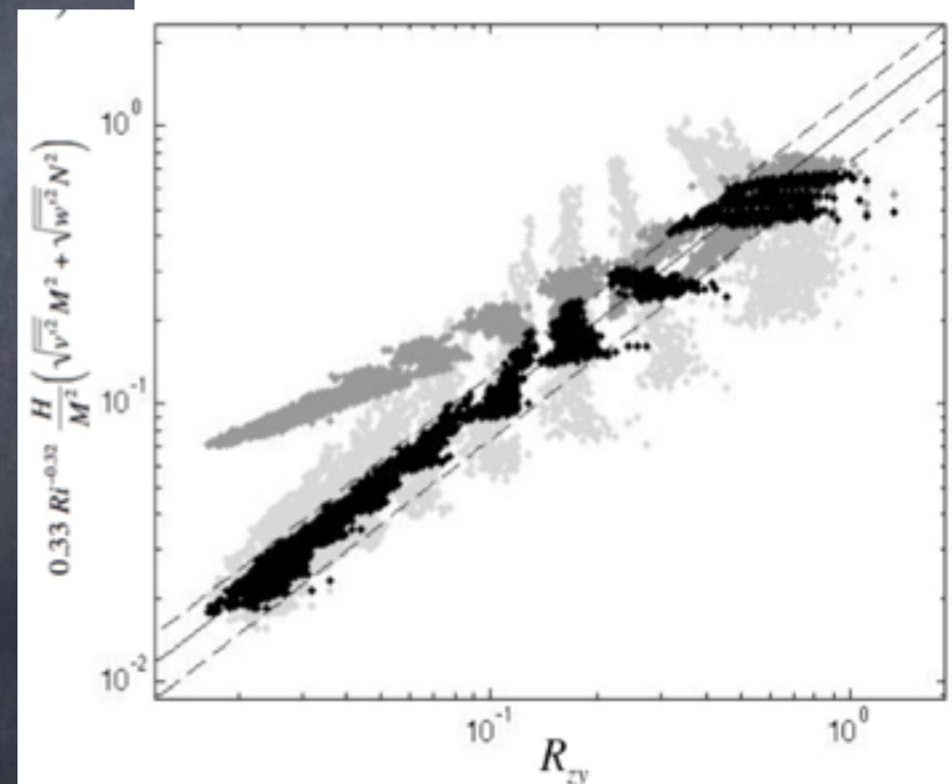

S. Bachman and B. Fox-Kemper. Eddy parameterization challenge suite. I: Eady spindown. Ocean Modelling, 64:12-28, 2013

Mixed Layer Eddy Restratification

Estimating eddy buoyancy/density fluxes:

$$\overline{\mathbf{u}'b'} \equiv \mathbf{\Psi} \times \nabla \bar{b}$$

A submeso eddy-induced overturning:

$$\mathbf{\Psi} = \frac{C_e H^2 \mu(z)}{|f|} \nabla \bar{b} \times \hat{\mathbf{z}}$$

in ML only:

$$\mu(z) = 0 \text{ if } z < -H$$

For a consistently restratifying,

$$\overline{w'b'} \propto \frac{H^2}{|f|} \left|\nabla_H \bar{b}\right|^2$$

and horizontally downgradient flux.

$$\overline{\mathbf{u}'_H b'} \propto \frac{-H^2 \frac{\partial \bar{b}}{\partial z}}{|f|} \nabla_H \bar{b}$$

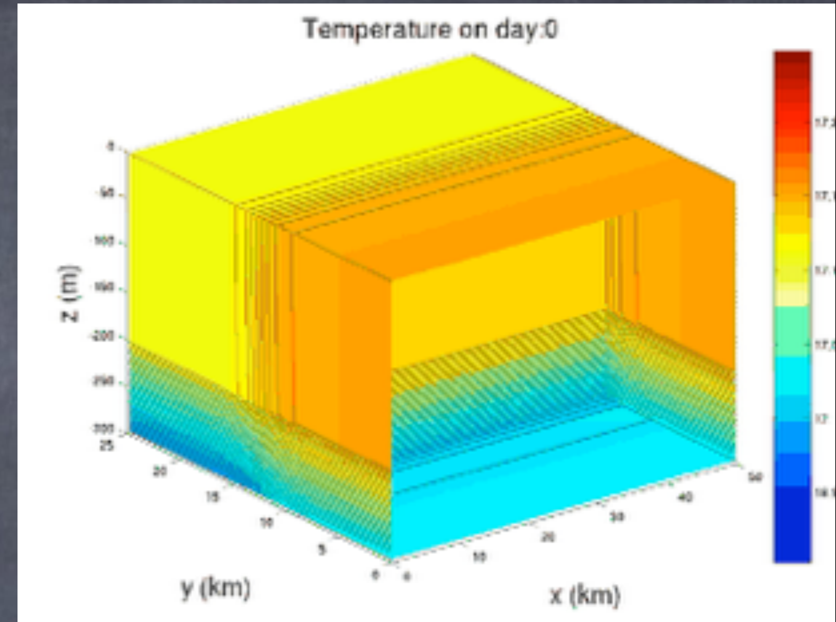

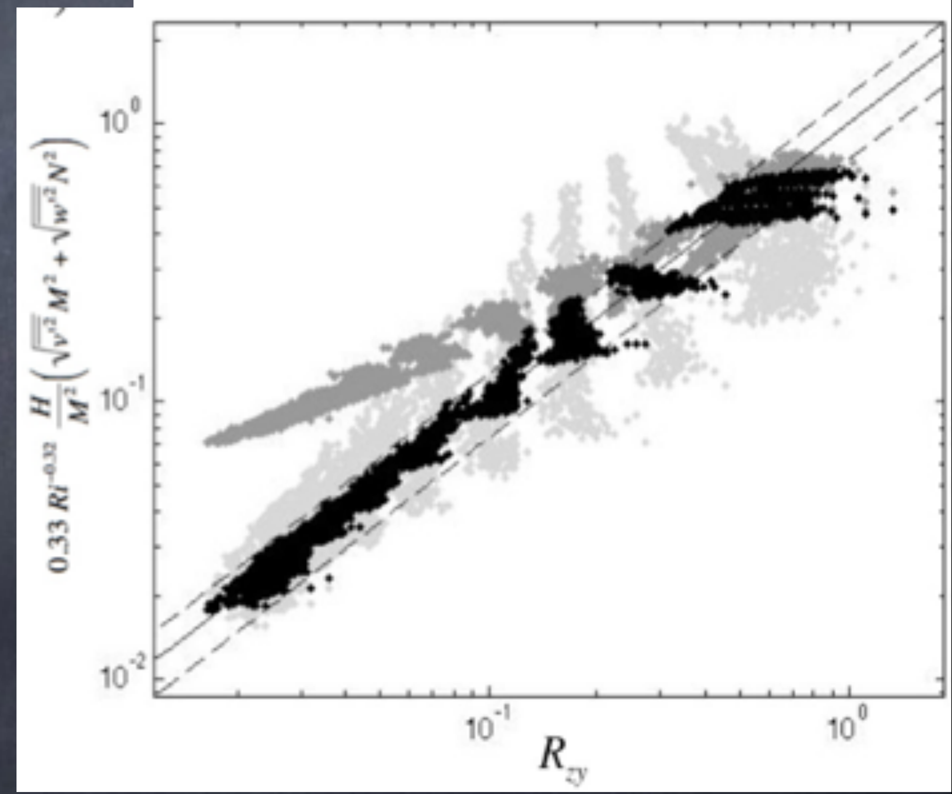

S. Bachman and B. Fox-Kemper. Eddy parameterization challenge suite. I: Eady spindown. Ocean Modelling, 64:12-28, 2013

Mixed Layer Eddy Res

Estimating eddy buoyancy/c

$$\overline{\mathbf{u}'b'} \equiv \mathbf{\Psi} \times \nabla \bar{b}$$

A submeso eddy-induced

$$\mathbf{\Psi} = \frac{C_e H^2 \mu(z)}{|f|} \nabla \bar{b} \times$$

in ML only:

$$\mu(z) = 0 \text{ if } z < -H$$

For a consistently restratifying,

$$\overline{w'b'} \propto \frac{H^2}{|f|} \left|\nabla_H \bar{b}\right|^2$$

and horizontally downgradient flux.

$$\overline{\mathbf{u}'_H b'} \propto \frac{-H^2 \frac{\partial \bar{b}}{\partial z}}{|f|} \nabla_H \bar{b}$$

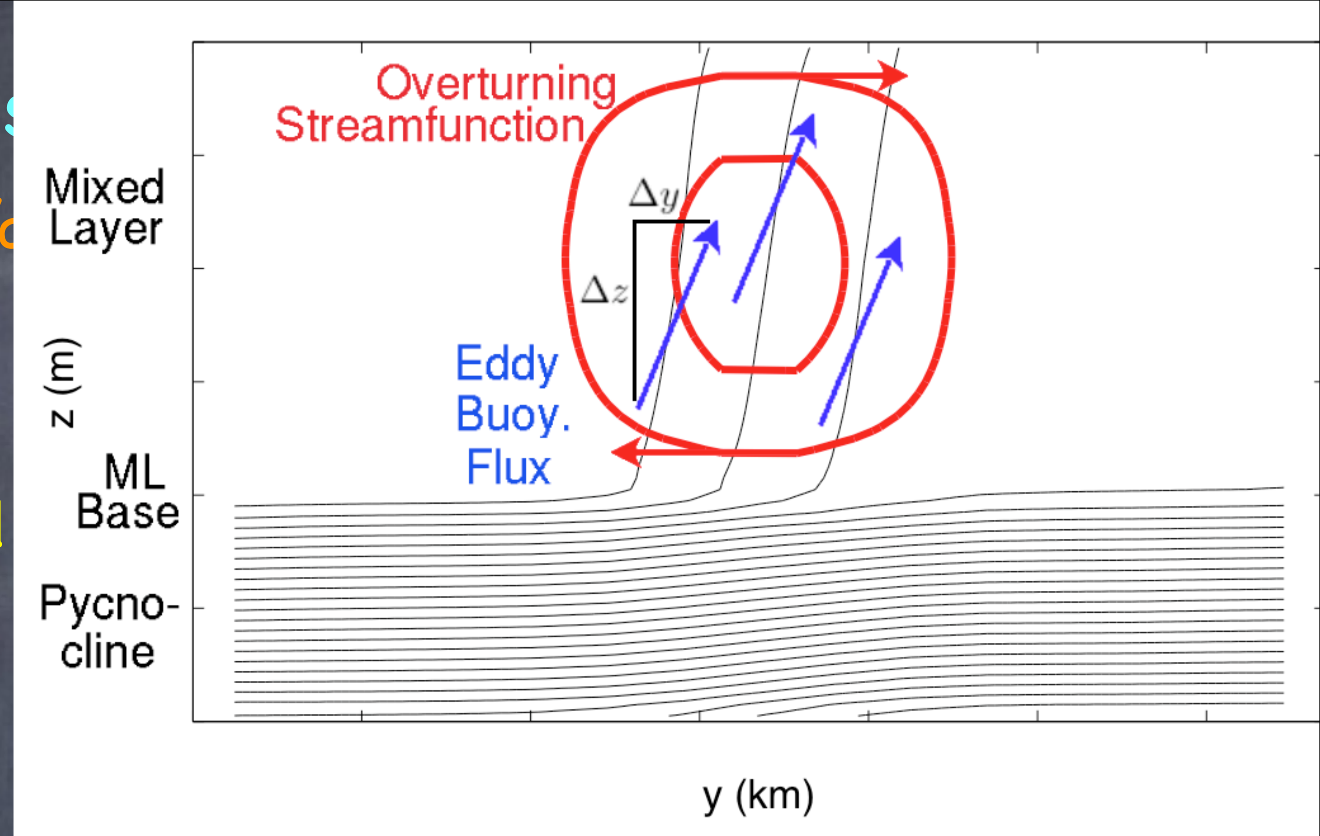

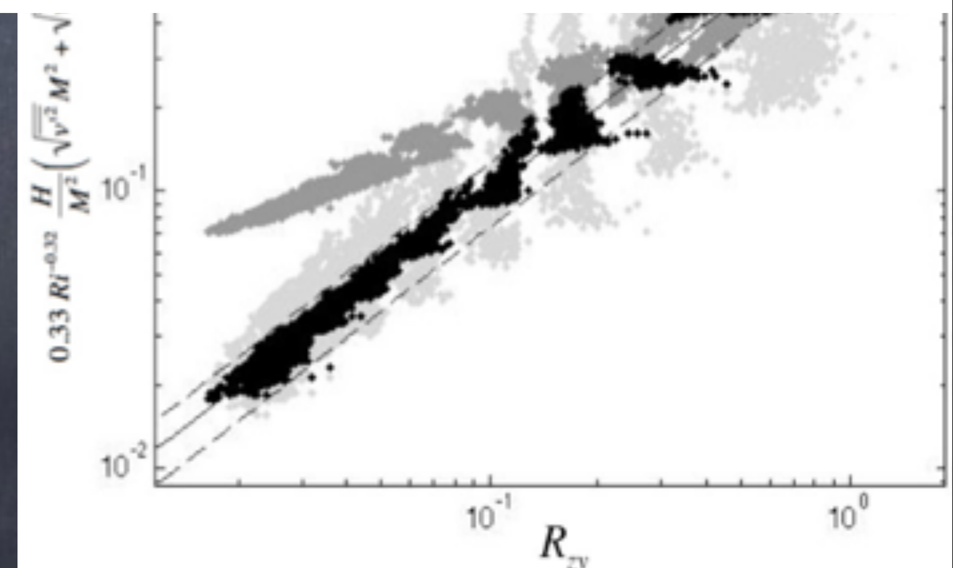

S. Bachman and B. Fox-Kemper. Eddy parameterization challenge suite. I: Eady spindown. Ocean Modelling, 64:12-28, 2013

Sensitivity of Climate to Submeso: AMOC & Cryosphere Impacts

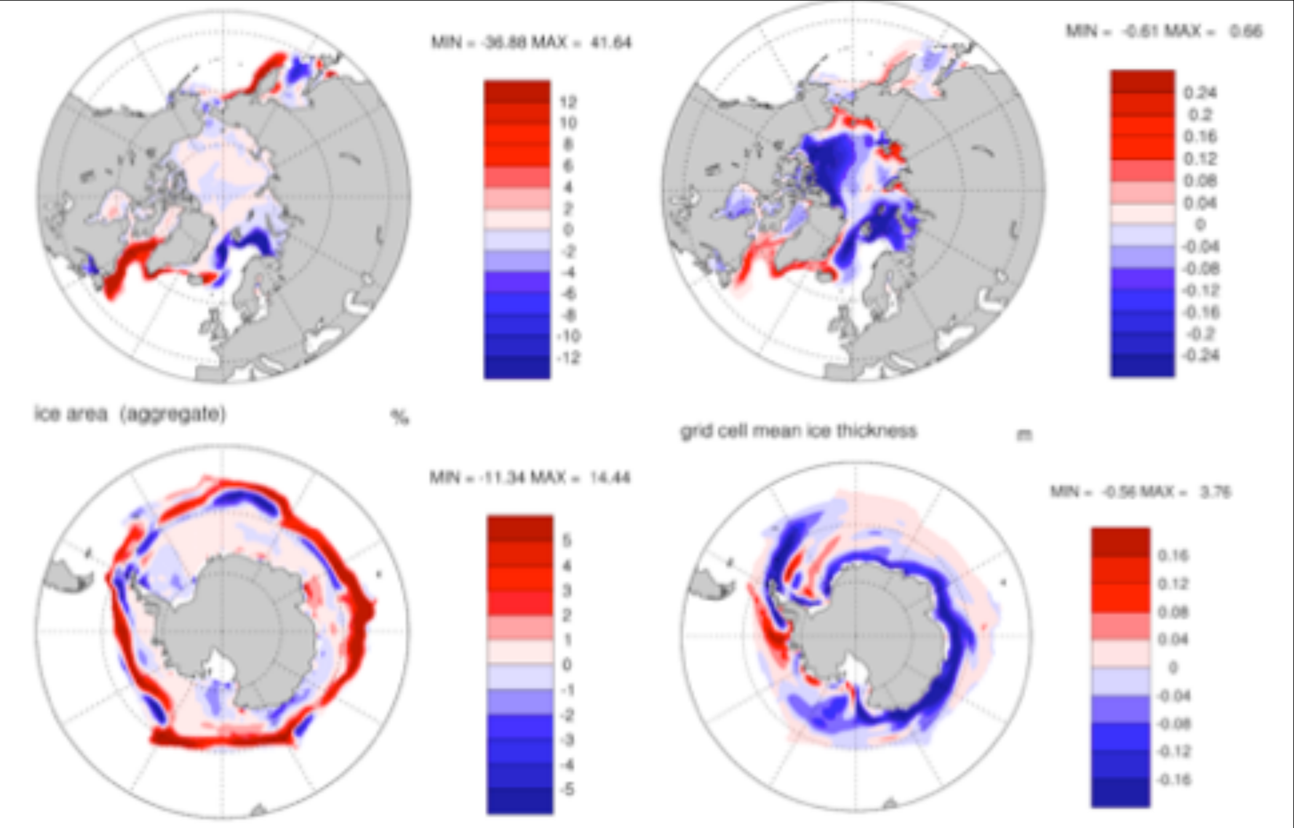

Figure 10: Wintertime sea ice sensitivity to introduction of MLE parameterization (CCSM$^+$ minus CCSM$^-$): January to March Northern Hemisphere a) ice area and b) thickness and July to September Southern Hemisphere c) ice area and d) thickness.

May Stabilize AMOC

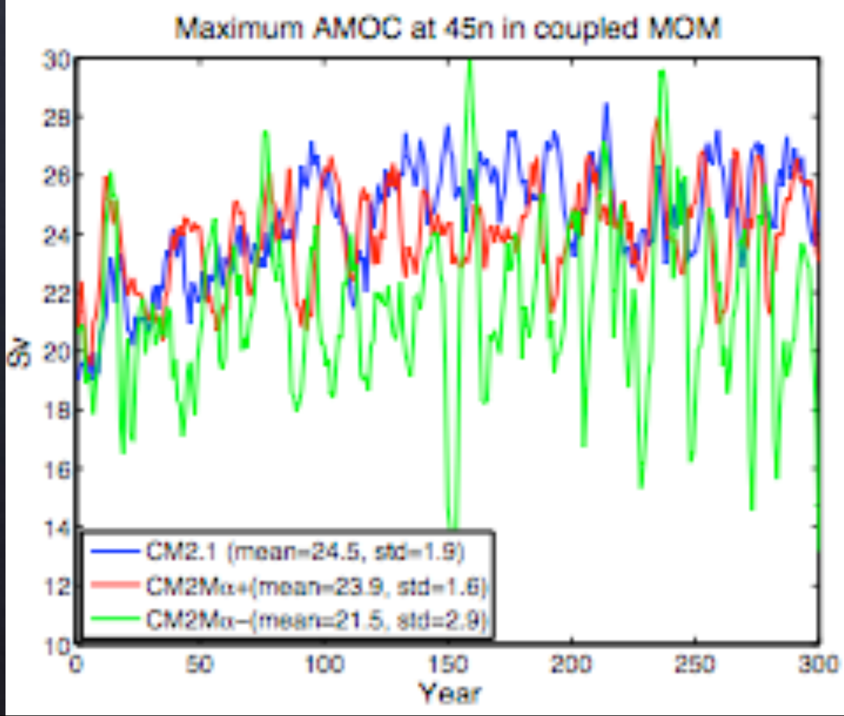

Affects sea ice

NO RETUNING NEEDED!!!

These are impacts: bias change unknown

CLB as equations for Large Eddy Simulations: Tricky: Misaligned Wind & Waves

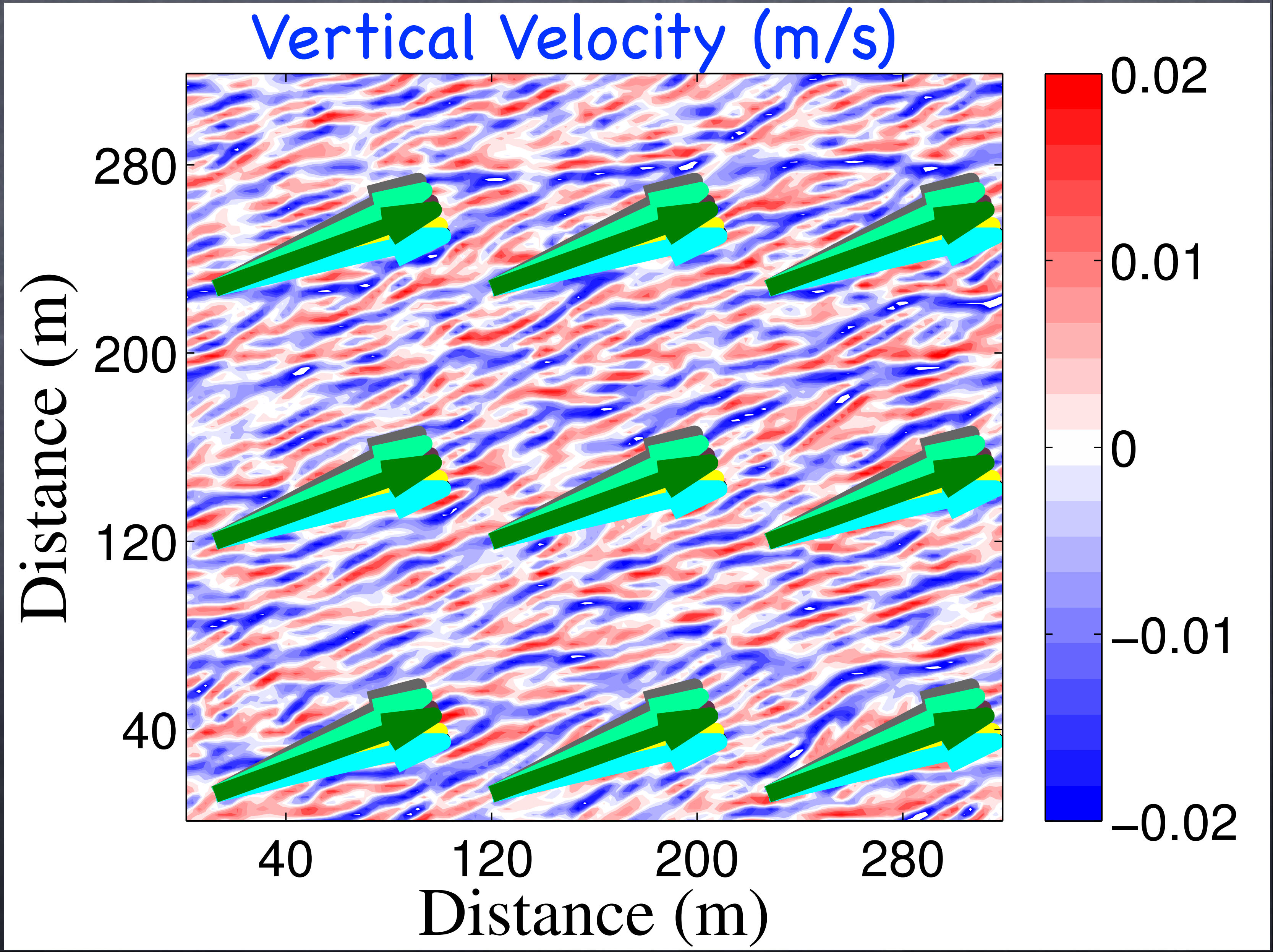

L. P. Van Roekel, B. Fox-Kemper, P. P. Sullivan, P. E. Hamlington, and S. R. Haney. The form and orientation of Langmuir cells for misaligned winds and waves. Journal of Geophysical Research-Oceans, 117:C05001, 22pp, May 2012.

Tricky: Misaligned Wind & Waves

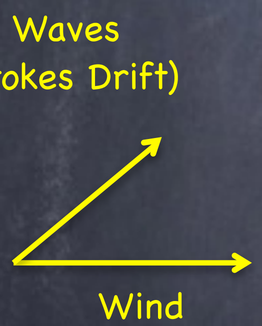

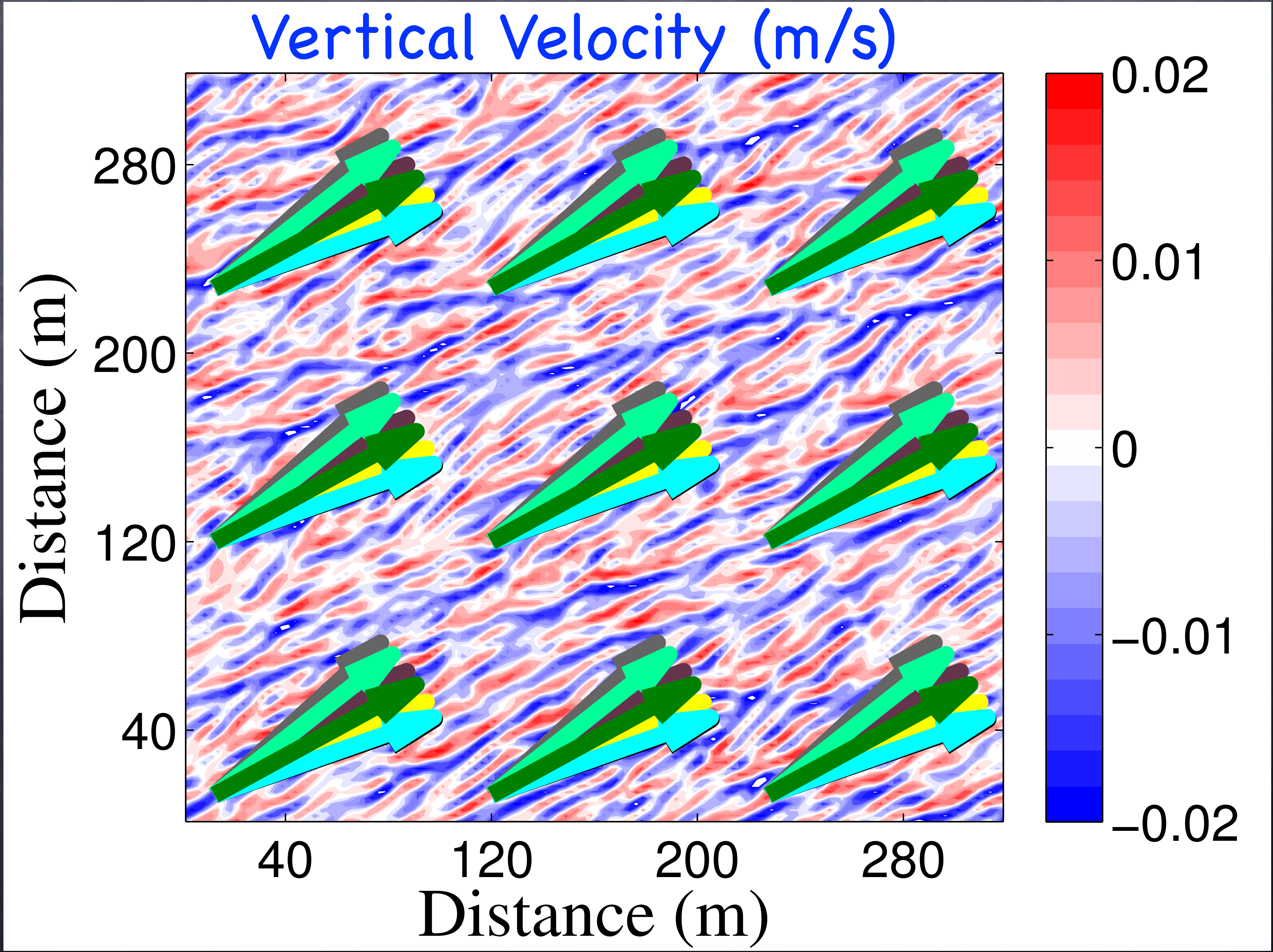

L. P. Van Roekel, B. Fox-Kemper, P. P. Sullivan, P. E. Hamlington, and S. R. Haney. The form and orientation of Langmuir cells for misaligned winds and waves. Journal of Geophysical Research-Oceans, 117:C05001, 22pp, May 2012.

Tricky: Misaligned Wind & Waves

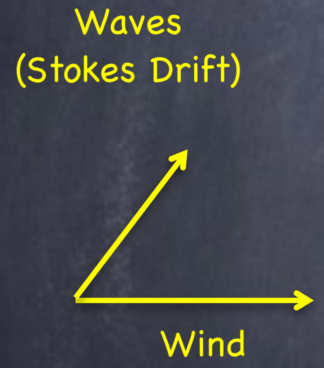

L. P. Van Roekel, B. Fox-Kemper, P. P. Sullivan, P. E. Hamlington, and S. R. Haney. The form and orientation of Langmuir cells for misaligned winds and waves. Journal of Geophysical Research-Oceans, 117:C05001, 22pp, May 2012.

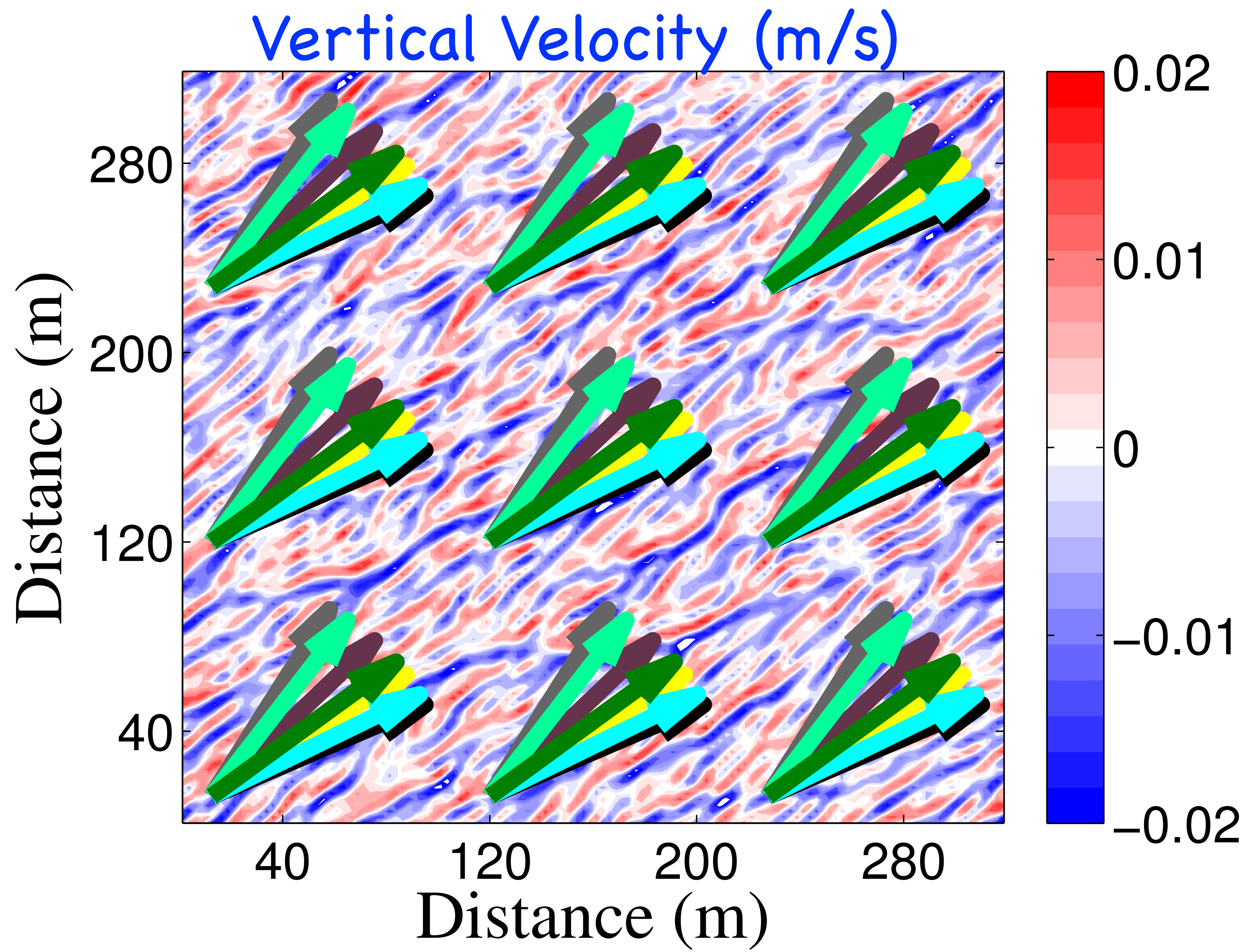

Tricky: Misaligned Wind & Waves

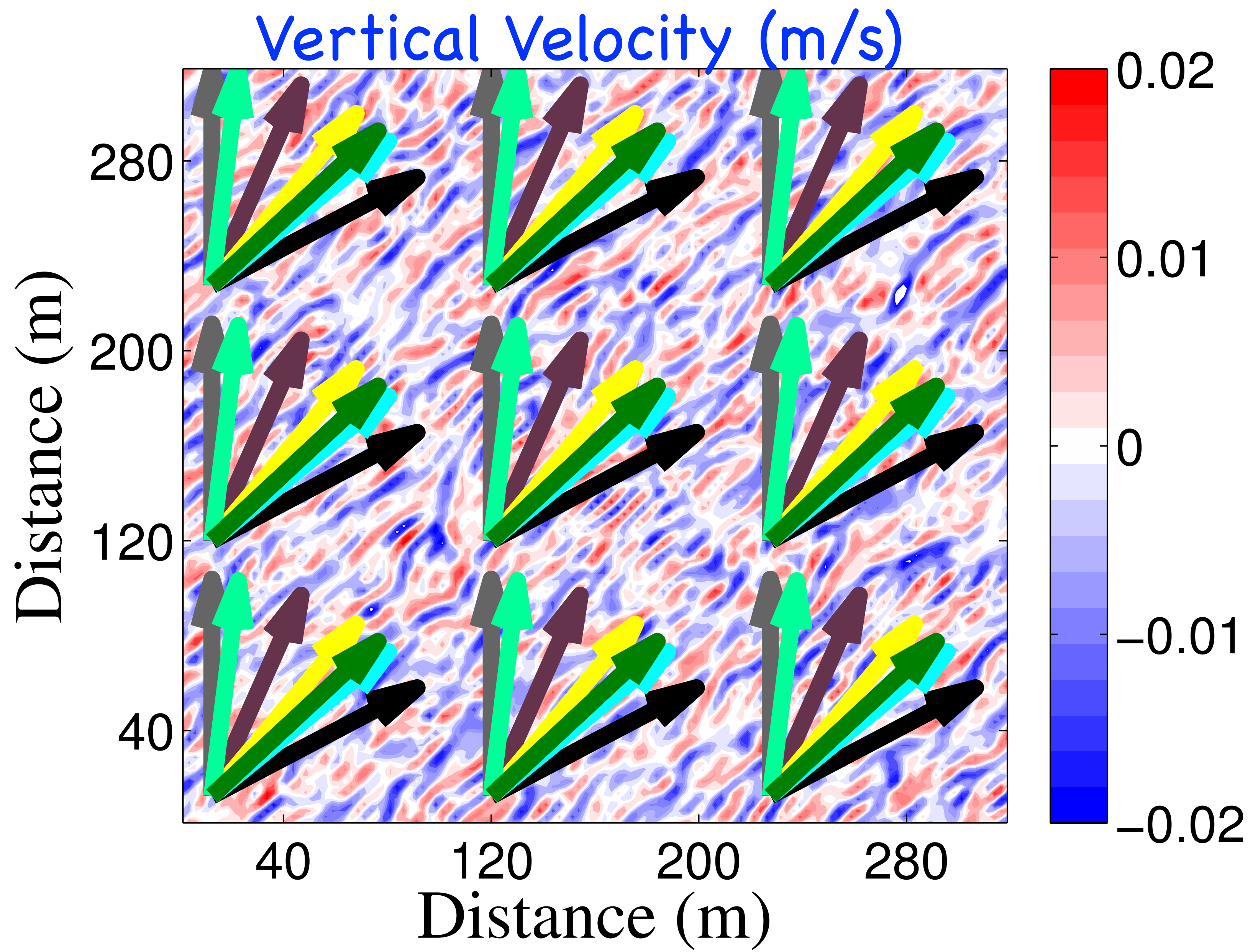

L. P. Van Roekel, B. Fox-Kemper, P. P. Sullivan, P. E. Hamlington, and S. R. Haney. The form and orientation of Langmuir cells for misaligned winds and waves. Journal of Geophysical Research-Oceans, 117:C05001, 22pp, May 2012.

Generalized Turbulent Langmuir No., Projection of u^*, u_s into Langmuir Direction

$\langle w^2 \rangle$

depth

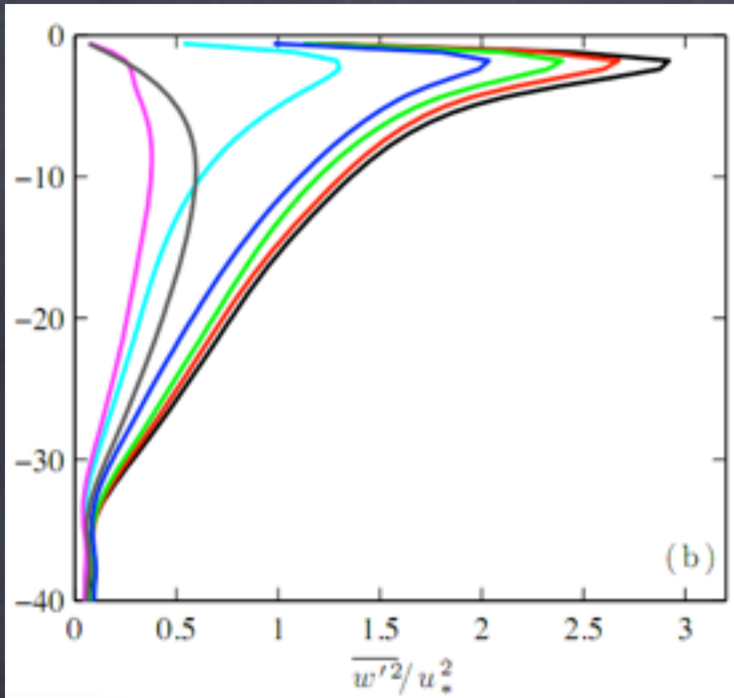

rescaled $\langle w^2 \rangle$

depth

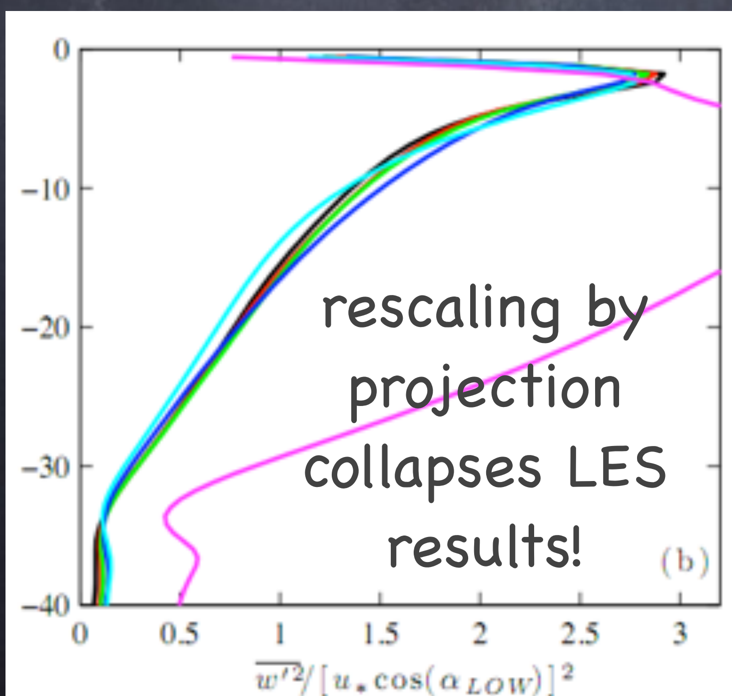

$$\frac{\left\langle \overline{w'^2} \right\rangle_{ML}}{u_*^2} = 0.6\cos^2(\alpha_{LOW})\left[1.0 + (3.1 La_{proj})^{-2} + (5.4 La_{proj})^{-4}\right],$$

$$La^2_{proj} = \frac{|u_*|\cos(\alpha_{LOW})}{|u_s|\cos(\theta_{ww}-\alpha_{LOW})},$$

$$\alpha_{LOW} \approx \tan^{-1}\left(\frac{\sin(\theta_{ww})}{\frac{u_*}{u_s(0)\kappa}\ln\left(\left|\frac{H_{ML}}{z_1}\right|\right)+\cos(\theta_{ww})}\right)$$

A scaling for LC strength & direction!

L. P. Van Roekel, B. Fox-Kemper, P. P. Sullivan, P. E. Hamlington, and S. R. Haney. The form and orientation of Langmuir cells for misaligned winds and waves. Journal of Geophysical Research-Oceans, 117:C05001, 22pp, 2012.

How well do we know Stokes Drift? <50% discrepancy

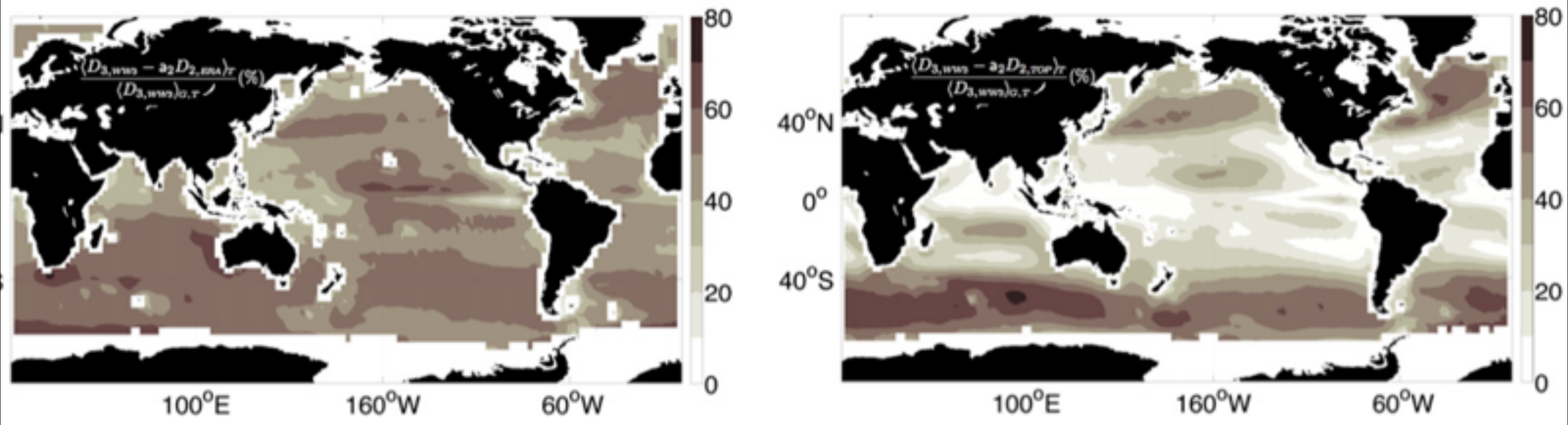

(e) $\langle D_{3,WW3} - a_2 D_{2,ERA}\rangle_T / \langle D_{3,WW3}\rangle_{G,T}$ (%) (f) $\langle D_{3,WW3} - a_2 D_{2,TOP}\rangle_T / \langle D_{3,WW3}\rangle_{G,T}$ (%)

RMS error in measures of surface Stokes drift, 2 wave models (left), model vs. altimeter (right)

Year 2000 data & models

A. Webb and B. Fox-Kemper. Wave spectral moments and Stokes drift estimation. *Ocean Modelling*, 40(3-4):273-288, 2011.

Why? Vortex Tilting Mechanism

In CLB: Tilting occurs in direction of $\mathbf{u}_L = \mathbf{v} + \mathbf{v}_s$

Misalignment enhances degree of wave-driven LT

$$\frac{\partial \xi}{\partial t} + \underbrace{(\mathbf{u}_L \cdot \nabla)\xi}_{\text{AD}} = \underbrace{(\omega_a \cdot \nabla)(\mathbf{u}_L \cdot \hat{\mathbf{x}}')}_{\text{TS}} + \underbrace{(\nabla b \times \hat{\mathbf{z}}) \cdot \hat{\mathbf{x}}'}_{\text{BV}} + \text{SGS},$$

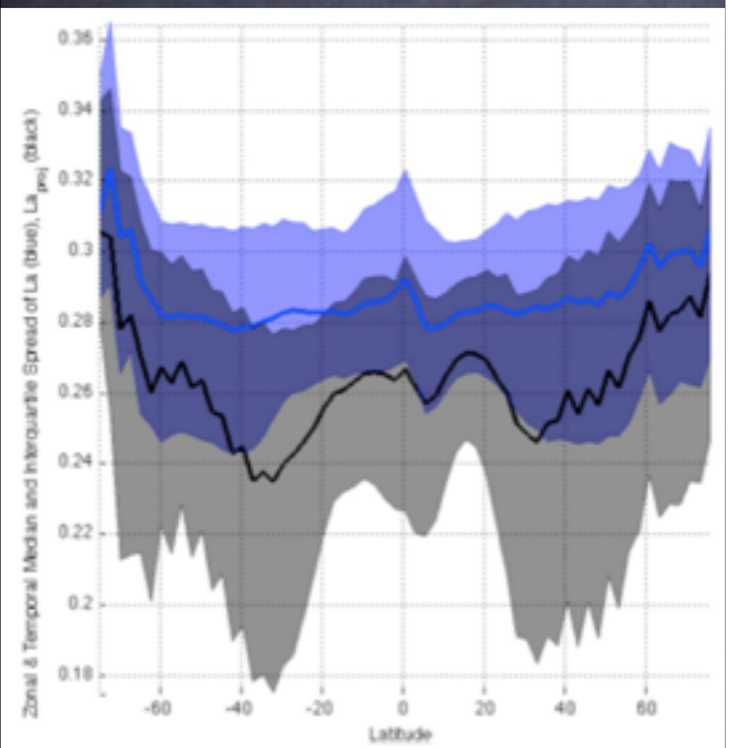

Figure 17. Temporal and zonal median and interquartile range of La_t and La_{proj} for a realistic simulation of 1994–2002 using Wave Watch III.

image: Thorpe, 04

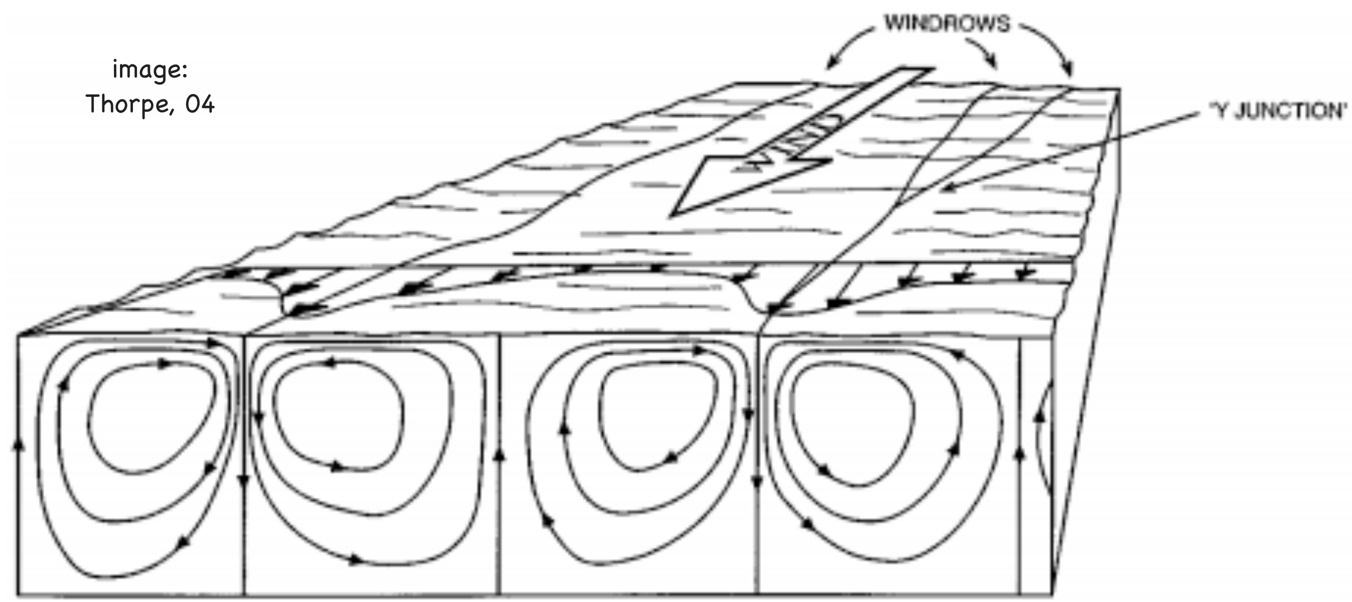

Figure 1 Sketch showing the pattern of mean flow in idealized Langmuir circulation. The windrows may be 2 m to 300 m apart, and the cell form is roughly square (as shown). In practice the flow is turbulent, especially near the water surface, and the windrows (Figure 2) amalgamate and meander in space and time. Bands of bubbles or buoyant algae may form within the downward-going (or downwelling) flow (see Figure 3).

Surface wave effects on oceanic fronts, filaments, and turbulence

Baylor Fox-Kemper
with contributions from Jim McWilliams (UCLA), Nobuhiro Suzuki (Brown), and Sean Haney (CU Boulder)

The upper ocean is home to many complex dynamical interactions—between the air and sea, between the waves, winds, and currents, between the gasses in the atmosphere and those dissolved in the ocean, and between spatiotemporal scales of variability. A standard approach to the upper ocean multiscale dynamical interaction was first proposed by Craik and Leibovich, and later improved by Holm, McWilliams, Lane, and Restrepo. The approach focuses on the Boussinesq equations averaged over the timescale of surface waves under the assumption that the fast scales are waves of limited steepness. Under this assumption, the leading order coupling between the fast and slow scales is through the Stokes drift of the surface waves, which affects the larger, slower scales through advection and the Coriolis and vortex forces. The approach is equivalent and complementary to the radiation stress theory of Longuet-Higgins. Analysis, theory, and Large Eddy Simulations of the wave-averaged equations will be presented that elucidate some effects of surface waves on upper ocean boundary layer turbulence and submesoscale fronts and filaments.

Particle motions

$$k = \frac{2\pi}{\text{wavelength}}$$

$$\omega = \sqrt{gk}$$

$$c_p = 2c_g = \sqrt{g/k}$$

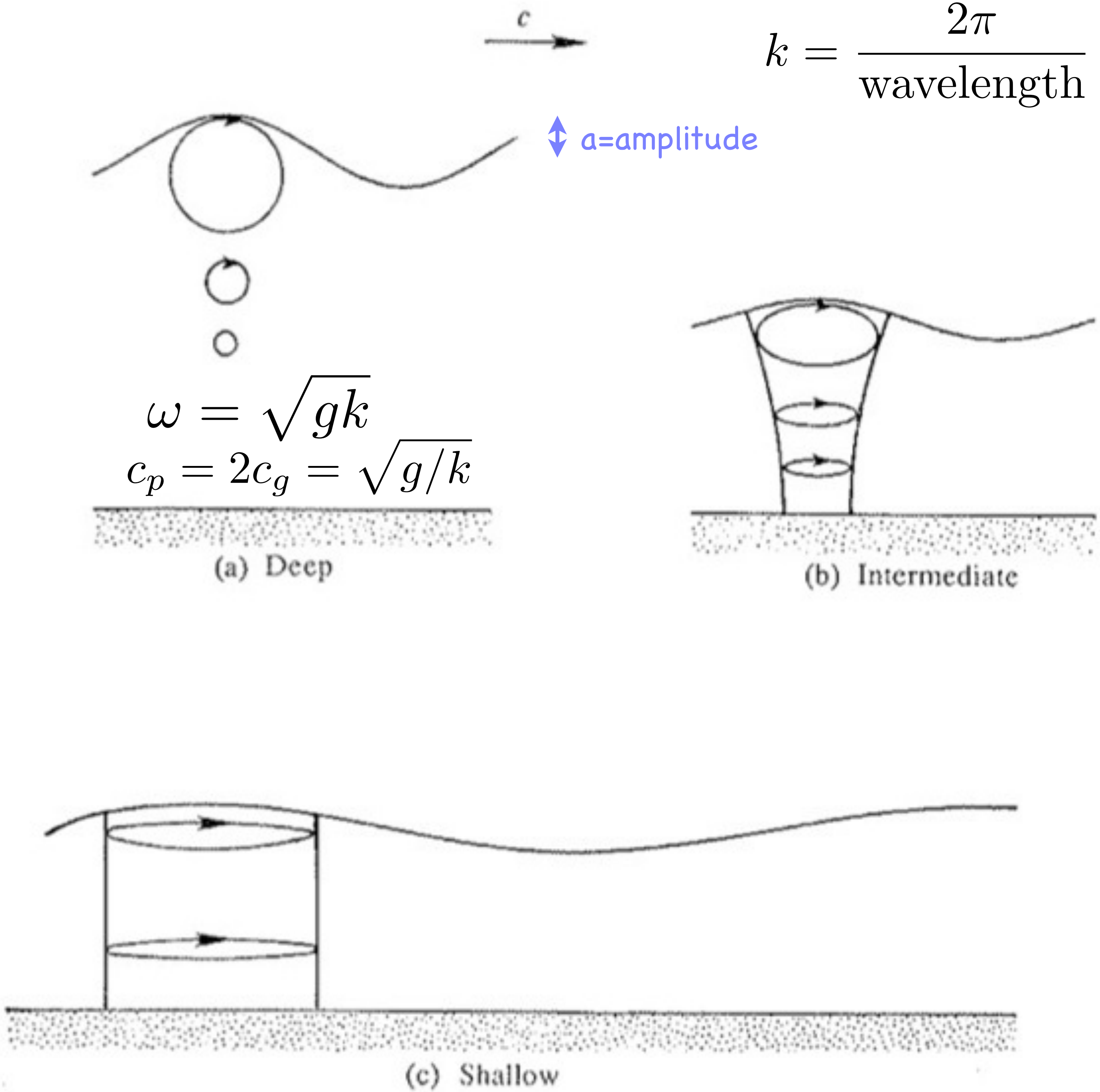

The u, v, decay exponentially toward the bottom with decay scale proportional to the wavelength.

Thus, kH is a measure of depth

ka is a measure of steepness

Deep water waves don't "feel" the bottom. Implies nonhydrostatic ($H \approx L$) & fast timescale (Ro>>1)

So, no problems? Just crunch away with CLB?

- Let's revisit our assumptions for scale separation:
  - CLB wave equations require limited *wave steepness* and irrotational flow
  - Real wind-waves are not monochromatic, but incorporate a spectrum of waves, and...

Power Spectrum of wave height

$$\langle \eta^2 \rangle = \int_0^\infty E(k)dk = C_0 + \int_{k_h}^\infty C_1 k^{-2} dk$$

Power Spectrum of wave steepness: INFINITE!

$$\langle k^2 \eta^2 \rangle = \int_0^\infty k^2 E(k)dk = D_0 + \int_{k_h}^\infty D_1 dk$$

Steep waves break->vortex motion & small scale turbulence!

So, no problems? Just crunch away with CLB?

- Let's revisit our assumptions for scale separation:
  - CLB wave equations require limited *wave steepness* and irrotational flow
  - Real wind-waves are not monochromatic, but incorporate a spectrum of waves, and...

Power Spectrum of wave height

$$\langle \eta^2 \rangle = \int_0^\infty E(k)dk = C_0 + \int_{k_h}^\infty C_1 k^{-2} dk$$

Power Spectrum of wave steepness: INFINITE!

$$\langle k^2 \eta^2 \rangle = \int_0^\infty k^2 E(k)dk = D_0 + \int_{k_h}^\infty D_1 dk$$

Steep waves break->vortex motion & small scale turbulence!